University of Nevada, Reno

Cracking Performance Evaluation of Asphalt Mixtures in Virginia

A thesis submitted in partial fulfillment of the requirements for the degree of Master of Science in Civil and Environmental Engineering

Submitted by

Habib El Hajj

Thesis Advisor

Elie Y. Hajj, Ph.D.

December 2023

UNIVERSITY OF NEVADA, RENO

THE GRADUATE SCHOOL

We recommend that the Thesis.

Prepared under our supervision by

Habib El Hajj

Entitled

Cracking Performance Evaluation of Asphalt Mixtures in Virginia

Be accepted in partial fulfillment of the

Requirements for the degree of

MASTER OF SCIENCE

Elie Y. Hajj, Ph.D., Thesis Advisor

Peter E. Sebaaly, Ph.D., P.E., Committee Member

Adam J.T. Hand, Ph.D., P.E., Committee Member

Anna Panorska, Ph.D., Committee Member

Markus Kemmelmeier, Ph.D., Dean Graduate School

December 2023

ABSTRACT

Asphalt plays an essential role in various transportation and infrastructure projects worldwide. Throughout its production and service life, asphalt binder undergoes aging influenced by factors like temperature and exposure to oxygen. Oxidative aging, for instance, alters the properties of the asphalt binder, leading to increased stiffness and a consequent decrease in resistance to cracking. This study aims to establish a long-term aging protocol specifically tailored for evaluating the cracking resistance of asphalt mixtures in Virginia. The research comprised two phases. The first phase focuses on establishing a practical aging protocol for dense-graded surface mixtures (SM) A and D that can be implemented in mix design and acceptance. According to Virginia Department of Transportation (VDOT), the A designation corresponds to mixtures with an equivalent single axle load (ESAL) of 0 to 3 million while the D designation corresponds to an ESAL range of 3 to 10 million. The second phase aims to establish initial test criteria for the CT index based on the current criteria for short-term aged asphalt mixtures. Given the challenges with aging of compacted specimens (e.g., aging gradient within the specimen), loose asphalt mixture aging was employed in this study. Eleven SMs from Virginia were selected, each comprising different combinations of reclaimed asphalt pavement (RAP), asphalt binder grade and content, aggregate gradation, and recycling agent (RA). Preliminary observations from 3 of the 11 SMs suggest a critical aging duration of 1 day at 95°C following 4 hours of aging at compaction temperature (4H_1D). This aging level demonstrates the ability to differentiate between the cracking resistance of the evaluated asphalt mixtures. Equivalent accelerated aging durations of 6 and 8 hours at compaction

temperature (6H_0D, 8H_0D) were evaluated and found to simulate the 4H_1D aging duration.

To set the criteria for CTindex at the critical aging found in the study, a thorough analysis of the test data was done. This analysis involved a combination of test parameters obtained from the different binder and mixture testing. Glover-Rowe parameter (GRP) was plotted against the CTindex for all mixtures and the cracking limits were obtained in terms of CTindex limits. Additionally, the CTindex was plotted against the aging duration and the cracking limits were also found in terms of aging duration.

The resulting CTindex limits for cracking were about 71 for an onset of cracking corresponding to a GRP of 180 kPa and 43 for significant cracking corresponding to a GRP of 600 kPa. Furthermore, the aging durations for cracking were 0.26 days (4 hrs at compaction temperature followed by 2.24 hrs at 95°C) for onset of cracking (i.e., GRP equal to 180 kPa) and 1.41 days (4 hrs at compaction temperature followed by 29.84 hrs at 95°C) for significant cracking (i.e., GRP equal to 600 kPa). The drop in CTindex after 4 hours of aging was calculated for each aging level and was found to have a strong correlation with the GRP of the recovered asphalt binder from the asphalt mixture at the respective aging level. A 10.8% drop in CTindex after 4 hours of aging corresponds to the asphalt binder onset of cracking (GRP of 180 kPa) and a further drop reaching 29.8% corresponds to the significant cracking level (GRP of 600 kPa). These preliminary findings will be verified in a follow up study using the remaining 8 SMs from Virginia.

Acknowledgments

I would like to thank all the Pavement Engineering and Science Program (PES) at the University of Nevada, Reno for all their support and motivation.

I would like to express my appreciation to my thesis advisor, Dr. Elie Y. Hajj for his constant guidance and effort.

Also, I would like to thank Dr. Peter E. Sebaaly and Dr. Adam J.T. Hand for all the knowledge they gave me and for being a good example and a role model for me.

I appreciate Dr. Anna Panorska for always being available and ready to help.

I would like to also thank our laboratory manager Siththarththan Arunthavabalan for his constant help and support.

Last but not least I would like to express my deep gratitude for my family and friends in Lebanon and in Reno for all the amazing memories and the constant encouragement.

Table of Contents

Chapter 1. Introduction 1

1.1 General Overview 1

1.2 Objective 2

1.3 Virginia Department of Transportation (VDOT) 2

1.3.1 VDOT BMD 3

1.4 Scope of Work 3

Chapter 2. Literature Review 6

2.1. History of Pavements 6

2.2. Definition of Cracking 6

2.3. Balanced Mix Design (BMD) 7

2.4. Aging Types 10

2.5. Past and current practices 10

Chapter 3. Materials Selection and Procurement 15

Chapter 4. Conditioning and Reheating Protocols 18

4.1. Reheating Protocols 18

4.1.1. Laboratory Mixed, Laboratory Compacted 18

4.1.2. Plant Mixed, Laboratory Compacted 20

4.2. RAP Quartering Procedure 22

Chapter 5. Results....24
5.1. Mix Design Verification....24
5.1.1. RAP....30
5.2. Long-Term aging at 95°C:....34
5.2.1. Mixture Testing....34
5.2.2. Binder Testing....50
5.3. Long-Term aging at Compaction Temperature:....79
5.3.1. Mixture Testing....82
5.3.2. Binder Testing....84
5.4. Comparison Plots....89
5.5. Aging Criteria....92
Chapter 6. Summary, Conclusion and Future Steps....94
6.1. Summary....94
6.2. Conclusion....96
6.3. Future Steps:....96

List of Tables

Table 1. Mixing and Compaction Temperatures Ranges for A and D designation 2

Table 2. VDOT Performance Testing Criteria. 3

Table 3. States with Efforts to address BMD and/or Mechanical Testing (Diefenderfer et al., 2021) 9

Table 4. Selected Asphalt Mixtures.....15

Table 5. JMF Information for Samples Asphalt Mixtures.....16

Table 6. JMF VTM and Gmm - All mixtures 17

Table 7. Binder Percentage and Gradation of M1 Plant Mixture 25

Table 8. Binder Percentage and Gradation of M2 Plant Mixture 26

Table 9. Binder Percentage and Gradation of M3 Plant Mixture 26

Table 10. Binder Percentage and Gradation of M4 Plant Mixture.....26

Table 11. Binder Percentage and Gradation of M5 Plant Mixture.....27

Table 12. Binder Percentage and Gradation of M6 Plant Mixture.....27

Table 13. Binder Percentage and Gradation of M7 Plant Mixture.....27

Table 14. Binder Percentage and Gradation of M8 Plant Mixture.....28

Table 15. Binder Percentage and Gradation of M9 Plant Mixture.....28

Table 16. Binder Percentage and Gradation of M10 Plant Mixture.....28

Table 17. RAP Binder Percentage LMLC 31

Table 18. RAP Gradation LMLC 32

Table 19. RAP fine Aggregate Specific Gravity.....33

Table 20. RAP Coarse Aggregate Specific Gravity 33

Table 21. JMF mixing and compaction temperatures for M4, M6, and M7 mixtures 34

Table 22. Maximum Theoretical Specific Gravity (Gmm) 35

Table 23. VDOT Max COV limits 36

Table 24. IDTL-CT results – M6 PMLC 38

Table 25. Initial Aging Durations and Temperatures LMLC 42

Table 26. IDT_CT LMLC 42

Table 27. IDT- CT comparison at each aging level - LMLC 43

Table 28. LMLC aging levels rank based on average CT value. 48

Table 29. ANOVA Interaction Test 49

Table 30. ΔTc - M4 54

Table 31. ΔTc - M6 57

Table 32. ΔTc - M7 60

Table 33. M4 FTIR test results – Virgin and Recovered Binder 64

Table 34. M6 FTIR test results – Virgin and Recovered Binder 66

Table 35. M7 FTIR test results – Virgin and Recovered Binder 68

Table 36. Experimental plan for Frequency Sweep test 69

Table 37. G* and Phase Angle - All mixtures 71

Table 38. Glover-Rowe (GRP) - Virgin and Recovered Binder (All Mixtures) 72

Table 39. G* vs Phase Angle - M4 mixture 73

Table 40. G* vs Phase Angle – M6 mixture 75

Table 41. G* vs Phase Angle - M7 76

Table 42. Time equivalence conversion table for different LTA temperatures (NCHRP 9-54) 79

Table 43. IDT- CT - LMLC all aging levels.....82

Table 44. FTIR Data Accelerated Aging levels - All mixtures.....86

List of Figures

Figure 1. Material Sampling Locations - Virginia 4

Figure 2. Experimental Plan.....5

Figure 3. Fatigue Cracking in Asphalt (google earth).....7

Figure 4. Schematic description of short-term and long-term aging of asphalt (Notani et al., 2020).....10

Figure 5. Loose mixture oven aging of asphalt (NC State University, 2015) 12

Figure 6. Pressure Aging Vessel (PAV), (Elwardany et., al, 2016).....13

Figure 7. Received Pallets at UNR campus. 17

Figure 8. LMLC Reheating Protocol.....19

Figure 9. PMLC Reheating Protocol 21

Figure 10. Quartering Procedure.....23

Figure 11. Centrifuge Extractor (left) and Rotary Evaporator (right) 24

Figure 12. Gradations - All mixtures.....29

Figure 13. Binder Contents - All mixtures.....30

Figure 14. Loose Mixture for Gmm (left), Loose Mixture in Vacuum machine. 35

Figure 15. IDT-CT machine (left), IDT-CT tested sample (right).....37

Figure 16. IDTL-CT Formula and Curve (ASTM D8225-19).....37

Figure 17. CT-Index vs aging duration - M6 PMLC.....39

Figure 18. Fracture Energy vs Aging Duration - M6 40

Figure 19. Peak Load vs Aging Duration - M6.....40

Figure 20. Post Peak Slops vs Aging Duration - M6 41

Figure 21. l75/m75 vs Aging Duration - M6 41

Figure 22. CT index for the LMLC mixtures.....43

Figure 23. l75/m75 for the LMLC mixtures 44

Figure 24. Peak Load for the LMLC mixtures.....44

Figure 25. Fracture Energy for the LMLC mixtures 45

Figure 26. Energy to Peak Load for LMLC mixtures 45

Figure 27. Gf vs l75/m75 - M4 46

Figure 28. Gf vs l75/m75 - M6 47

Figure 29. Gf vs l75/m75 - M7 47

Figure 30. Bending Beam Rheometer (BBR) 51

Figure 31. Rolling Thin Film Oven (RTFO).....51

Figure 32. Pressure Aging Vessel (PAV) 51

Figure 33. S-value (left), m-value (right) - M4 Virgin Binder.....53

Figure 34. S-value (left), m-value (right) - M4 Recovered Binder 53

Figure 35. Virgin True low PG (left), Virgin Standardized low PG (right) - M4.....55

Figure 36. Recovered True low PG (left), Recovered Standardized low PG (right) - M4. 55

Figure 37. S-value (left), m-value (right) - M6 Virgin Binder.....56

Figure 38. S-value (left), m-value (right) - M6 Recovered Binder 56

Figure 39. Virgin True low PG (left), Virgin Standardized low PG (right) - M6.....58

Figure 40. Recovered True low PG (left), Recovered Standardized low PG (right) - M6. 58

Figure 41. S-value (left), m-value (right) - M7 Virgin Binder.....59

Figure 42. S-value (left), m-value (right) - M7 Recovered Binder 59

Figure 43. Virgin True low PG (left), Virgin Standardized low PG (right) - M7.....61

Figure 44. Recovered True low PG (left), Recovered Standardized low PG (right) - M761

Figure 45. Fourier Transform Infrared Machine (FTIR) 62

Figure 46. FTIR - M4 Virgin Binder.....63

Figure 47. FTIR - M4 Recovered Binder 63

Figure 48. FTIR - M6 Virgin Binder.....65

Figure 49. FTIR - M6 Recovered Binder 65

Figure 50. FTIR - M7 Virgin Binder.....67

Figure 51. FTIR - M7 Recovered Binder 67

Figure 52. Black Space Diagram– Virgin Binders.....70

Figure 53. Black Space Diagram - Recovered Binders.....70

Figure 54. Black Space Diagram - M4.....72

Figure 55. Black Space Diagram- M6.....74

Figure 56. Black Space Diagram - M7.....76

Figure 57. Carbonyl Growth vs Aging Duration.....77

Figure 58. CTindex vs Aging Duration 78

Figure 59. Time equivalence conversion curve for different LTA temperatures (NCHRP 9-54).....80

Figure 60. CT-Index M4 - LMLC all aging levels.....83

Figure 61. CT-Index M6 - LMLC all aging levels.....83

Figure 62. CT-Index M7 - LMLC all aging levels.....84

Figure 63. FTIR - M4 all aging Levels.....85

Figure 64. FTIR - M6 all aging Levels.....85

Figure 65. FTIR - M7 all aging Levels.....85

Figure 66. Black Space Diagram - M4 all aging levels.....87

Figure 67. Black Space Diagram - M6 all aging levels.....88

Figure 68. Black Space Diagram - M7 all aging levels.....88

Figure 69. GRP vs Aging level – LMLC all mixtures.....89

Figure 70. CA vs aging level – LMLC all mixtures.....90

Figure 71. CAg(2h) vs Aging levels - LMLC all mixtures 90

Figure 72. CTindex vs Aging levels - LMLC all mixtures.....91

Figure 73. CTindex vs GRP - All mixtures 92

Figure 74. CTindex vs Aging Duration - All mixtures.....93

Figure 75. DCTindex (4h) vs GRP - All Mixtures.....93

Chapter 1. Introduction

1.1 General Overview

Asphalt is a naturally occurring substance found in crude oil deposits and it is refined to obtain the binder used in pavement construction. Asphalt pavement is widely used around the world for several transportation and infrastructure applications as it is a cost-effective material that offers various advantages in road construction and maintenance. Asphalt binder undergoes aging during its production and service life. Aging is influenced by several factors such as temperature and exposure to oxygen. Oxidative aging increases the asphalt mixture's stiffness and decreases its cracking resistance.

Two approaches are typically used to evaluate the effects of aging, the first one involves aging the asphalt binder in the laboratory and measuring the aging index parameters that provide relative resistance to cracking. One downside to this technique is that it does not consider the effect of the aggregates on the aging and the overall performance of the asphalt mixture. The second approach is specified in the American Association of State Highway and Transportation Officials (AASHTO) R 30 *Standard Practice for Mixture Conditioning of Hot Mix Asphalt*. This standard practice is based on oven-aging of compacted asphalt mixture specimens at 85°C for 5 days following a short-term loose mixture conditioning for 4 hours at 135°C. Aging the compacted specimens may not be accurate in simulating the real effect of climate and depth into the asphalt concrete (AC) layer due to the aging gradient in the specimen. This gradient might introduce increased variability due to alterations in the shape, size of compacted specimens, and air void content. This issue can be mitigated by opting for conditioning the loose mixture instead (Kim et al., 2013).

Recycled materials are often added to the mixtures for cost and environmental reasons, inclusion of recycled material in the mix design makes the mechanical evaluation even more critical as it highlights the effects of recycled material, binder type and quality, additives, and their interaction with aggregates characteristics on the long-term cracking performance of the asphalt mixture.

1.2 Objective

This research aims to establish an effective long-term aging procedure for asphalt mixtures in Virginia that can be used for mix design, verification, and acceptance. Thus, the primary focus is on examining the extended aging of loose asphalt mixtures to address the concerns associated with aging of compacted specimens.

1.3 Virginia Department of Transportation (VDOT)

VDOT currently specifies the use of the Indirect Tensile Cracking Test (IDT-CT) as part of its Balanced Mix Design (BMD) approach. This test assesses the cracking resistance of dense-graded asphalt surface mixtures (SM) with A and D designations. The A designation corresponds to an equivalent single axle load (ESAL) range of 0 to 3 million, while the D designation pertains to an ESAL range of 3 to 10 million. The short-term aging duration for the IDT-CT is 4 hours at the compaction temperature. The mixing and compaction temperatures for mixture designations A and D are shown in Table 1.

Table 1. Mixing and Compaction Temperatures Ranges for A and D designation

Mixture Designation	**A**	**D**
Mixing Temperature Range (°C)	148.9-154.4	154.4-160.0
Compaction Temperature Range (°C)	140.5-143.3	146.1-148.9

1.3.1 VDOT BMD

For BMD specifications, VDOT requires the JMF to meet the performance test criteria shown in Table 2. VDOT uses the Cantabro test, Asphalt Pavement Analyzer (APA), and IDT-CT for durability, rutting, and cracking, respectively.

Table 2. VDOT Performance Testing Criteria.

Mixture	LMLC	PMLC	RPMLC
Durability (Cantabro, AASHTO TP 108)			
Specimens	3	–	3
Mass loss	≤ 7.5%	–	≤ 7.5%
Rutting (APA test AASHTO T 340)			
Specimens	4	4	4
APA rut depth	≤ 8 mm	–	≤ 8 mm
Cracking (ASTM D8225)			
Specimens	5 replicates	5 replicates	5 replicates
Air Void (%)	7 ± 0.5	7 ± 0.5	7 ± 0.5
Sample Size (mm)	150 x 62	150 x 62	150 x 62
Conditioning	STA of 4 hrs at compaction temp.	None (i.e., no reheat).	Reheated
Cracking Tolerance (CT) index	≥ 70	≥ 95	≥ 70

1.4 Scope of Work

This study, titled "Developing Long-term Aging Protocols for Cracking Performance Evaluation of Asphalt Mixtures in Virginia" is part of the Virginia Transportation Research Council (VTRC) initiative and it involves the examination of 11 SM mixtures. These mixtures include a combination of reclaimed asphalt pavement (RAP) percentages, asphalt binder performance grades (PG), and other constituent elements. The project is structured into three distinct tasks:

Task 1 – Material Selection and Procurement: This phase involves acquiring raw materials, including aggregates, binders, additives, RAP, and plant mixtures sampled from various

locations in Virginia. The aim is to capture variations in aggregate mineralogy and the crude oil sources of asphalt binders. Figure 1 shows the material sampling locations in Virginia.

Figure 1. Material Sampling Locations - Virginia

Task 2 – Experimental Plan: The research focuses on the extended aging of loose asphalt mixtures at two distinct temperatures: 95°C and 135°C. Following each conditioning phase, the specimens undergo compaction and a series of tests to evaluate aging's impact on performance. Additionally, asphalt binders extracted from these tested specimens undergo rheological and chemical characterization. Figure 2 outlines the experimental plan for each asphalt mixture, considering specific aging conditions (temperature and duration). Subsequently, the reheated plant mixed, laboratory compacted (PMLC) specimens are tested without further aging, and the corresponding extracted and recovered asphalt binders undergo rheological and chemical characterization.

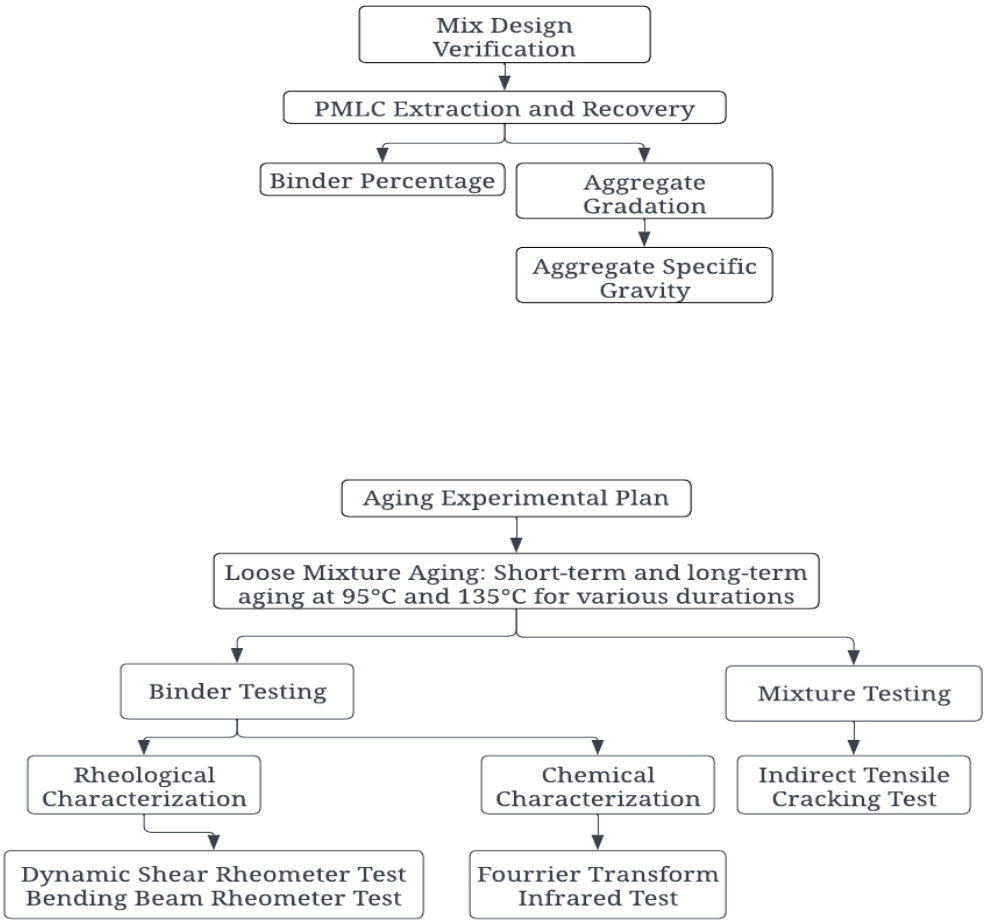

Figure 2. Experimental Plan

Task 3 – Data Analyses: Comprehensive analysis is undertaken to compare and establish correlations among the test results within each long-term aging protocol and across different protocols. The scope involves an evaluation of mechanistic performance to assess how aging impacts pavement performance. Initial test criterion for the long-term aged asphalt mixtures is determined, drawing from the established correlations with the short-term aged CT index criterion of 70.

Chapter 2. Literature Review

2.1. History of Pavements

Over ninety percent of the roads in the United States are made of a mixture of asphalt and other materials. The use of asphalt started around 625 BC for road building in Babylon where the romans took the road system from Carthaginians and built roads for easier military travel. The first modern asphalt road was built in 1824 where large blocks of natural asphalt rock were used to pave the Champ-Élysées in Paris, France.

The first modern asphalt facility was built in 1901 by Warren Brothers in East Cambridge, Massachusetts where the production of refined petroleum asphalt outstripped the use of natural asphalt. With the fast growth of the automobile, better roads were a necessity, and the demand grew leading to innovations in production and layoff.

2.2. Definition of Cracking

In asphalt pavements cracking refers to the development of fractures in the asphalt surface, this can occur due to many reasons including environmental, traffic and asphalt mix design and quality. Cracking can significantly affect the performance and the life of the pavement in terms of structural integrity. Cracking can have many names depending on the cause and looks of the cracks such as Fatigue/ Alligator cracking which is characterized by a pattern of interconnected cracks that look like alligator skin texture and is caused by repeated traffic loads in high stress concentration areas. Other types of cracking include block cracking, transverse cracking, longitudinal cracking, and edge cracking.

Figure 3. Fatigue Cracking in Asphalt (google earth)

2.3. Balanced Mix Design (BMD)

The objective of BMD methodology is to optimize the performance of asphalt mixtures by harmonizing various elements, such as gradation and binder percentage. This approach aims to achieve specific performance targets that ensure enhanced durability throughout the pavement's lifespan. Key aspects considered in BMD encompass performance metrics, material characterization, laboratory testing, a mechanistic-empirical approach, optimization strategies, and field validation.

Several states have initiated the incorporation of BMD into their current and future projects. In Virginia, efforts to tackle rutting in Marshall mixtures prompted the adoption of the Superpave system in 1997. However, initial findings revealed coarse and dry mixtures, leading to premature failures and shorter pavement life span. Subsequent adjustments were made by VDOT, altering the compaction effort to 50 gyrations along with aggregate gradation and volumetric modifications (Diefenderfer et al., 2018).

California has embraced a framework for BMD mixtures, integrating performance-based specifications and its own mechanistic empirical design program known as CalME. The specification criteria were based on repeated simple shear test results showing 5% permanent deformation shear strain, 50% loss of stiffness, and flexural stiffness at 20°C with a test frequency of 10 Hz for the bending beam fatigue (BBF) test (Harvey et al., 2014).

Illinois DOT is currently in the process of implementing BMD, incorporating requirements such as the Hamburg wheel track test (HWTT) for rutting evaluation, Illinois flexibility index test (I-FIT) for fatigue evaluation, and a modified version of the tensile strength ratio (TSR) test for moisture susceptibility evaluation.

The Texas DOT applies BMD for various mixtures including porous friction course, stone matrix, overlays. Testing involves HWTT and overlay tester (OT) at different asphalt binder contents around the optimum binder content (OBC) range. The final OBC should meet specific criteria related to rut depth and number of passes for different binder high-performance grades, alongside fracture energy and crack propagation rate for OT. Table 3 shows the BMD efforts and mechanical testing of select State DOTs.

Table 3. States with Efforts to address BMD and/or Mechanical Testing (Diefenderfer et al., 2021)

State	BMD/ Mechanical testing Efforts
Florida (west et al., 2018)	• Use FN, HWTT, and APA rut tests to evaluate rutting. • Use IDT energy ratio and OT to evaluate cracking
Georgia (west et al., 2018)	• Use APA and moisture susceptibility test as part of the mix design approval and field verification of all asphalt mixtures. • Use different APA test temperatures depending on mix location in pavement structure. • Currently looking into CTindex and FI parameters
Minnesota (Newcomb and Zhou, 2018)	• Use the DCT fracture energy, Gf, to evaluate cracking performance. • Require DCT testing on both mix design and production mix samples. • Considering applying the DCT as a mix design test and the IDT as a QC/QA test • Need further work to define failure criteria for all cracking tests
New Mexico (west et al., 2018)	• Constructed test sections on existing projects by using asphalt mixtures designed following a BMD procedure. • Use HWTT to evaluate rutting and stripping potentials of asphalt mixtures
Ohio (Rodezno et al., 2018)	• Use APA testing for mixtures with more than 15% fine aggregates and that do not meet the fine aggregate angularity criteria. • Use BBF tests for bridge deck waterproofing mixtures. • Selected the I-FIT to assess the cracking resistance and durability of mixtures with recycled materials; however, with the emergence of the IDT, are evaluating the suitability of both tests for implementation in mix design approval and QC/QA. Will recommend specification limits and test standards
Oklahoma (Cross and Li, 2019)	• Are considering potential implementation of BMD Approach II • Constructed several BMD trial projects in spring 2018. • Use the HWTT, I-FIT, IDT, and Cantabro test to evaluate mix design and production samples. • Recommended the IDT if Oklahoma DOT decides to move forward with BMD. • Recommended a minimum CTindex of 80 as the criterion for short-term aged specimens; recommended consideration of dropping the binder grade in case failure to meet this criterion occurs
Oregon (Coleri et al., 2020)	• Previous research efforts established a performance-based BMD framework that suggested the use of the I-FIT with typical FI values ranging from 9-14 for production mixtures. • Recently completed efforts developed a long-term aging protocol to be implemented consisting of aging mixtures at 95°C for 24 hours to simulate not more than 3-5 years of aging in the field; FI threshold was refined to a minimum of 6 for Level 3 mixtures (1-10 million ESALs on rural highways and 1-3 million ESALs on urban highways) and 8 for Level 4 mixtures (>10 million ESALs on rural highways and >3 million ESALs on urban highways). A rut depth threshold of 3 mm for Level 3 mixtures and 2.5 mm for Level 4 mixtures was recommended.
South Dakota (west et al., 2018)	• Currently follows the conventional Superpave volumetric mix design. • Uses APA and TSR tests to evaluate rutting and moisture damage of asphalt mixtures, respectively
Utah (west et al., 2018)	• Uses Superpave volumetric approach to design asphalt mixtures. • Uses HWTT to evaluate resistance to rutting. • Is exploring the use of the BBR sliver test and I-FIT to evaluate the mixture resistance to low temperature and intermediate temperature cracking, respectively
Wisconsin (west et al., 2018)	• Lowered the mixture design air-void target from 4.0% to 3.5% • Increased the minimum TSR requirement from 0.70 to 0.75. • Uses HWTT to evaluate moisture susceptibility and rutting. • Uses DCT test to evaluate low temperature cracking. • Uses SCB test for fatigue cracking. • Evaluates the PG grading of the recovered asphalt binder. • Is exploring and evaluating the feasibility of using the HWTT, confined FN, and SCB tests at intermediate and low temperatures. • Identified potential for increase of asphalt contents by regressed air voids using the HWTT, DCT, and I-FIT tests

APA = Asphalt Pavement Analyzer; BBF = bending beam fatigue; BBR = bending beam rheometer; BMD = balanced mix design; DCT = disk-shaped compact tension; ESALs = equivalent single axle loads; FI = flexibility index; FN = flow number. HWTT = Hamburg wheel-tracking test; IDT = indirect tensile test; OT = overlay test; PG = performance grade; QC/QA = quality control/quality assurance; SCB = semi-circular bend; TSR = tensile strength ratio.

2.4. Aging Types

Two types of aging exist in the laboratory, short term aging (STA) that usually simulates the aging that the asphalt mixture undergoes while being mixed in the mixing plant. The second type of aging is the long-term aging (LTA), which simulates the aging that the asphalt mixture undergoes during the service life. Typically, the LTA temperatures are lower than the STOA since the pavement temperatures in the field do not reach the high mixing plant temperatures (around 300-350°F).

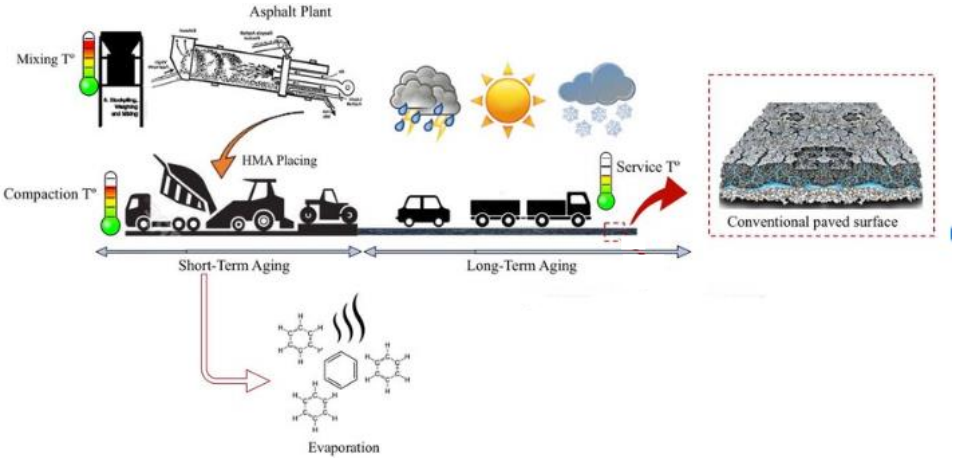

Figure 4. Schematic description of short-term and long-term aging of asphalt (Notani et al., 2020)

2.5. Past and current practices

In 2015, the National Center for Asphalt Technology (NCAT) collaborated with the Minnesota Department of Transportation's Road Research Facility (MnROAD) to initiate a nationwide cracking study. As part of this research, the significance of age hardening in asphalt mixtures underwent evaluation. Both LMLC (laboratory mixed laboratory compacted) and PMLC (plant mixed laboratory compacted) specimens underwent short-term and long-term aging prior to testing. The standard practice for laboratory long-term

aging (LTA), initially developed in a pre-SHRP (Strategic Highway Research Program) study by Bell et al. according to AASHTO R 30, involves conditioning the compacted specimens for 5 days at 85°C, intended to simulate 7 to 10 years of field aging. However, findings from the National Cooperative Highway Research Program (NCHRP) project 09-52 indicated that this protocol approximated 1 to 2 years of aging in warmer and colder climates, respectively. This estimation was derived after conducting tests on LMLC and field cores extracted from over 40 asphalt mixtures. Islam et al., in their study, reported similar conclusions in BBF analysis.

A significant finding highlighted in Howard and Doyle's study indicated that subjecting specimens to 28 days of oven aging at 60°C closely approximated one year of outdoor aging. Aside from conditioning compacted specimens, LTA can be achieved by aging loose asphalt mixtures before the compaction phase. This alternate method typically induces a more noticeable level of aging, given its exposure to heightened oxygen levels and

hightemperatures. Furthermore, accelerating the aging process of loose mixtures by elevating the temperature can be performed without concerns about specimen distortion.

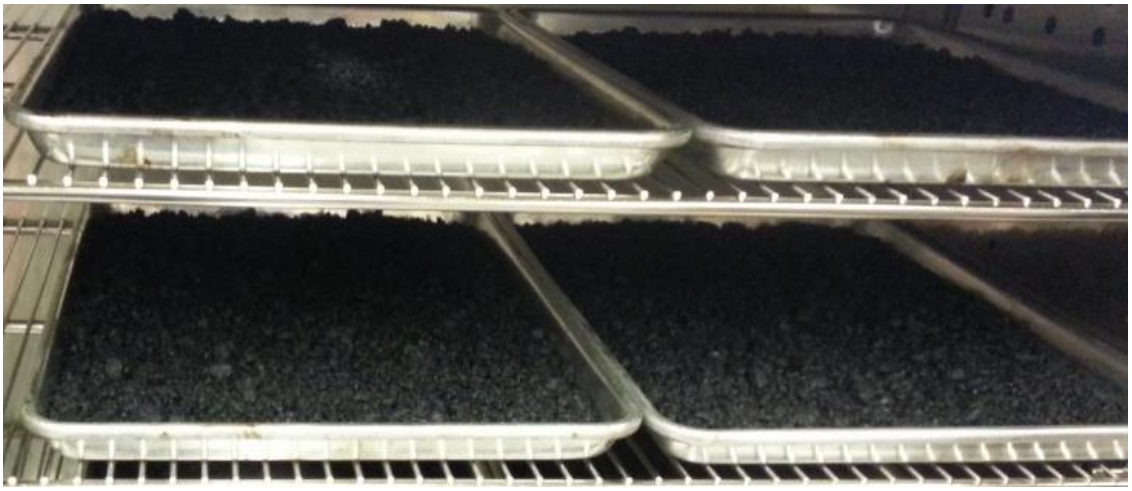

Figure 5. Loose mixture oven aging of asphalt (NC State University, 2015)

Numerous aging protocols for loose asphalt mixtures have been developed and implemented. Braham et al. assessed aging protocols considering both mixture and binder physical properties, which are thought to correlate with various pavement cracking types. Their study subjected the asphalt mixture to 135°C and assessed the impact of aging on fracture energy via the disk-shaped compact tension test (DCT). The research indicated that 24 hours at 135°C was conservative, suggesting the need for distinct aging protocols for modified and unmodified binders.

In a separate investigation by Reinke et al., loose mixtures from MnROAD underwent conditioning at 135°C for durations of 12 and 24 hours. The NCHRP 09-54 study examined loose asphalt mixture aging across temperatures ranging from 70°C to 135°C. Findings revealed a notable shift in the relationship between binder rheology and chemistry as

temperatures increased from 95°C to 135°C. Moreover, reduced fatigue resistance was observed in mixtures aged at 95°C.

Elwardany et al. conducted a study aiming to establish laboratory aging procedures simulating long-term aging for mechanical testing. Aging was conducted using the pressure aging vessel (PAV) on loose asphalt mixture and compacted specimens, ensuring specimen integrity, efficiency, practicality, and versatility.

Two remedial approaches were explored: applying pressure to aid oxygen diffusion and diminish oxidation gradients and utilizing smaller specimens (38mm in diameter by 100mm in height) to reduce diffusion path and self-weight-induced slump. The study concluded that pressure releases compromised specimen integrity despite accelerating the oxidation process. Compaction efforts for long-term aged loose asphalt mixture remained quite similar to short-term aged mixture without adjustments to compaction temperature. A temperature of 95°C exhibited the most promising condition for mechanical testing.

Figure 6. Pressure Aging Vessel (PAV), (Elwardany et., al, 2016)

Some research endeavors have centered on delineating the non-uniform aging of asphalt mixtures in real-world conditions via laboratory assessments (Fan Yin et al.). The absence

of uniformity in air voids and temperature distribution signifies that pavement surfaces age at a quicker rate than their subsurface. In this specific study, field cores were procured from four diverse locations, each with varying in-service durations. These cores underwent non-destructive evaluation using the Viscoelastic Characterization Direct Tension Test (VEC-DT), followed by extraction and recovery of binders for testing using the Dynamic Shear Rheometer (DSR) and Fourier Transform Infrared Spectroscopy (FTIR). Findings from these tests revealed that surface binders exhibited high maximum complex modulus, GRP, and carbonyl area (CA).

Chapter 3. Materials Selection and Procurement

A total of eleven dense-graded SM mixtures were selected from BMD and non-BMD projects. Aggregates, binders additives and RAP were procured and laboratory-mixed, laboratory compacted (LMLC) specimens were prepared for testing.

In addition, plant-mixed, laboratory compacted (PMLC) specimens were tested to investigate the link between design and production. Asphalt mixtures were selected in a way that covers a range of cracking potential based on CT results. The asphalt mixtures were obtained from across the state of Virginia to capture differences in aggregates mineralogy and asphalt binder source. Table 4 represents the various asphalt mixtures that were sampled for this study. Note that the typical PG for the state of Virginia is PG 64-22 but that was not the only PG used in all mixtures.

Table 4. Selected Asphalt Mixtures

Mixture ID	VDOT ID	Mixture Type	Design Type	Contractor	Plant	Sample Date	Binder PG
M0	22-1010	–	–	Boxley	Salem	04/12/2022	-
M1	22-1015	SM_12.5D	BMD	Lee-Hy Paving	Mountcastle	05/19/2022	58-28
M2	22-1025	SM-9.5D	BMD	Adams	Rockydale	06/28/2022	64S-22
M3	22-1030	SM-9.5D	BMD	Allan Myers	Leesburg	06/30/2022	64S-22
M4	22-1035	SM-9.5D	BMD	JC Joyce	Martinsville	07/11/2022	64S-22
M5	22-1036	SM-12.5A	BMD	SL Williamson	Shadwell	07/08/2022	64S-22
M6	22-1038	SM-9.5D	BMD	Boxley	Lynchburg	07/12/2022	64S-22
M7	22-1039	SM-12.5A	BMD	Superior Paving	Stafford	07/29/2022	64S-22
M8	22-1043	SM-9.5D	Superpave	Bransome	Chesterfield	07/21/2022	58-28
M9	22-1059	SM-12.5D	Superpave	Lee-Hy Paving	Rockville	08/05/2022	64S-22
M10	22-1076	SM-9.5A P+VO	BMD	Superior Paving	Leesburg	08/23/2022	64S-22 +RA

Other mixtures characteristics such as RAP percentages, total asphalt binder content as well as additives are given in the JMF and are shown in Table 5. An asphalt JMF is a detailed recipe that outlines various properties of the mixture such as aggregate gradation, binder content, additives, modifiers and much more. The JMF is crucial to ensure that the desired performance is achieved in terms of durability, flexibility, resistance of several factors such as traffic and climate.

Table 5. JMF Information for Samples Asphalt Mixtures

Mixture ID	RAP (%)	Total Binder Content (%)	Reclaimed Binder Ratio (RBR)	Additive	Additives (%)	Rut Depth Average (mm)	CT index
M0	na	na	na	na	na	na	na
M1	30	6.1	na	Zycotherm	0.30	na	na
M2	30	5.9	na	Ad-here 62-40	na	na	150
M3	30	5.6	na	Zycotherm SP2	0.04	na	na
M4	26	6.1	19.3	Ad-here LOF 6500	0.50	3.0	103
M5	30	5.7	na	Zycotherm	0.03	na	na
M6	26	5.9	21.4	Evotherm J1	0.30	na	92
M7	30	5.3	27.4	Zycotherm	0.05	na	na
M8	30	5.7	na	PC 2550	0.03	na	na
M9	30	5.8	na	Zycotherm	0.03	na	na
M10	40	5.5	na	Evotherm J1	0.30	na	na

Na: not available

The RBR data is missing the remaining mixture data since it has not been tested and the RAP properties are not known yet. All the mixtures summarized in Table 5 were received by UNR during the summer of 2022. Upon receival, each mixture was checked for inventory and stored in a specific location safe from the elements to prevent contamination and aging. Each mixture received had 26 cardboard boxes of plant mixed material, 40 buckets of aggregates including RAP and 6 buckets of binder. Figure 7 shows an example of how the pallets were received.

Figure 7. Received Pallets at UNR campus.

Additionally, each JMF had a value for void in total mixture (VTM) and for theoretical maximum specific gravity (Gmm). Table 6 shows the different JMF VTM and Gmm values. This information was used to verify the asphalt mixtures specifications.

Table 6. JMF VTM and Gmm - All mixtures

Mixture ID	VTM (%)	Gmm
M0	–	–
M1	3.5	2.436
M2	3.5	2.612
M3	4.0	2.668
M4	3.4	2.580
M5	4.2	2.600
M6	3.5	2.577
M7	3.6	2.671
M8	4.0	2.507
M9	3.1	2.448
M10	3.2	2.673

Chapter 4. Conditioning and Reheating Protocols

4.1. Reheating Protocols

4.1.1. Laboratory Mixed, Laboratory Compacted

Conditioning and reheating protocols were set for both laboratory-mixed, laboratory-compacted mixtures and for plant-mixed, laboratory-mixed mixtures. These protocols are set to ensure consistency and repeatability in the overall process. The following steps were followed for the reheating of laboratory mixed, laboratory compacted specimens:

- Loose Samples were mixed in the laboratory.
- The mixture is heated in a metal pan with a uniform thickness of 2 ± 0.5 inches in a preheated oven. Note that the timing starts when the sample is placed in the oven.
- The mixture is stirred every 60 ± 5 minutes to maintain uniform conditioning.
- The compaction stars if the internal temperature of the mixture has reached the desired compaction temperature, if not the mixture is kept in the oven and monitored every 15 minutes and then compacted when the temperature reaches the desired compaction temperature.

Figure 8 represents the conditioning and reheating protocol for laboratory-mixed, laboratory-compacted mixtures.

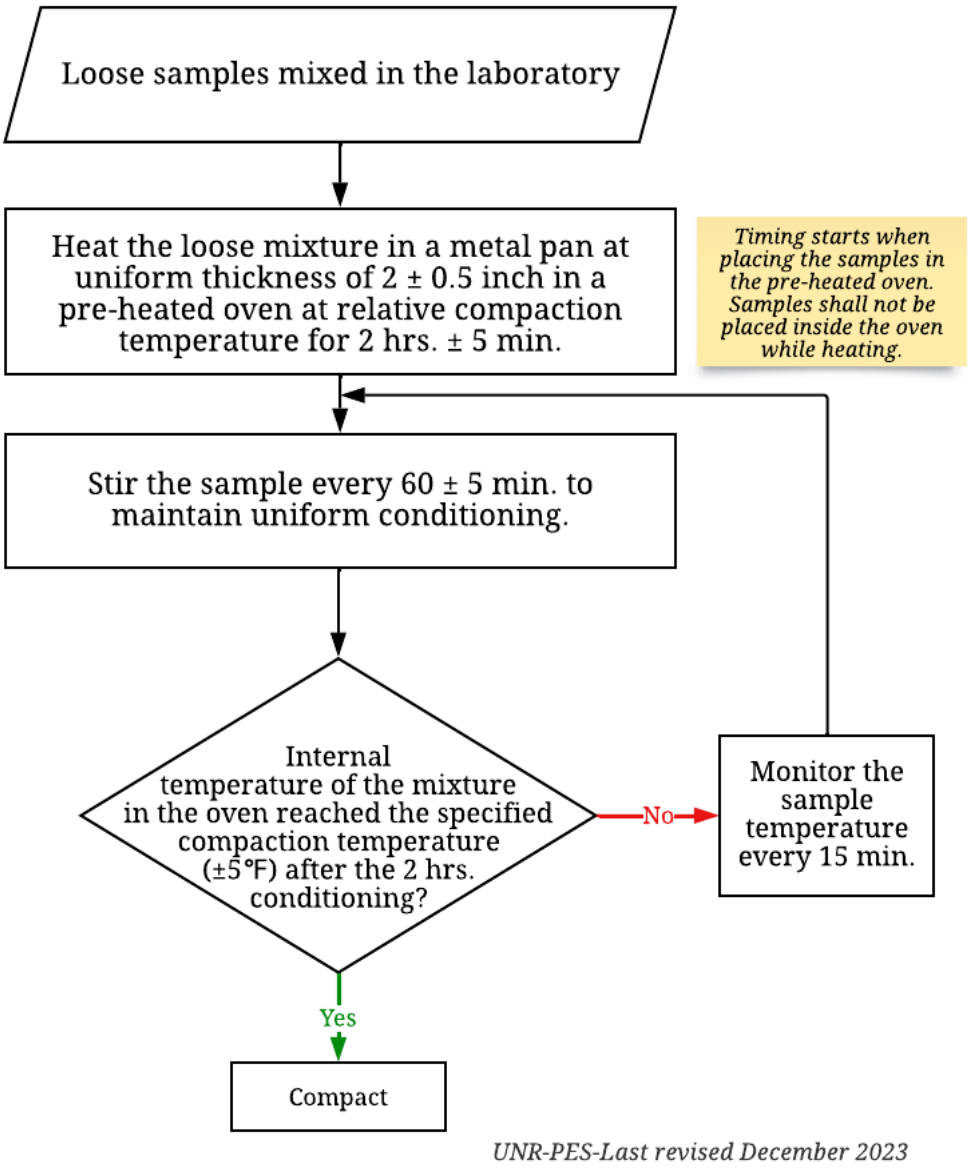

Figure 8. LMLC Reheating Protocol

4.1.2. Plant Mixed, Laboratory Compacted

Similar protocols were established for the plant/field mixed, laboratory compacted samples shown in Figure 9. Eight steps were followed for the conditioning of the RPMLC mixtures:

- First, the loose mixtures are obtained in cardboard boxes cooled to room temperature for at least 24 hours.
- The boxes are heated for 1.5 hours at the compaction temperature. Timing starts when the oven reaches the desired temperature.
- The samples are then transferred to large metal pans while being mixed thoroughly.
- The metal pans are heated in the oven for 1 hour at compaction temperature for further splitting.
- The samples are split into the required sample weight as per AASHTO R 47.
- The samples are then placed in metal pans with a uniform thickness of 2 ± 0.5 inches and placed in the oven at compaction temperature.
- The samples are stirred every 30 ± 5 minutes to maintain uniform conditioning.
- The compaction starts if the compaction temperature is reached ± 5°F, if not the sample is kept in the oven till it reaches the desired temperature while being monitored every 15 minutes.

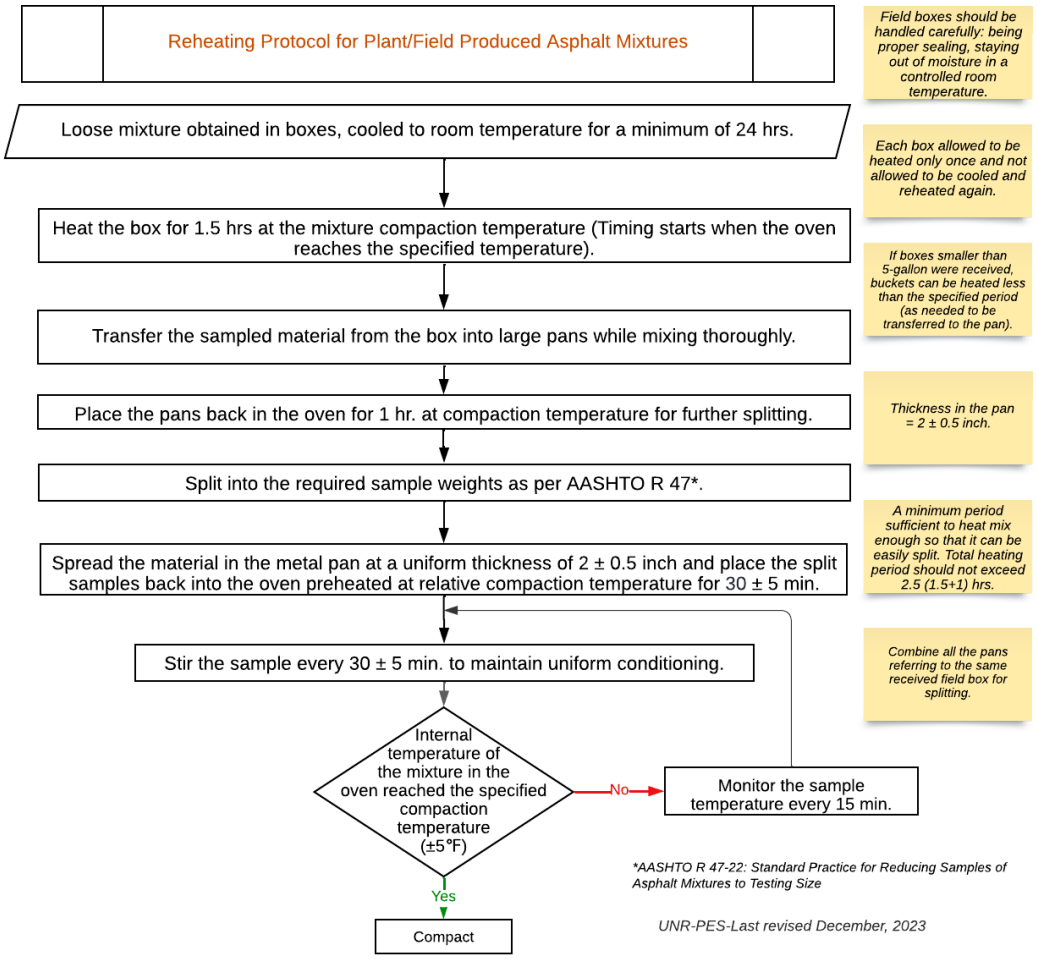

Figure 9. PMLC Reheating Protocol

4.2. RAP Quartering Procedure

Specifications for asphalt mixtures require samples for material testing, therefore it is imperative to reduce large samples to a convenient representative size of the material. Quartering of asphalt mixtures is typically done to ensure representative samples for testing various properties like gradation, density, moisture content and other characteristics. The adopted quartering procedure is summarized in Figure 10 and is in accordance with AASHTO R 47.

These steps include:

- Place RAP in metal tray and dry in the oven overnight at 140°F
- Place RAP on clean metal surface
- Mix and shape into a cone
- Trim the top of the cone
- Split cone into 4 identical sections
- Mix opposite parts to obtain two smaller cones
- Split each small cone into 4 identical sections and collect material from opposite sides of each cone
- Weigh sample according to desired weight.

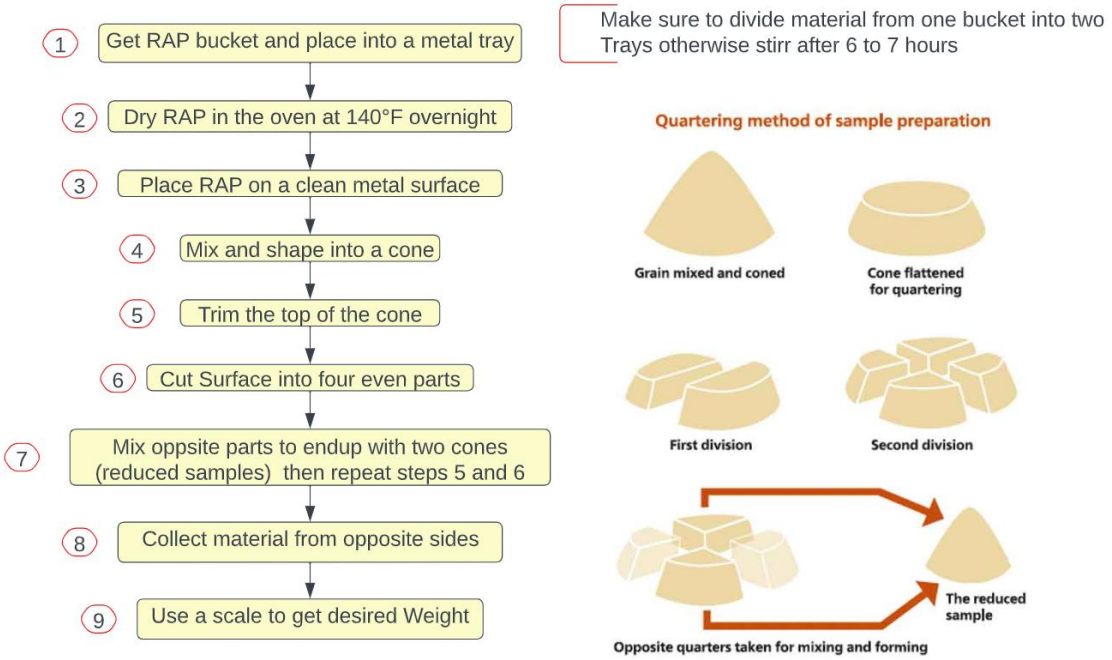

Figure 10. Quartering Procedure

Chapter 5. Results

5.1. Mix Design Verification

All plant mixed material and three RAP mixtures were evaluated to determine the binder content as well as the gradation and specific gravity. The extraction and recovery of the binder was performed as per AASHTO T 164-22 (A). In this method, the binder is extracted using n-propyl bromide through a centrifuge machine and recovered using the rotary evaporator machine (Figure 11). The sieve analysis to determine the aggregate gradation was performed following AASHTO T 30, this procedure involves washing the aggregates and drying them overnight then sieving the dried material.

Figure 11. Centrifuge Extractor (left) and Rotary Evaporator (right)

Two replicates were extracted and recovered from PMLC and RAP to ensure high repeatability. The results of each mixture were compared with the JMF to check the limits as well as Standard deviation (1s) and the range (d2s). For sieve analysis the two extracted replicates were used to get the gradation of each mixture. (1s) and (d2s) limits were multi

laboratory limits from AASHTO T 164-22 (A) for asphalt binder content and form AASHTO T 30 for sieve analysis.

The apparatus used in these tests were:

1. For Extraction and Recovery:

   Oven, Pan, Balance, Beakers, Extraction Bow, Filter, Rings, Rotary Evaporator machine, Centrifugal machine capable of 3600 R/min, Fuming hood, Gloves, masks and protective glasses, n-Propyl Bromide conforming to ASTM D6368.

2. For Sieve Analysis:

   Balance, Sieves conforming to ASTM E11, Mechanical Sieve Shaker, Oven, Wetting Agent, Container, Spoon or mixing utensil, mechanical washing equipment.

Tables 7 to 16 represent the various recovered asphalt binder contents and gradation as well as the JMF limits and Figures 12 and 13 show the gradation and binder contents for all the mixtures respectively.

Table 7. Binder Percentage and Gradation of M1 Plant Mixture

Property	**AASHTO T 164-22 (A)**					**JMF**			**Check**
	Rep 1	**Rep 2**	**1s (≤ 0.30%)**	**d2s (≤ 0.85%)**	**Average**	**Value**	**Min**	**Max**	**Pass/Fail**
Recovered Binder Content	5.93%	6.06%	0.09%	0.13%	6.00%	6.10%	5.89%	6.31%	Pass
Percent Passing	**AASHTO T 30**					**JMF**			**Check**
Sieve Size	**Rep 1**	**Rep 2**	**1s**	**d2s**	**Average**	**Value**	**Min**	**Max**	**Pass/Fail**
3/4 inch	100.0%	100.0%	0%	0%	100.0%	100.0%	100.0%	100.0%	Pass
1/2 inch	95.8%	95.5%	0.21%	0.30%	95.7%	96.0%	93.2%	98.8%	Pass
3/8 inch	87.8%	87.1%	0.49%	0.70%	87.5%	85.0%	82.2%	87.8%	Pass
No. 4	-	-	-	-	-	-	-	-	Pass
No. 8	38.8%	38.0%	0.57%	0.80%	38.4%	36.0%	33.2%	38.8%	Pass
No. 200	4.3%	4.4%	0.07%	0.10%	4.4%	4.7%	4.0%	5.4%	Pass

Table 8. Binder Percentage and Gradation of M2 Plant Mixture

Property	AASHTO T 164-22 (A)					JMF			Check
	Rep 1	Rep 2	1s (≤ 0.30%)	d2s (≤ 0.85%)	Average	Value	Min	Max	Pass/Fail
Recovered Binder Content	5.82%	5.89%	0.05%	0.07%	5.86%	5.90%	5.69%	6.11%	Pass
Percent Passing	**AASHTO T 30**					**JMF**			**Check**
Sieve Size	**Rep 1**	**Rep 2**	**1s**	**d2s**	**Average**	**Value**	**Min**	**Max**	**Pass/Fail**
3/4 inch	-	-	-	-	-	-	-	-	Pass
1/2 inch	100.0%	100.0%	0.00%	0.00%	100.0%	100.0%	99.0%	100.0%	Pass
3/8 inch	95.6%	95.2%	0.25%	0.36%	95.4%	96.0%	93.2%	98.8%	Pass
No. 4	61.3%	60.9%	0.33%	0.47%	61.1%	59.0%	56.2%	61.8%	Pass
No. 8	39.3%	38.7%	0.46%	0.66%	39.0%	41.0%	38.2%	43.8%	Pass
No. 200	5.4%	5.2%	0.08%	0.12%	5.3%	6.0%	5.3%	6.7%	Pass

Table 9. Binder Percentage and Gradation of M3 Plant Mixture

Property	AASHTO T 164-22 (A)					JMF			Check
	Rep 1	Rep 2	1s (≤ 0.30%)	d2s (≤ 0.85%)	Average	Value	Min	Max	Pass/Fail
Recovered Binder Content	5.51%	5.56%	0.04%	0.05%	5.54%	5.60%	5.39%	5.81%	Pass
Percent Passing	**AASHTO T 30**					**JMF**			**Check**
Sieve Size	**Rep 1**	**Rep 2**	**1s**	**d2s**	**Average**	**Value**	**Min**	**Max**	**Pass/Fail**
3/4 inch	-	-	-	-	-	-	-	-	Pass
1/2 inch	100.0%	100.0%	0.00%	0.00%	100.0%	100.0%	99.0%	100.0%	Pass
3/8 inch	94.9%	94.0%	0.64%	0.90%	94.5%	93.0%	90.2%	95.8%	Pass
No. 4	55.9%	54.8%	0.78%	1.10%	55.4%	54.0%	51.2%	56.8%	Pass
No. 8	41.5%	40.1%	0.99%	1.40%	40.8%	39.0%	36.2%	41.8%	Pass
No. 200	4.9%	4.8%	0.07%	0.10%	4.9%	5.5%	4.8%	6.2%	Pass

Table 10. Binder Percentage and Gradation of M4 Plant Mixture

Property	AASHTO T 164-22 (A)					JMF			Check
	Rep 1	Rep 2	1s (≤ 0.30%)	d2s (≤ 0.85%)	Average	Value	Min	Max	Pass/Fail
Recovered Binder Content	6.06%	6.04%	0.01%	0.02%	6.05%	6.10%	5.89%	6.31%	Pass
Percent Passing	**AASHTO T 30**					**JMF**			**Check**
Sieve Size	**Rep 1**	**Rep 2**	**1s**	**d2s**	**Average**	**Value**	**Min**	**Max**	**Pass/Fail**
3/4 inch	-	-	-	-	-	-	-	-	Pass
1/2 inch	100.0%	100.0%	0.00%	0.00%	100.0%	100.0%	99.0%	100.0%	Pass
3/8 inch	97.4%	97.4%	0.00%	0.00%	97.4%	95.0%	92.2%	97.8%	Pass
No. 4	67.5%	67.4%	0.07%	0.10%	67.5%	66.0%	63.2%	68.8%	Pass
No. 8	40.3%	40.9%	0.42%	0.60%	40.6%	43.0%	40.2%	45.8%	Pass
No. 200	5.0%	4.9%	0.07%	0.10%	5.0%	4.7%	4.0%	5.4%	Pass

Table 11. Binder Percentage and Gradation of M5 Plant Mixture

Property	AASHTO T 164-22 (A)					JMF			Check
	Rep 1	Rep 2	1s (≤ 0.30%)	d2s (≤ 0.85%)	Average	Value	Min	Max	Pass/Fail
Recovered Binder Content	5.52%	5.61%	0.06%	0.09%	5.57%	5.70%	5.49%	5.91%	Pass
Percent Passing	**AASHTO T 30**					**JMF**			**Check**
Sieve Size	**Rep 1**	**Rep 2**	**1s**	**d2s**	**Average**	**Value**	**Min**	**Max**	**Pass/Fail**
3/4 inch	100.0%	100.0%	0%	0%	100.0%	100.0%	100.0%	100.0%	Pass
1/2 inch	97.8%	98.1%	0.21%	0.30%	98.0%	97.0%	94.2%	99.8%	Pass
3/8 inch	86.3%	86.5%	0.14%	0.20%	86.4%	85.0%	82.2%	87.8%	Pass
No. 4	-	-	-	-	-	-	-	-	Pass
No. 8	40.6%	40.7%	0.07%	0.10%	40.7%	39.0%	36.2%	41.8%	Pass
No. 200	6.6%	6.6%	0.00%	0.00%	6.6%	5.9%	5.2%	6.6%	Pass

Table 12. Binder Percentage and Gradation of M6 Plant Mixture

Property	AASHTO T 164-22 (A)					JMF			Check
	Rep 1	Rep 2	1s (≤ 0.30%)	d2s (≤ 0.85%)	Average	Value	Min	Max	Pass/Fail
Recovered Binder Content	6.03%	5.91%	0.08%	0.12%	5.97%	5.90%	5.69%	6.11%	Pass
Percent Passing	**AASHTO T 30**					**JMF**			**Check**
Sieve Size	**Rep 1**	**Rep 2**	**1s**	**d2s**	**Average**	**Value**	**Min**	**Max**	**Pass/Fail**
3/4 inch	-	-	-	-	-	-	-	-	Pass
1/2 inch	100.0%	100.0%	0.00%	0.00%	100.0%	100.0%	99.0%	100.0%	Pass
3/8 inch	95.4%	95.4%	0.00%	0.00%	95.4%	94.0%	91.2%	96.8%	Pass
No. 4	61.5%	61.4%	0.07%	0.10%	61.5%	62.0%	59.2%	64.8%	Pass
No. 8	42.2%	42.1%	0.07%	0.10%	42.2%	42.0%	39.2%	44.8%	Pass
No. 200	7.0%	6.5%	0.35%	0.50%	6.8%	6.5%	5.8%	7.2%	Pass

Table 13. Binder Percentage and Gradation of M7 Plant Mixture

Property	AASHTO T 164-22 (A)					JMF			Check
	Rep 1	Rep 2	1s (≤ 0.30%)	d2s (≤ 0.85%)	Average	Value	Min	Max	Pass/Fail
Recovered Binder Content	5.41%	5.40%	0.01%	0.01%	5.41%	5.30%	5.09%	5.51%	Pass
Percent Passing	**AASHTO T 30**					**JMF**			**Check**
Sieve Size	**Rep 1**	**Rep 2**	**1s**	**d2s**	**Average**	**Value**	**Min**	**Max**	**Pass/Fail**
3/4 inch	100.0%	100.0%	0%	0%	100.0%	100.0%	100.0%	100.0%	Pass
1/2 inch	98.5%	98.5%	0.00%	0.00%	98.5%	97.0%	94.2%	99.8%	Pass
3/8 inch	90.2%	89.9%	0.21%	0.30%	90.1%	88.0%	85.2%	90.8%	Pass
No. 4	-	-	-	-	-	-	-	-	Pass
No. 8	44.2%	42.6%	1.13%	1.60%	43.4%	42.0%	39.2%	44.8%	Pass
No. 200	5.4%	5.3%	0.07%	0.10%	5.4%	5.5%	4.8%	6.2%	Pass

Table 14. Binder Percentage and Gradation of M8 Plant Mixture

Property	AASHTO T 164-22 (A)					JMF			Check
	Rep 1	Rep 2	1s (≤ 0.30%)	d2s (≤ 0.85%)	Average	Value	Min	Max	Pass/Fail
Recovered Binder Content	5.83%	5.75%	0.06%	0.08%	5.79%	5.70%	5.49%	5.91%	Pass
Percent Passing	**AASHTO T 30**					**JMF**			**Check**
Sieve Size	**Rep 1**	**Rep 2**	**1s**	**d2s**	**Average**	**Value**	**Min**	**Max**	**Pass/Fail**
1/2 inch	99.6%	99.8%	0%	0%	99.7%	100.0%	99.0%	100.0%	Pass
3/8 inch	94.3%	94.2%	0.07%	0.10%	94.3%	94.0%	91.2%	96.8%	Pass
No. 4	67.0%	67.1%	0.07%	0.10%	67.1%	66.0%	63.2%	68.8%	Pass
No. 8	45.6%	45.9%	0.21%	0.30%	45.8%	45.0%	42.2%	47.8%	Pass
No. 30	24.9%	24.7%	0.14%	0.20%	24.8%	23.0%	20.9%	25.1%	Pass
No. 200	4.8%	5.1%	0.21%	0.30%	5.0%	5.5%	4.8%	6.2%	Pass

Table 15. Binder Percentage and Gradation of M9 Plant Mixture

Property	AASHTO T 164-22 (A)					JMF			Check
	Rep 1	Rep 2	1s (≤ 0.30%)	d2s (≤ 0.85%)	Average	Value	Min	Max	Pass/Fail
Recovered Binder Content	5.79%	5.69%	0.07%	0.10%	5.74%	5.80%	5.59%	6.01%	Pass
Percent Passing	**AASHTO T 30**					**JMF**			**Check**
Sieve Size	**Rep 1**	**Rep 2**	**1s**	**d2s**	**Average**	**Value**	**Min**	**Max**	**Pass/Fail**
3/4 inch	100.0%	100.0%	0%	0.00%	100.0%	100.0%	100.0%	100.0%	Pass
1/2 inch	96.8%	97.0%	0%	0.20%	96.9%	96.0%	93.2%	98.8%	Pass
3/8 inch	88.9%	89.0%	0.07%	0.10%	89.0%	88.0%	85.2%	90.8%	Pass
No. 4	62.1%	61.3%	0.57%	0.80%	61.7%	61.0%	58.2%	63.8%	Pass
No. 8	45.6%	44.5%	0.78%	1.10%	45.1%	44.0%	41.2%	46.8%	Pass
No. 30	25.1%	23.7%	0.99%	1.40%	24.4%	22.0%	19.9%	24.1%	Fail
No. 200	5.1%	5.0%	0.07%	0.10%	5.1%	5.0%	4.3%	5.7%	Pass

Table 16. Binder Percentage and Gradation of M10 Plant Mixture

Property	AASHTO T 164-22 (A)					JMF			Check
	Rep 1	Rep 2	1s (≤ 0.30%)	d2s (≤ 0.85%)	Average	Value	Min	Max	Pass/Fail
Recovered Binder Content	5.31%	5.37%	0.04%	0.06%	5.34%	5.50%	5.29%	5.71%	Pass
Percent Passing	**AASHTO T 30**					**JMF**			**Check**
Sieve Size	**Rep 1**	**Rep 2**	**1s**	**d2s**	**Average**	**Value**	**Min**	**Max**	**Pass/Fail**
1/2 inch	100.0%	99.8%	0%	0.20%	99.9%	100.0%	99.0%	100.0%	Pass
3/8 inch	94.9%	93.3%	1.13%	1.60%	94.1%	94.0%	91.2%	96.8%	Pass
No. 4	66.2%	65.9%	0.21%	0.30%	66.1%	65.0%	62.2%	67.8%	Pass
No. 8	46.0%	46.2%	0.14%	0.20%	46.1%	44.0%	41.2%	46.8%	Pass
No. 200	5.8%	5.6%	0.14%	0.20%	5.7%	6.2%	5.5%	6.9%	Pass

Passing the criteria means that the obtained test value falls within the JMF limits and falls within the single laboratory and multi laboratory standard deviation and range for the two replicates. In summary, all mixtures cleared the JMF assessment, indicating a successful replication of the mixtures in the laboratory with some exceptions.

Gradations show that all the mixtures are fine graded as shown in the JMFs and the binder content ranged from 5.3 to 6.1.

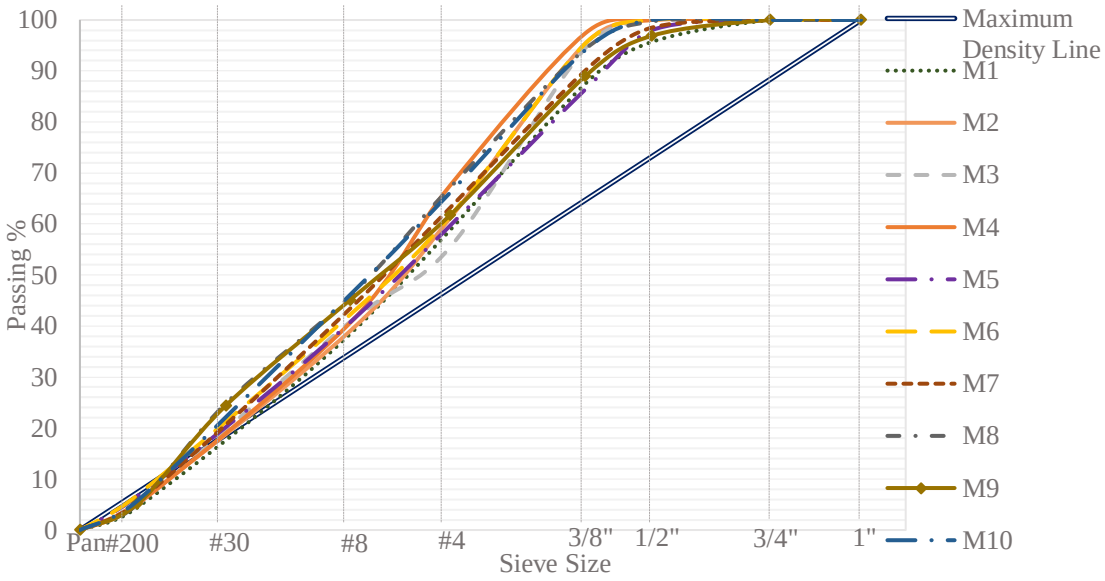

Figure 12. Gradations - All mixtures

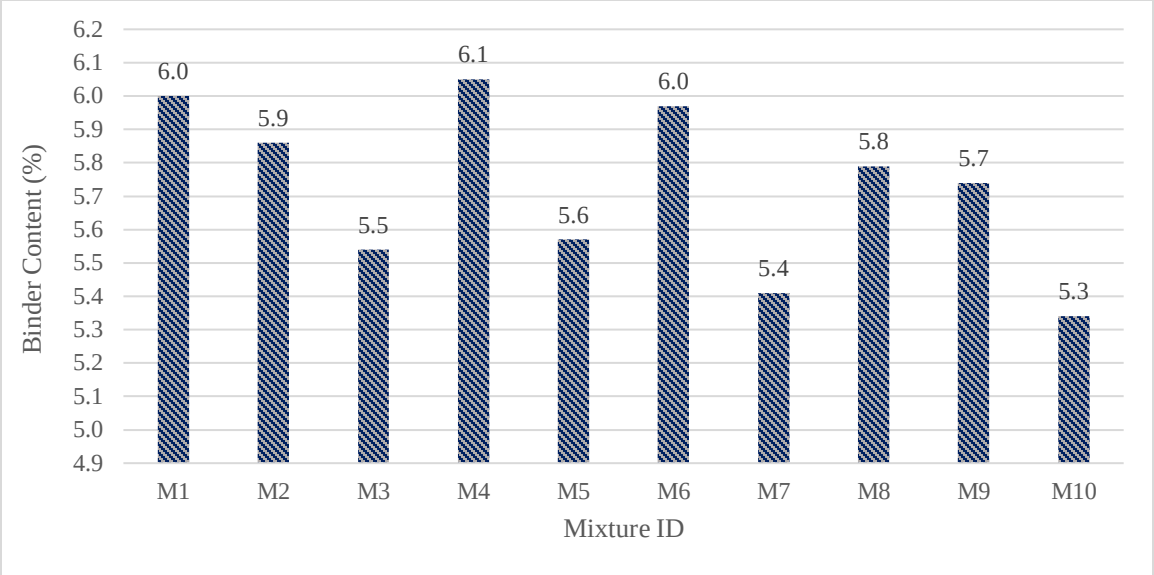

Figure 13. Binder Contents - All mixtures

5.1.1. RAP

In order to replicate the JMF mixtures accurately in the laboratory, a comprehensive knowledge of all mixture parameters was required, including the gradations and binder contents of the RAP utilized in each mixture. The RAP associated with each of the three mixtures underwent division and sampling, followed by extraction and recovery using AASHTO T 164-22 (A) and ASTM D5404 methodologies. These processes were employed to ascertain the binder percentage, gradation, as well as the specific gravity of coarse and fine aggregates. Three mixtures (M4, M6 and M7) were chosen to be investigated because they offer a variety of binder contents, gradations, additives, and cracking performances.

5.1.1.1 RAP Binder Percentage

Four RAP replicates were extracted and recovered for each of the three mixtures, two were used to find the RAP binder percentage as per AASHTO T 164-22 (A) and gradation as per AASHTO T 30 and the other two were used to determine the RAP aggregate specific gravities as per AASHTO T 84 and AASHTO T 85. The RAP binder percentages are summarized in Table 17 where 1s and d2s are the single laboratory precision and bias limits for Standard deviation and range respectively. The same apparatus used in mix design verification for extraction and recovery as well as sieve analysis was used to determine RAP properties.

Table 17. RAP Binder Percentage LMLC

Sample ID	M4(1)	M4(2)	M6(1)	M6(2)	M7(1)	M7(2)
% Binder by TWM	**4.40**	**4.64**	**5.01**	**4.70**	**4.82**	**4.85**
% Binder by DWA	4.60	4.86	5.27	4.94	5.07	5.09
AVERAGE	**4.52**		**4.85**		**4.83**	
1s (max 0.30)	0.17		0.21		0.02	
d2s (max 0.85)	0.24		0.30		0.02	

5.1.1.2. RAP Gradation

Following extraction and reclamation, the aggregates undergo drying and washing procedures following the guidelines outlined in AASHTO T 11. Subsequently, the aggregates are oven dried. The initial and post-washing weights of the aggregates are measured, after which the materials are sieved to determine their gradation. Table 18 presents the summarized gradations for the RAP of each of the three mixtures.

Table 18. RAP Gradation LMLC

	M4			M6			M7		
	Sample 1	**Sample2**	**AVERAGE**	**Sample 1**	**Sample2**	**AVERAGE**	**Sample 1**	**Sample2**	**AVERAGE**
3/4"							100.0%	100.0%	**100.0%**
1/2"	100%	100%	**100.0%**	100.0%	100.0%	**100.0%**	99.8%	100.0%	**99.9%**
3/8"	93.7%	93.6%	**93.7%**	97.4%	97.6%	**97.5%**	96.2%	96.8%	**96.5%**
#4	67.2%	67.0%	**67.1%**	74.0%	71.8%	**72.9%**			
#8	24.5%	23.6%	**24.1%**	58.3%	54.7%	**56.5%**	59.9%	63.2%	**61.5%**
#200	6.13%	5.42%	**5.8%**	6.82%	6.05%	**6.4%**	6.07%	6.16%	**6.1%**

5.1.1.3 RAP aggregate Fine and Coarse Specific Gravity

The aggregates reclaimed from the RAP are categorized into fine aggregates, passing through the #4 sieve, and coarse aggregates, consisting of everything retained on the #4 sieve and larger. To determine the fine aggregate specific gravity, the aggregates are soaked in at least 6% of their weight in water overnight, following the testing protocol outlined in AASHTO T 84. Conversely, for the coarse aggregates, they undergo submersion underwater overnight and are then tested in accordance with AASHTO T 85.

<u>The apparatus used in coarse and fine specific gravities is the following:</u>

1. For Coarse Specific Gravity:

   Balance, Sample Container, Water Tank, Sieves, Oven, Thermometer.

2. For Fine Specific Gravity:

   Balance, Pycnometer, Mold, Tamper, Oven, Thermometer.

Tables 19 and 20 present the results for fine and coarse aggregate specific gravity, respectively. 1s and d2s are the standard deviation and range for a single-operator precision.

Table 19. RAP fine Aggregate Specific Gravity

Sample ID	M4(1)	M4(2)	M6(1)	M6(2)	M7(1)	M7(2)
Specific Gravity Bulk (DRY)	2.749	2.759	2.671	2.664	2.868	2.855
Average Bulk Dry	2.754		2.667		2.861	
Specific Gravity Bulk (SSD)	2.770	2.777	2.691	2.681	2.891	2.872
Apparent Specific Gravity	2.808	2.811	2.725	2.708	2.937	2.906
Absorption	0.763	0.681	0.748	0.609	0.825	0.616
(1s) max 0.009	0.007		0.005		0.009	
(d2s) max 0.025	0.010		0.006		0.013	

Table 20. RAP Coarse Aggregate Specific Gravity

Sample ID	M4(1)	M42)	M6(1)	M6(2)	M7(1)	M7(2)
Specific Gravity Bulk (DRY)	2.622	2.638	2.499	2.492	2.651	2.639
Average Bulk Dry	2.630		2.495		2.645	
Specific Gravity Bulk (SSD)	2.666	2.685	2.560	2.555	2.723	2.710
Apparent Specific Gravity	2.742	2.768	2.661	2.662	2.857	2.841
Absorption	1.664	1.788	2.434	2.564	2.714	2.696
(1s) max 0.011	0.011		0.005		0.009	
(d2s) max 0.032	0.016		0.007		0.013	

The specific gravity test outcomes are the bulk specific gravity, the saturated surface dry (SSD) bulk specific gravity, the apparent specific gravity, and the absorption of the aggregates. These parameters help understand the structure and properties of the aggregates used in the mixture and are useful in mixture calculation and volumetrics.

5.2. Long-Term aging at 95°C:

Three LMLC mixtures were chosen to be investigated in detail, M4, M6 and M7. The reason behind choosing these mixtures specifically is because they offer a variety of binder sources, RAP sources, gradations, additives, and cracking performances. The JMF mixing and compaction temperatures for the three mixtures are shown in Table 21.

Table 21. JMF mixing and compaction temperatures for M4, M6, and M7 mixtures

	M4	M6	M7
Mixing Temperature (°C)	176.7	176.7	176.7
Compaction Temperature (°C)	148.9	148.9	143.3

5.2.1. Mixture Testing

5.2.1.1. Theoretical Maximum Specific Gravity Test

The theoretical maximum specific gravity (Gmm) is a parameter used in the mix design process and in the replication of the job mix formula (JMF) mixtures in the laboratory. Gmm of a mixture plays a role in determining air void level of laboratory compacted specimens thus providing target values for compaction of asphalt mixtures therefore it is critical to know the Gmm of each mixture before the start of any laboratory testing. This test was conducted on uncompacted specimens as per AASHTO T 209-22 where a mixture's coated aggregates are separated by hand so that the particles of the fine aggregate portion are not larger than 6.3mm (1/4 in.) then placed underwater in a vacuum machine of 27.5 ± 2.5 mmHg pressure for 15 ± 1 min to remove air trapped. After that the vacuum is released by increasing the pressure at a rate that does not exceed 60 mmHg per second. The weight is measured dry and under water.

The apparatus used in this test is the following:

Vacuum container, Bowl for mass determination in water, Flask for mass determination in air, Pycnometer for mass determination in air, Balance, Vacuum pump, Vacuum measuring device.

Figure 14 shows the loose mixture preparation for Gmm as well as in the vacuum machine.

Figure 14. Loose Mixture for Gmm (left), Loose Mixture in Vacuum machine.

Table 22 shows the different Gmm values for the chosen mixtures.

Table 22. Maximum Theoretical Specific Gravity (Gmm)

Mixture ID	Gmm
M4	2.560
M6	2.575
M7	2.677

The results shown in Table 22 are an average of two samples and shows that the three mixtures have relatively different Gmm values indicating a different air void levels for the same sample weight

5.2.1.2. IDT- CT Test

The IDT-CT test described in ASTM D8225-19 assesses an asphalt mixture's resistance to cracking at intermediate temperatures, notably at 25°C in this research. Specimens are created by compacting the asphalt mixture using a superpave gyratory compactor, forming cylinders with dimensions of 150 ± 2 mm in diameter and 62 ± 1 mm in height (for nominal maximum aggregate size, NMAS of 19 mm or smaller). Prior to testing, these specimens are conditioned at 25°C for two hours. The CT-Index of an asphalt mixture is derived from the failure energy, the post-peak slope of the load-displacement curve, and the deformation at 75% of the peak load. This index serves as an indicator of the mixture's cracking resistance generally, a higher CT-Index value implies better resistance to cracking and, consequently, reduced cracking throughout the pavement's lifespan. VDOT has a limit imposed on the maximum coefficient of variation (COV) for 5 samples and for trimmed data of 3 samples shown in Table 23. This limit serves as a condition to determine whether to trim the IDT-CT data or keep considering the 5 tested replicates.

Table 23. VDOT Max COV limits

Max COV (%) – 5 Replicates	18.3
Max COV (%) – 3 Replicates	11.2

The apparatus used in this test was the following:

Axial loading device, Load cell, loading strips, Internal displacement measuring device, External displacement measuring device, Data acquisition system, Conditioning chamber, Gyratory compactor, Sample measuring device.

Figure 15 depicts both the IDT-CT machine and an IDT-CT sample post-testing.

Figure 15. IDT-CT machine (left), IDT-CT tested sample (right)

Figure 16 represents the IDT-CT formula and curve with all its parameters.

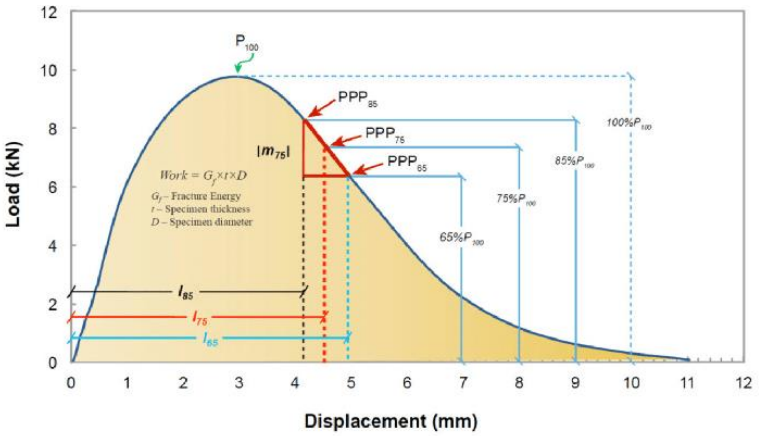

$$CT_{index} = \frac{t}{62} * G_f * \frac{l_{75}}{|m_{75}|} * \frac{1}{D}$$

Figure 16. IDTL-CT Formula and Curve (ASTM D8225-19)

With:

P100: Peak Load (kN)

m75: Post Peak Slope

l75: Displacement at 75% of Peak Load (mm)

Gf: Fracture Energy (Joules/m2)

D: Diameter of the sample (mm)

t: Thickness of the sample (mm)

5.2.1.2.1. PMLC

Five replicates were tested for each aging level to ensure precision and accuracy in the results. The IDT-CT data underwent input into an Excel file for thorough analysis and validation. Parameters like fracture energy (Gf), post-peak slope (m75), peak load (P100), energy to peak load (energy to P100), and deformation at 75% of peak load (l75) were extracted from these Excel files and graphed for visual scrutiny. Table 24 showcases the assorted IDT-CT outcomes for the M6 PMLC blend. It's important to note that the PMLC mixture detailed in this table underwent a single reheating before testing at three distinct long-term aging levels, without any short-term aging.

Table 24. IDTL-CT results – M6 PMLC

Mixture ID	CTindex	Gf (Joules/m^2)	l_{75}/m_{75}	P100 (kN)	Energy to P100 (Joules/m2)
M6[0hrs; 0d]	118.1	11,673	1.5	17.0	3627.3
M6[0hrs; 4d]	43.1	10,342	0.6	21.2	3467.2
M6[0hrs; 6.5d]	38.5	9,264	0.6	19.6	3309.1

*: H is hours of aging at compaction temperature and the D is days of aging at 95°C

The CT-Index fluctuates across durations from 0 days to 6.5 days of LTA at 95°C. A reduced CT-Index signifies decreased resistance to cracking, consistent with the notion that aging diminishes a mixture's ability to resist cracking. Figure 17 shows the varied IDT-CT values for the M6 PMLC across the three LTA durations.

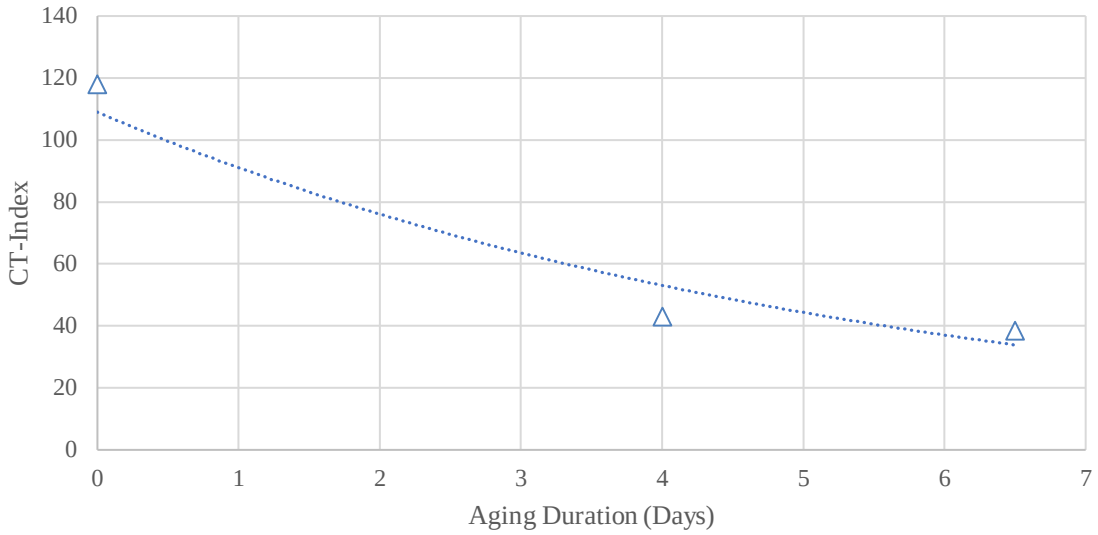

Figure 17. CT-Index vs aging duration - M6 PMLC

The data in Table 24 and Figures 17 present a clear trend in the CT-Index values concerning aging duration at 95°C for the PMLC mixture. Initially, at 0 days of aging, the CT-Index peaks at 118.1, indicating superior resistance to cracking. However, as the aging duration increases, there's a significant decrease in the CT-Index values. For instance, after 4 days of aging, the CT-Index drops to 43.1, and further declines to 38.5 after 6.5 days.

This consistent decline in CT-Index suggests a correlation between increased aging time and decreased resistance to cracking. The oxidation process occurring during aging is a likely cause for this decline. Oxidation tends to make the asphalt binder stiffer and more brittle, making the mixture more susceptible to cracking under stress.

Figures 18, 19, 20 and 21 complement this analysis by showcasing various CT parameters, providing a comprehensive view of how different aging durations impact the mixture's properties. These figures likely detail parameters like stiffness, ductility, and brittleness, further supporting the observed trend in CT-Index with increasing aging duration. Overall, these findings underscore the importance of considering aging duration in evaluating asphalt mixtures for their susceptibility to cracking, particularly in relation to oxidation effects on binder properties.

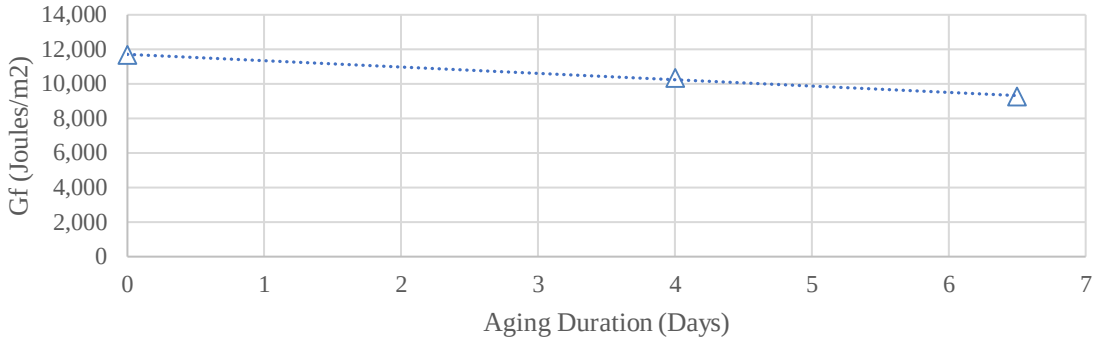

Figure 18. Fracture Energy vs Aging Duration - M6

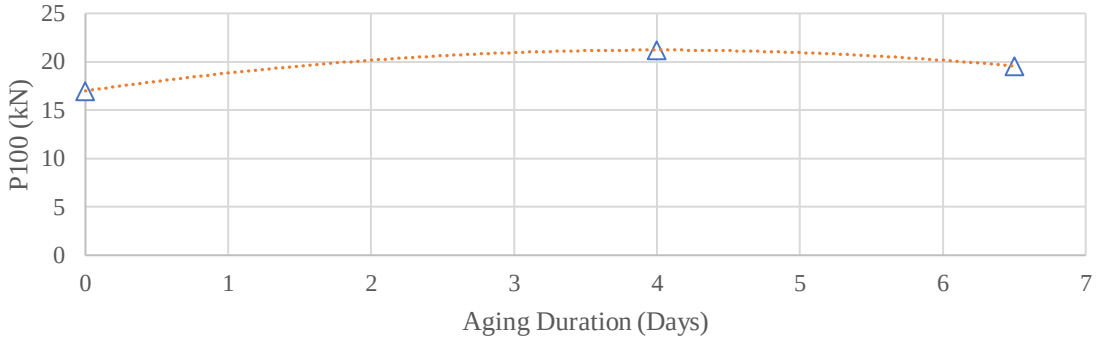

Figure 19. Peak Load vs Aging Duration - M6

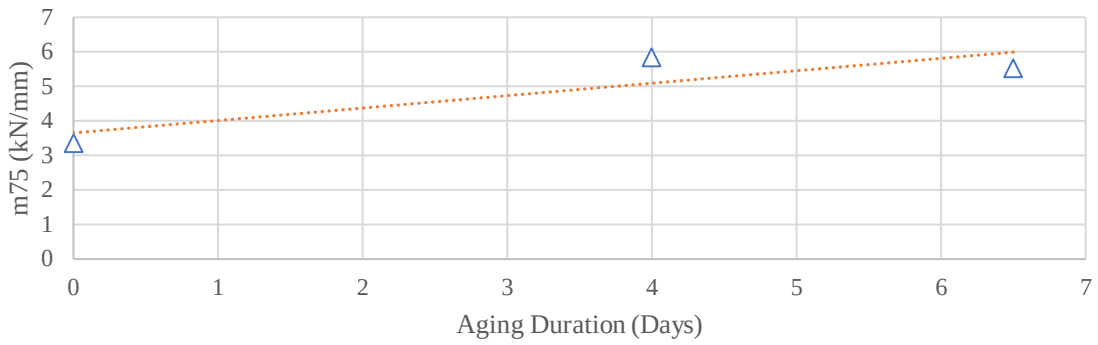

Figure 20. Post Peak Slops vs Aging Duration - M6

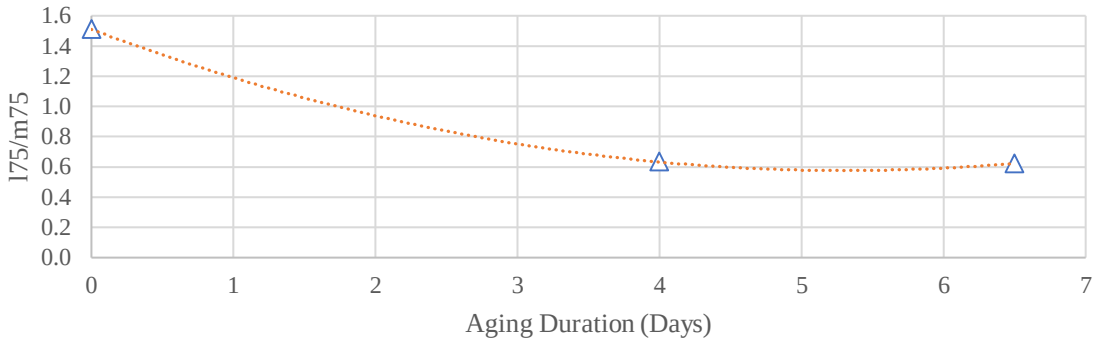

Figure 21. l75/m75 vs Aging Duration - M6

5.2.1.2.2. LMLC

Understanding the properties of the RAP enables the reproduction of mixtures based on the JMF, followed by testing on both the mixture and the binder. Five aging levels were recommended for the laboratory-mixed samples, outlined comprehensively in Table 25

Table 25. Initial Aging Durations and Temperatures LMLC

Short-Term Aging (Hours)	Temperature (°C)	Long Term Aging (Days)	Temperature (°C)
2	Compaction Temperature	0	-
4		0	-
4		1	95
4		2	95
4		4	95

A total of 25 samples (5 samples per aging level) were manufactured and evaluated for each of the three selected LMLC mixtures, maintaining air voids within the range of 7 ± 0.5%. Table 26 provides an overview of the IDT-CT test outcomes for the LMLC mixtures, while Table 27 offers a comparison of the CT-index across various aging stages.

Table 26. IDT_CT LMLC

M4						
Mixture ID*	**CTindex**	**l75/m75**	**Gf (Joules/m2)**	**m75 (kN/mm)**	**P100 (kN)**	**Energy to P100 (Joules/m2)**
M4[2hrs; 0d]	99.6	1.79	8361.7	2.83	13.019	3245.1
M4[4hrs; 0d]	61.9	1.21	7702.6	3.57	14.124	2962.6
M4[4hrs; 1d]	35.1	0.73	7195.6	4.62	16.404	2727.6
M4[4hrs; 2d]	31.2	0.67	6995.8	4.97	16.253	2654.2
M4[4hrs; 4d]	20.2	0.43	7009.0	6.73	18.681	2718.8
M6						
Mixture ID*	**CTindex**	**l75/m75**	**Gf (Joules/m2)**	**m75 (kN/mm)**	**P100 (kN)**	**Energy to P100 (Joules/m2)**
M6[2hrs; 0d]	144.5	2.07	10429.4	2.54	14.640	3279.2
M6[4hrs; 0d]	70.9	1.03	10314.8	4.25	17.552	3538.8
M6[4hrs; 1d]	38.4	0.63	9158.1	5.41	19.628	3087.1
M6[4hrs; 2d]	31.0	0.58	7969.5	5.74	21.164	2963.4
M6[4hrs; 4d]	28.6	0.50	8552.1	6.15	20.859	2840.3
M7						
Mixture ID*	**CTindex**	**l75/m75**	**Gf (Joules/m2)**	**m75 (kN/mm)**	**P100 (kN)**	**Energy to P100 (Joules/m2)**
M7[2hrs; 0d]	101.4	1.50	10139.1	3.11	15.820	3349.3
M7[4hrs; 0d]	75.5	1.13	10113.0	3.91	17.428	3508.6
M7[4hrs; 1d]	72.9	1.12	9769.0	3.84	16.831	3405.3
M7[4hrs; 2d]	65.4	0.99	9956.5	4.08	18.357	3545.4
M7[4hrs; 4d]	46.6	0.72	9644.1	5.11	19.611	3347.4

*: H is hours of aging at compaction temperature and the D is days of aging at 95℃

Table 27. IDT- CT comparison at each aging level - LMLC

	CTindex		
Mixture ID	**M4**	**M6**	**M7**
M4[2hrs; 0d]	99.6	144.5	101.4
M4[4hrs; 0d]	61.9	70.9	75.5
M4[4hrs; 1d]	35.1	38.4	72.9
M4[4hrs; 2d]	31.2	31.0	65.4
M4[4hrs; 4d]	20.2	28.6	46.6

*: H is hours of aging at compaction temperature and the D is days of aging at 95℃

As indicated in the preceding tables, the M7 blend exhibited superior performance in terms of crack resistance, consistently displaying the highest CTindex across nearly every aging stage. To enhance visual clarity, the comparative analysis of the three mixtures was presented in unified plots depicted in Figures 22 through 26. These visuals aimed to show the diverse parameters and their impact on the mixtures' behavior.

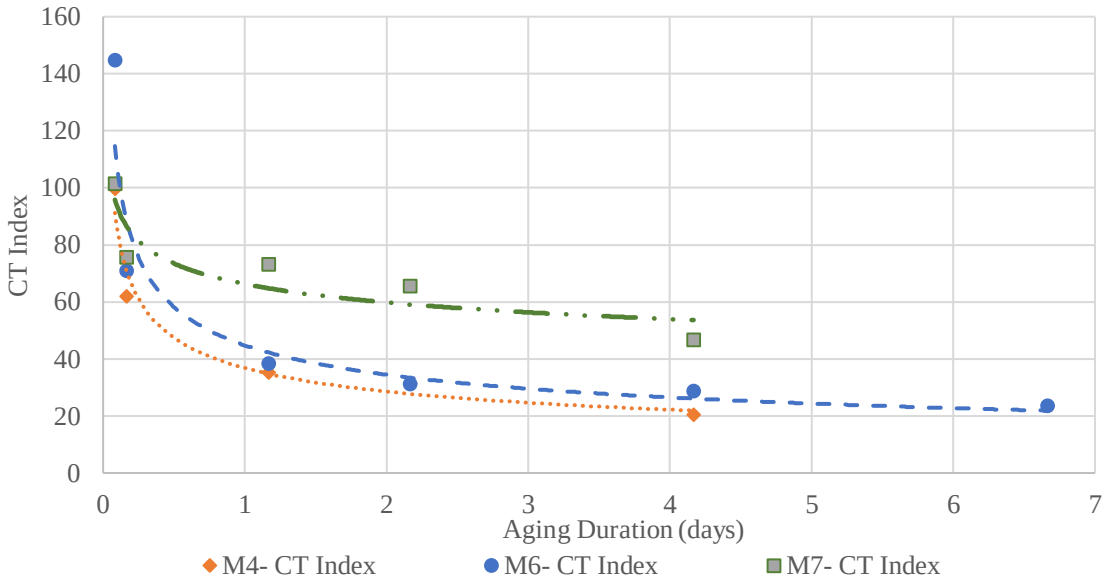

Figure 22. CT index for the LMLC mixtures

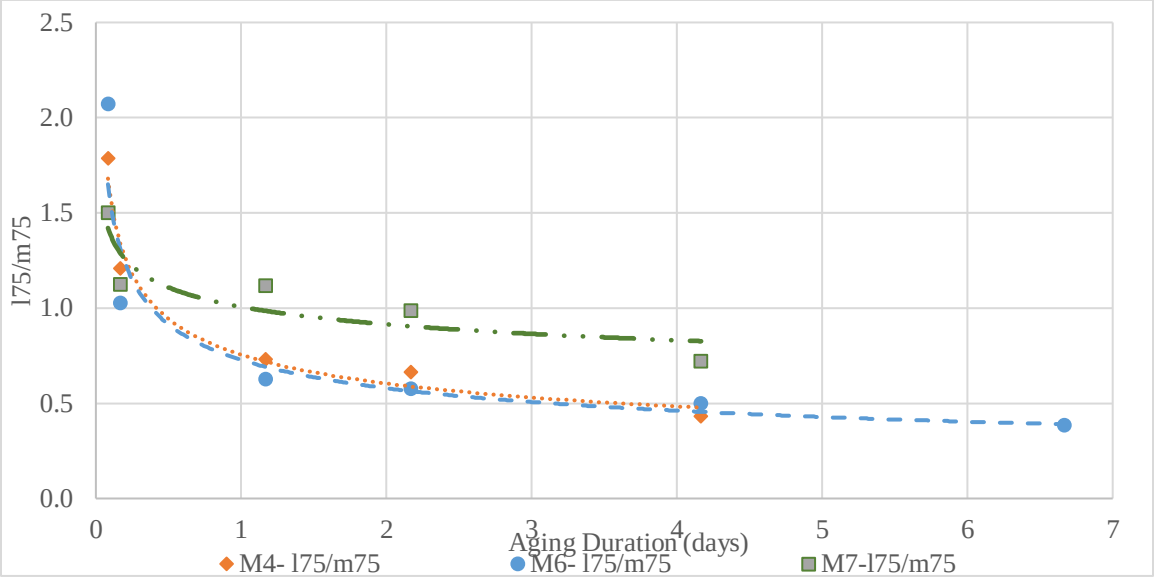

Figure 23. l75/m75 for the LMLC mixtures

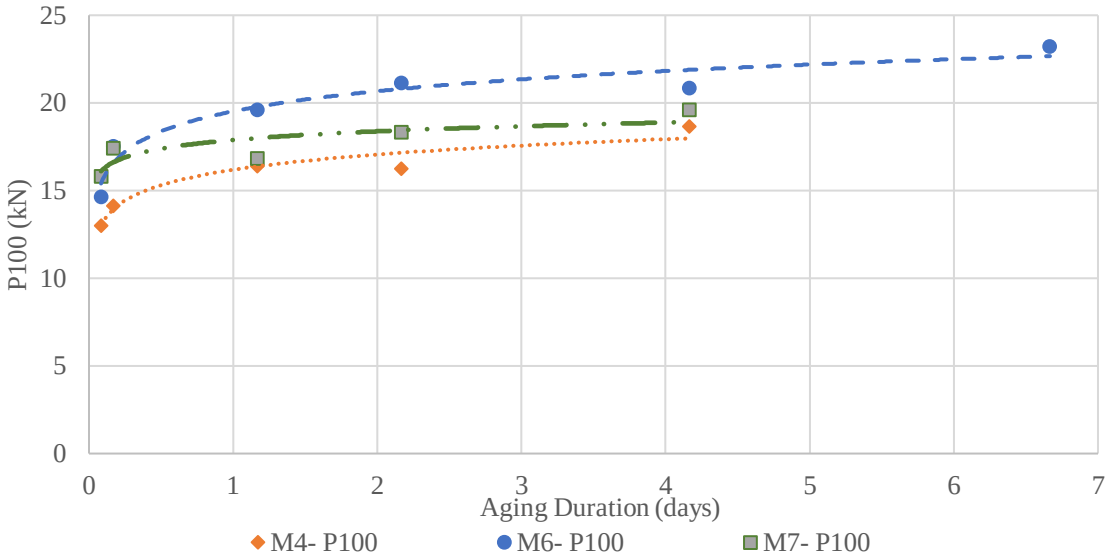

Figure 24. Peak Load for the LMLC mixtures

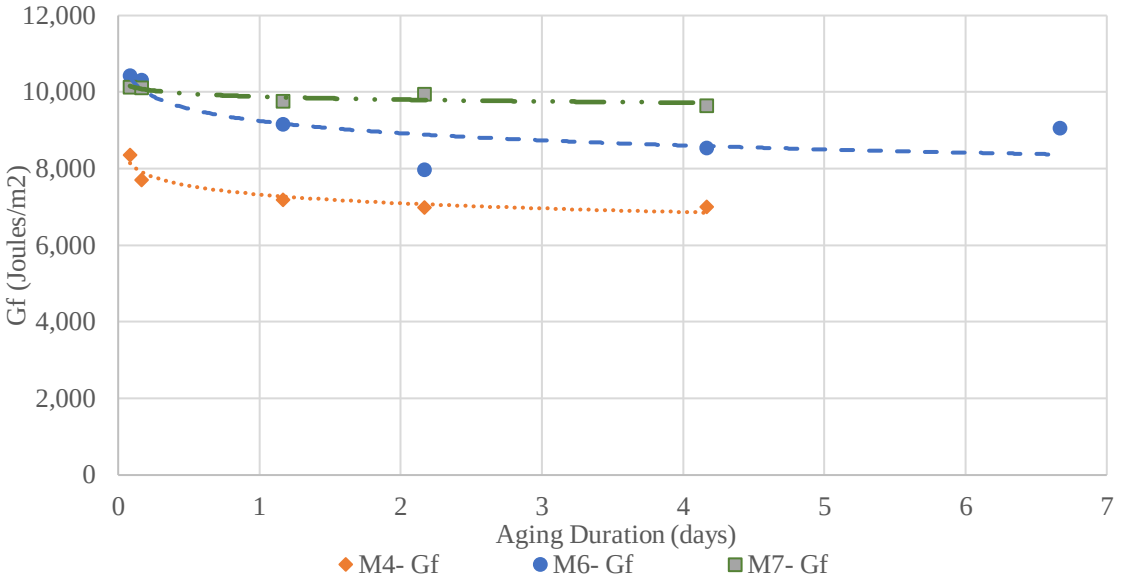

Figure 25. Fracture Energy for the LMLC mixtures

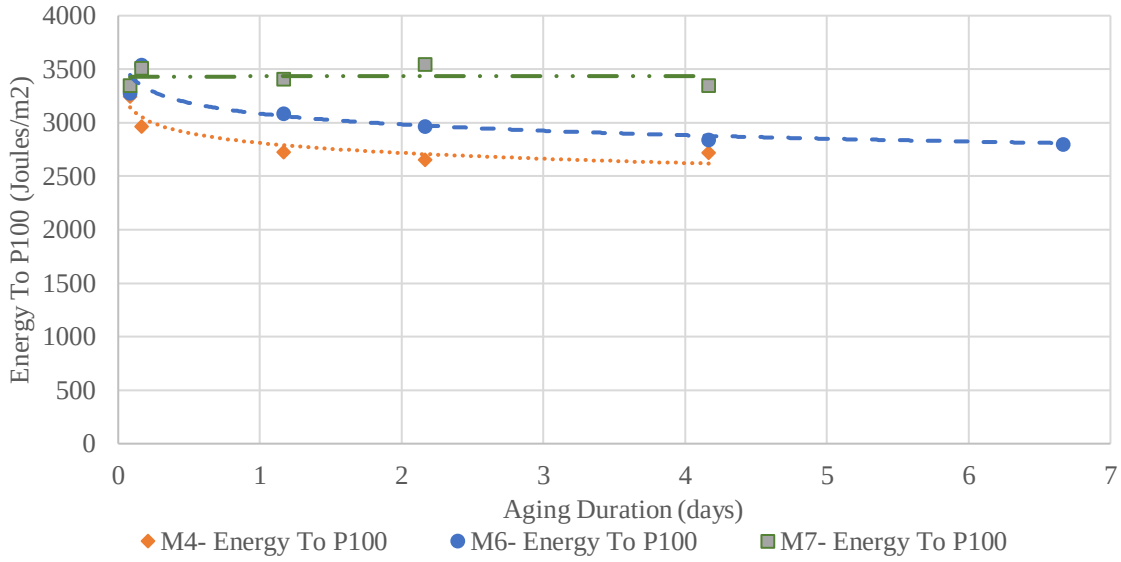

Figure 26. Energy to Peak Load for LMLC mixtures

As depicted in Figure 22, the CTindex trends for the M4 and M6 mixtures run in close parallel, exhibiting nearly identical behaviors at corresponding aging levels. Notably, the M6 blend demonstrates a marginal advantage over the M4 mixture. Conversely, the performance of the M7 mixture stands out, showcasing superior behavior compared to both M4 and M6, presenting a similar parallel trend but marked by significantly higher CTindex values at equivalent aging stages. Figure 23 reveals a strong correlation between the l75/m75 parameter and the CTindex, with both graphs displaying a comparable overall shape, indicating a similar pattern of change between l75/m75 and CTindex. Additionally, there is a noticeable formation of an elbow shape in the curve following 1 day of extended aging at 95°C, succeeded by a plateau, signifying a stabilized CT value beyond that period. Figures 27, 28 and 29 demonstrate the relationship between Gf, l75/m75 and CTindex.

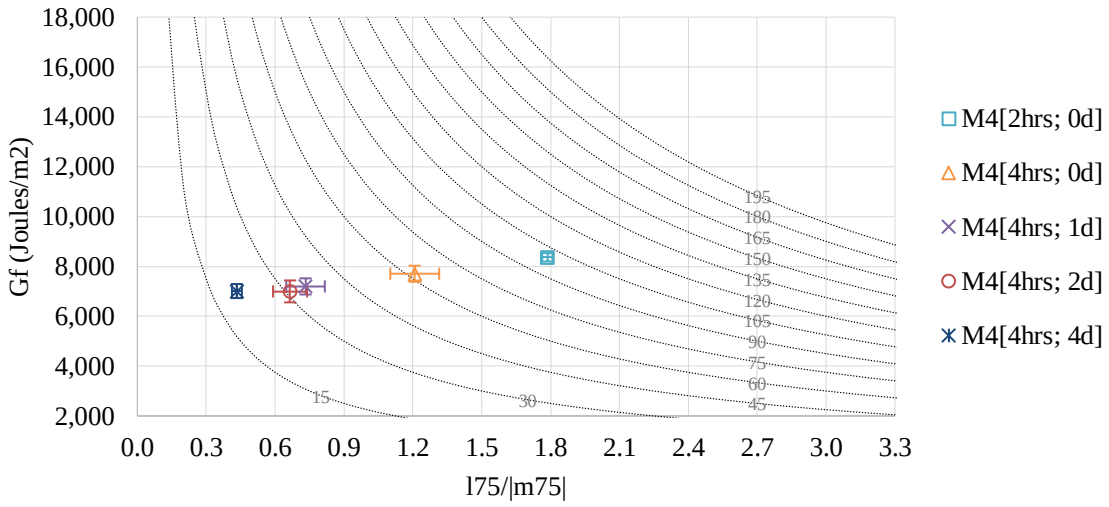

Figure 27. Gf vs l75/m75 - M4

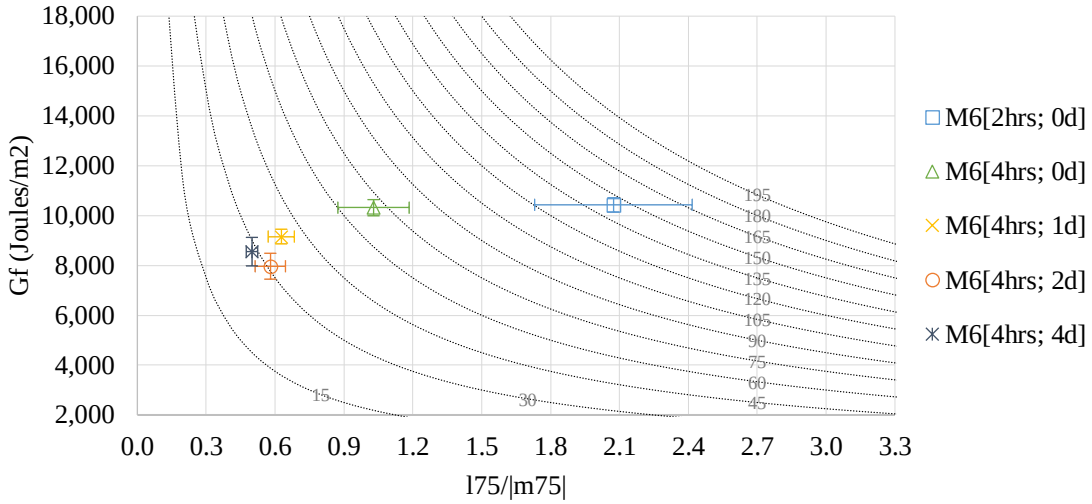

Figure 28. Gf vs l75/m75 - M6

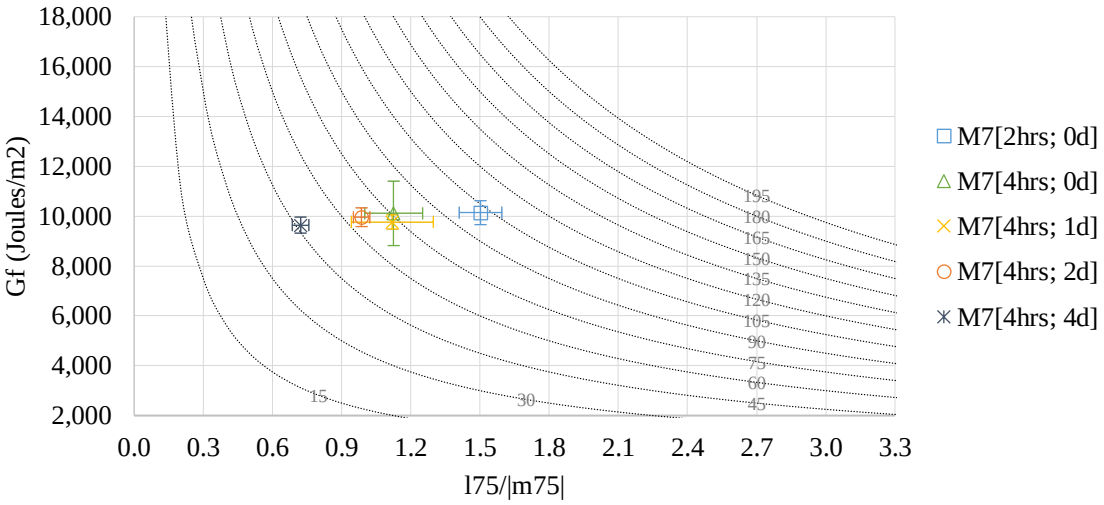

Figure 29. Gf vs l75/m75 - M7

When observing the relationship between fracture energy and the l75/m75 parameter for all three mixtures M4, M6 and M7s, it's evident that after 1 day of long-term aging, the data points congregate closely, suggesting a minor variance compared to the data points linked to lesser aging.

The IDT-CT data for the three mixtures was ranked according to average CT value for individual aging levels and is shown in Table 28.

Table 28. LMLC aging levels rank based on average CT value.

Rank based on Average CT value					
Aging Level*	**2H_0D**	**4H_0D**	**4H_1D**	**4H_2D**	**4H_4D**
M4	3	3	3	2	3
M6	1	2	2	3	2
M7	2	1	1	1	1

*: H is hours of aging at compaction temperature and the D is days of aging at 95℃

The data in Table 28 demonstrates that the M7 mixture consistently showcased superior performance across nearly every aging level compared to both M4 and M6 mixtures, with M6 following closely and M4 displaying the least performance among the three. Furthermore, alongside the ranking established from the average CT value, an additional ranking based on statistical analysis using the analysis of variance method (ANOVA) of the CTindex was suggested. This analysis consists of comparing the CTindex means using all three mixtures and all aging levels. Means that do not share a letter are significantly different. The suggested grouping was using the Tukey method and a 95% confidence interval. Before analyzing the ANOVA output, statistical interaction was tested, an interaction signifies that a variable depends on another variable or influences it’s behavior.

The output generated by the software indicated the presence of interaction between aging duration and mixture ID. To summarize, the mixture ID impacts the CTindex, the aging duration impacts the CTindex but also the interaction between the mixture ID and the aging duration impacts the CTindex. Therefore, the analysis of variance is not valid. The ANOVA output is as follows:

Table 29. ANOVA Interaction Test

	Df	Sum Sq	Mean Sq	F Value	Pr(>F)
Mixture	2	5596	2798	9.887	0.000194
Aging Level	4	62742	15685	55.43	< 2e-16
Mixture: Aging	8	7974	997	3.522	0.002119
Residuals	60	16979	283		

5.2.2. Binder Testing

To evaluate how binder aging influences mixture behavior, the virgin and recovered binders from mixtures M4, M6, and M7 underwent testing. These tests involved conducting the Bending Beam Rheometer (BBR) as per AASHTO T 313, alongside the Fourier Transform Infrared Test and the Frequency Sweep Test to determine the Glover-Rowe parameter. These tests were conducted at four aging levels (Original binder, Rolling Thin Film Oven (RTFO) aged binder, Pressure Aging Vessel (PAV) aged binder for 20 hours and PAV aged binder for 40 hours) for the virgin binder and at 5 different aging levels (2H_0D, 4H_0D, 4H_1D, 4H_2D and 4H_4D) for the recovered binders with H being the time at compaction temperature in hours and D being the time at 95°C in days. The RTFO procedure described in AASHTO T 240 is used to simulate the short-term aging that the asphalt binder undergoes during the mixing and transportation phase of the production, this process involves placing a thin film of asphalt binder inside a rotating platform and exposed to high temperatures for a specified duration (typically 163°C for 85-90 minutes). Conversely, the PAV aging process, as outlined in AASHTO R 28, seeks to replicate the prolonged aging experienced throughout the lifespan of pavement. The asphalt binder undergoes exposure to high temperature and increased pressure for an extended duration, usually at 100°C for either 20 or 40 hours. Figure 30, 31 and 32 portray the BBR machine, RTFO machine and PAV machine respectively.

Figure 30. Bending Beam Rheometer (BBR)

Figure 31. Rolling Thin Film Oven (RTFO)

Figure 32. Pressure Aging Vessel (PAV)

5.2.2.1. Beam Bending Rheometer Test (BBR)

The beam bending rheometer test was conducted on all virgin and recovered binders to evaluate various ΔTc values. The recovered binder was extracted from two IDT-CT samples that exhibited CTindex values closest to the mean CT value of the respective aging level under consideration. The ΔTc parameter assists in characterizing the asphalt binders' thermal traits and their behavior concerning stiffness and deformation under specific temperature circumstances. The BBR test involves evaluating an asphalt binder beam measuring 6.35 ± 0.05 mm in thickness, 12.7 ± 0.05 mm in width, and 127 ± 2 mm in length while under a consistent load of 980 ± 50 mN. Throughout the test, the sample beam is immersed in a bath of ethanol set at the specified test temperature. Notably, the BBR machine undergoes calibration at each test temperature, ensuring precise outcomes while minimizing potential errors. Two temperatures underwent assessment to determine the ΔTc parameter. One passing temperature, while the other failing. Each temperature was tested with two beams to ensure precision and bias are within the specified criterion. The stiffness (s-value) and the m-value at 60 seconds were recorded for each replicate.

<u>The apparatus used in this test is the following:</u>

Bending Beam Rheometer (BBR) test system, loading frame, loading system, Sample supports, loading shaft, Load cell, Linear variable differential transducer (LVDT), Controlled temperature fluid bath, Bath agitator, circulating bath (Optional), Data acquisition system, Signal filtering, Temperature measuring equipment, Test beam molds.

5.2.2.1.1. M4 Mixture

Figures 33 and 34 show the stiffness and the m-value of the M4 mixture at 60s for different temperatures and aging levels.

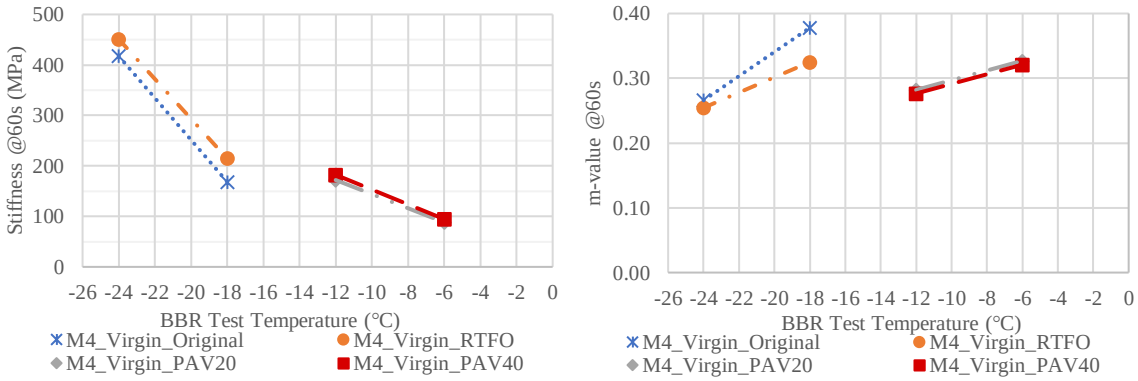

Figure 33. S-value (left), m-value (right) - M4 Virgin Binder

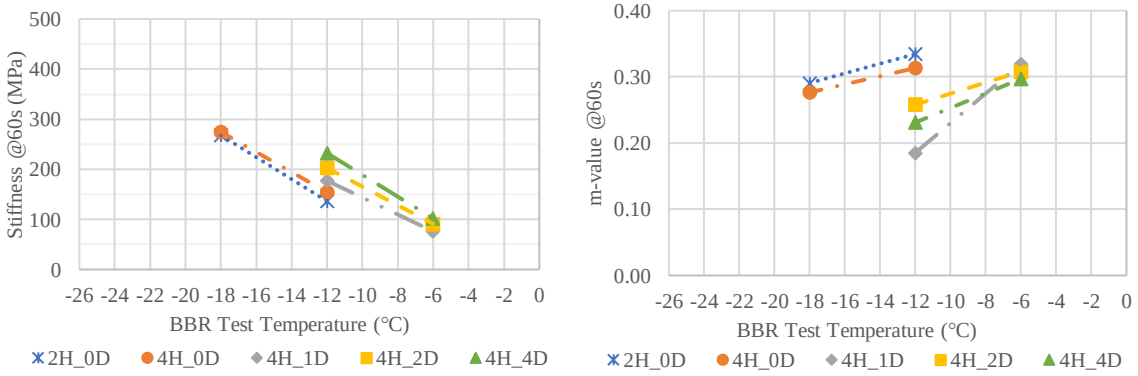

Figure 34. S-value (left), m-value (right) - M4 Recovered Binder

The m-value dictates the lower performance grade observed in the M4 mixture, evident in both the virgin and recovered binders, transitioning from -22 to -16 for the recovered binder after only one day of long-term aging (4H_1D). It's notable that the stiffness value of the recovered binder never surpassed the set maximum limit of 300 MPa at any temperature. Table 30 shows the different ΔTc values for the M4 mixture.

Table 30. ΔTc - M4

Binder	ΔTc (°C)
Virgin Original – M4	0.4
Virgin RTFO – M4	-0.6
Virgin PAV20 – M4	-7.4
Virgin PAV40 – M4	-7.7
Recovered 2H_0D – M4*	-2.2
Recovered 4H_0D – M4*	-4.7
Recovered 4H_1D – M4*	-6.5
Recovered 4H_2D – M4*	-8.0
Recovered 4H_4D – M4*	-8.1

*: H is hours of aging at compaction temperature and the D is days of aging at 95℃

A more negative ΔTc parameter generally indicates heightened stiffness and decreased ability to deform. Table 30 data reveals that the ΔTc for the virgin binder in the M4 mixture remained relatively consistent until subjected to PAV20 aging. In contrast, the ΔTc for the recovered binder gradually decreased until stabilizing around -8°C. It's noteworthy that the recovered binder aged more significantly after only 2 hours of STA at compaction temperature (2H_0D) than both the Virgin original and Virgin RTFO binders, evident in its more negative ΔTc. Moreover, the ΔTc values for PAV20 and 4H_1D were relatively close, suggesting the critical significance of the 4H_1D aging duration once again. Figures 35 and 36 illustrate the true and standardized low performance grade of the M4 mixture.

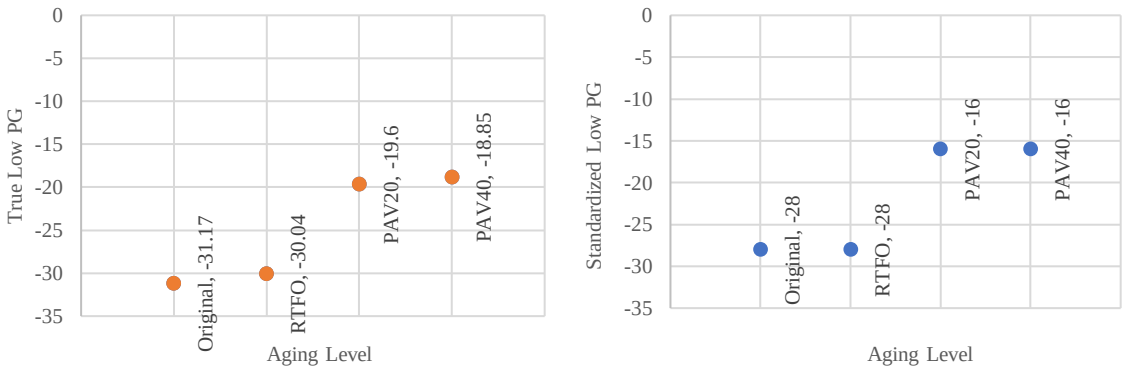

Figure 35. Virgin True low PG (left), Virgin Standardized low PG (right) - M4

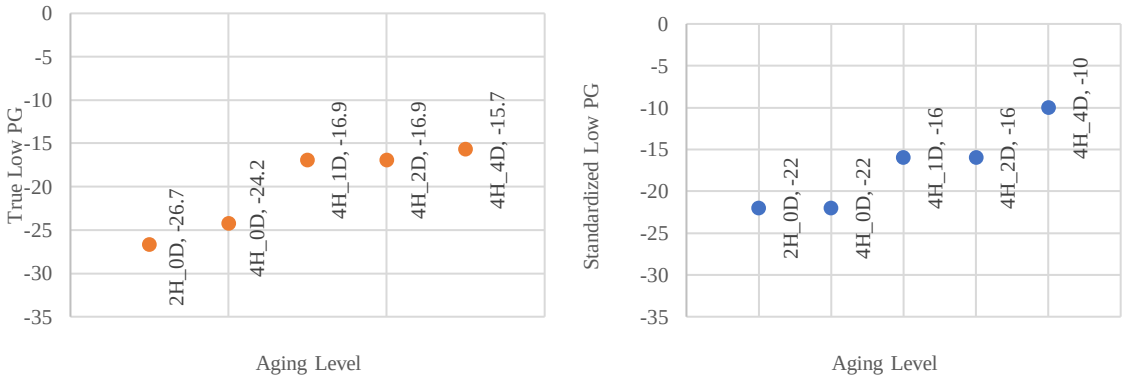

Figure 36. Recovered True low PG (left), Recovered Standardized low PG (right) - M4.

Once more, the 4H_1D marks a significant turning point for the M4 mixture, showcasing a notable jump in true and standardized low PG equally.

5.2.2.1.2. M6 Mixture

Shown in Figures 37 and 38 is the stiffness and the m-value of the M6 mixture at 60s for different temperatures and aging levels.

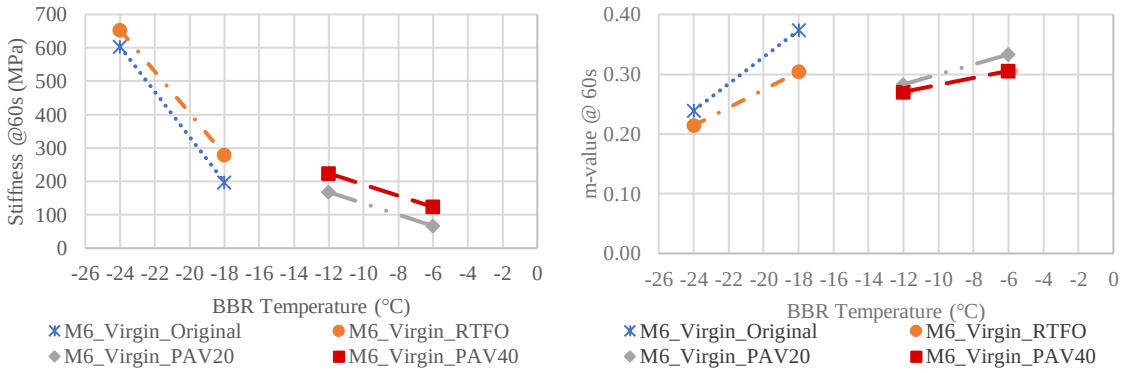

Figure 37. S-value (left), m-value (right) - M6 Virgin Binder

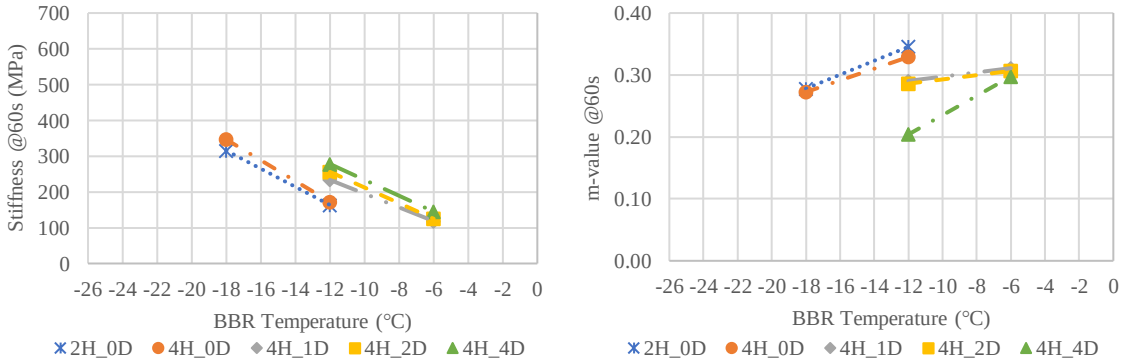

Figure 38. S-value (left), m-value (right) - M6 Recovered Binder

The 300 MPa and even the 600 MPa threshold is surpassed by the S value in both RTFO and Original at -24°C. Additionally, the m-value contributes to the low PG of the M6 binder. The true PG spans from -29.51 to -16.98. Omission of the -22°C low grade implies an escalated aging response unique to this particular virgin binder. Table 31 shows the different ΔTc values for the M6 mixture.

Table 31. ΔTc - M6

Binder	ΔTc (°C)
Virgin Original – M6	1.0
Virgin RTFO – M6	-0.2
Virgin PAV20 – M6	-5.8
Virgin PAV40 – M6	-8.0
Recovered 2H_0D – M6*	-1.5
Recovered 4H_0D – M6*	-1.7
Recovered 4H_1D – M6*	-5.0
Recovered 4H_2D – M6*	-5.4
Recovered 4H_4D – M6*	-6.9

*: H is hours of aging at compaction temperature and the D is days of aging at 95℃

The rate of change in ΔTc for the M6 mixture remained slow until reaching the 4H_1D aging level, where a noticeable negative shift occurred, aligning closely with the value observed in PAV20. Figures 39 and 40 illustrate the true and standardized low performance grade of the M6 mixture.

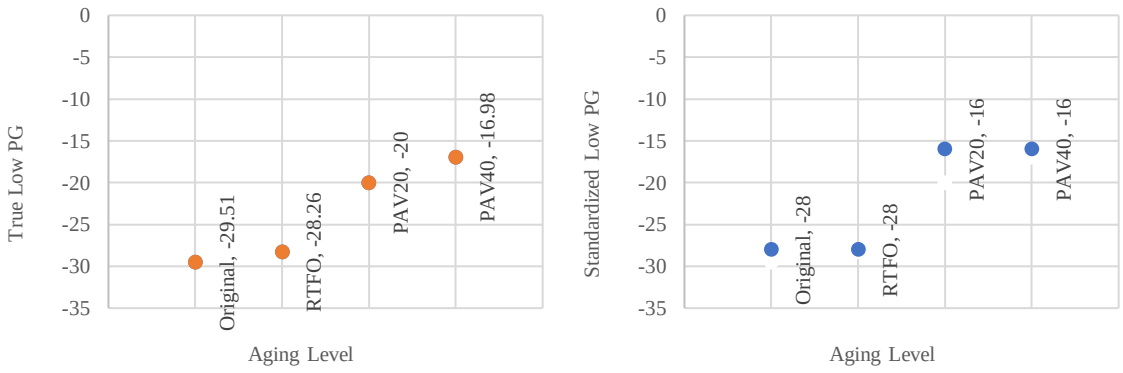

Figure 39. Virgin True low PG (left), Virgin Standardized low PG (right) - M6.

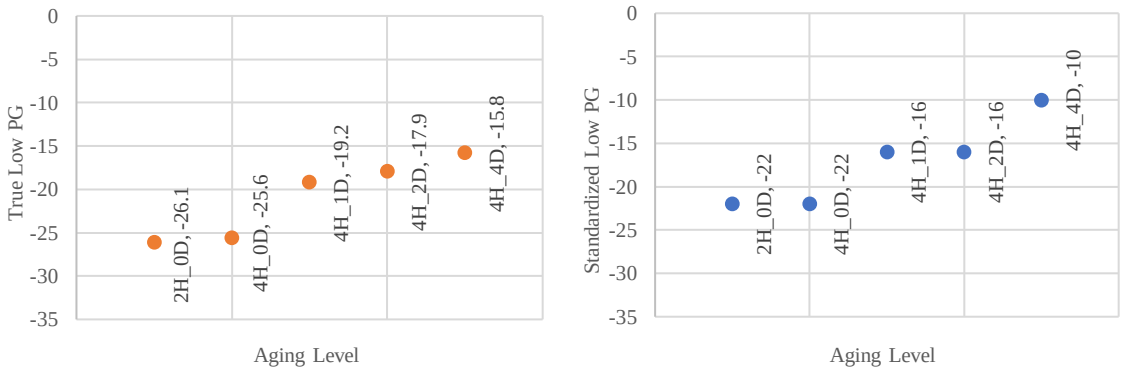

Figure 40. Recovered True low PG (left), Recovered Standardized low PG (right) - M6.

Also, for the M6 mixture, the 4H_1D marks a significant turning point showcasing a notable jump in true and standardized low PG equally.

5.2.2.1.3. M7 Mixture

Shown in Figures 41 and 42 is the stiffness and the m-value of the M6 mixture at 60s for different temperatures and aging levels.

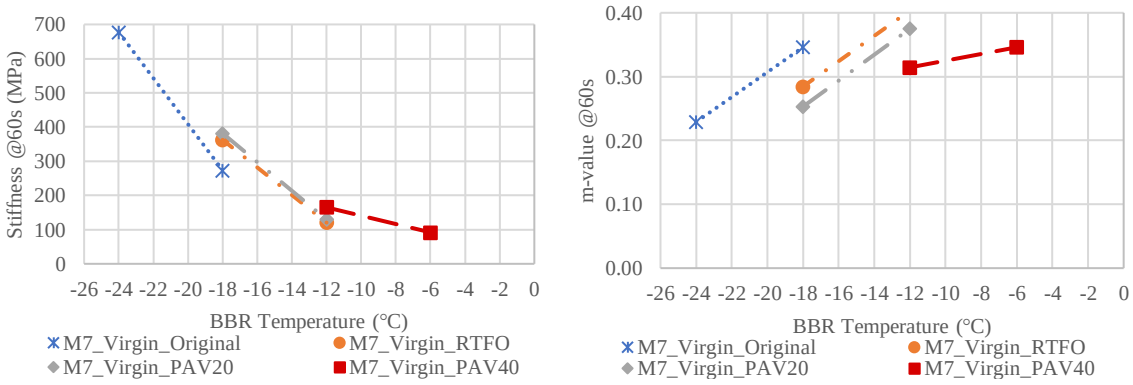

Figure 41. S-value (left), m-value (right) - M7 Virgin Binder

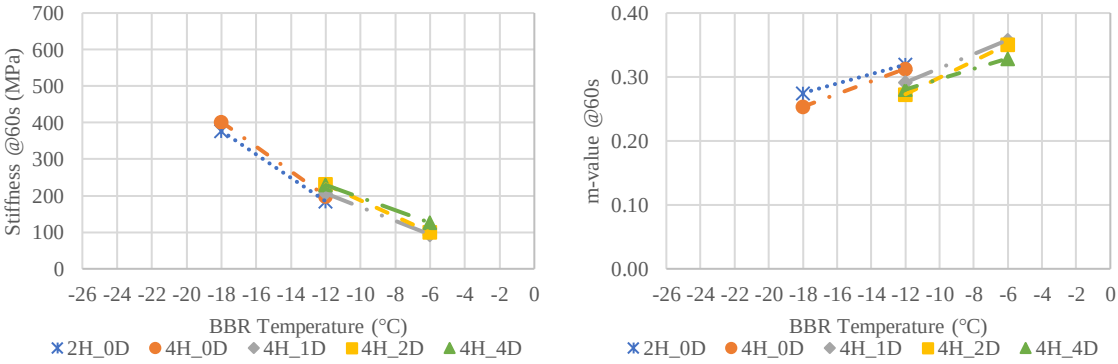

Figure 42. S-value (left), m-value (right) - M7 Recovered Binder

The s-value seems to breach the 600 MPa limit for virgin original binder at -24°C, indicating a potential failure. Additionally, the m-value plays a pivotal role in governing the low PG characteristics of the M7 recovered binder. Table 32 shows the different ΔTc values for the M7 mixture.

Table 32. ΔTc - M7

Binder	ΔTc (°C)
Virgin Original – M7	1.7
Virgin RTFO – M7	0.2
Virgin PAV20 – M7	-1.0
Virgin PAV40 – M7	-3.4
Recovered 2H_0D – M7*	-1.5
Recovered 4H_0D – M7*	-2.2
Recovered 4H_1D – M7*	-3.6
Recovered 4H_2D – M7*	-3.9
Recovered 4H_4D – M7*	-5.3

*: H is hours of aging at compaction temperature and the D is days of aging at 95℃

In contrast to the M4 and M6 mixtures, the ΔTc of the recovered binder for the M7 mixture reached parity with the virgin binder's ΔTc at PAV40 following the 4H_1D duration, rather than at PAV20. Figures 43 and 44 illustrate the true and standardized low performance grade of the M7 mixture.

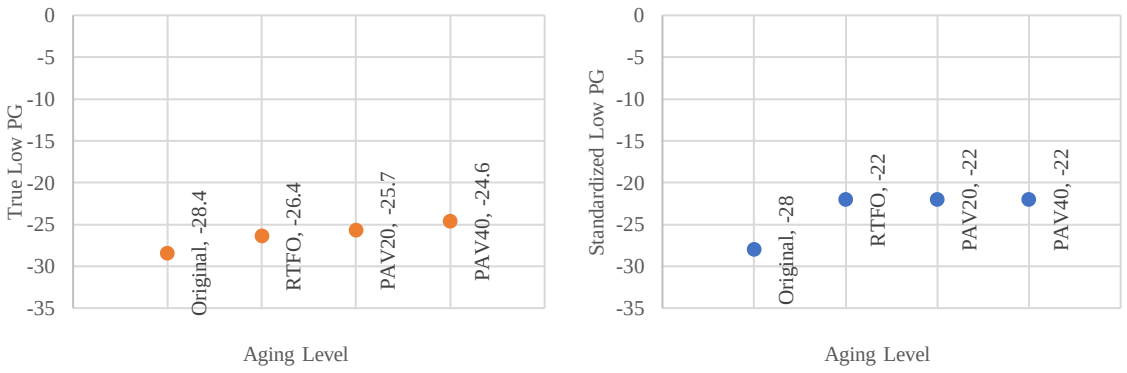

Figure 43. Virgin True low PG (left), Virgin Standardized low PG (right) - M7.

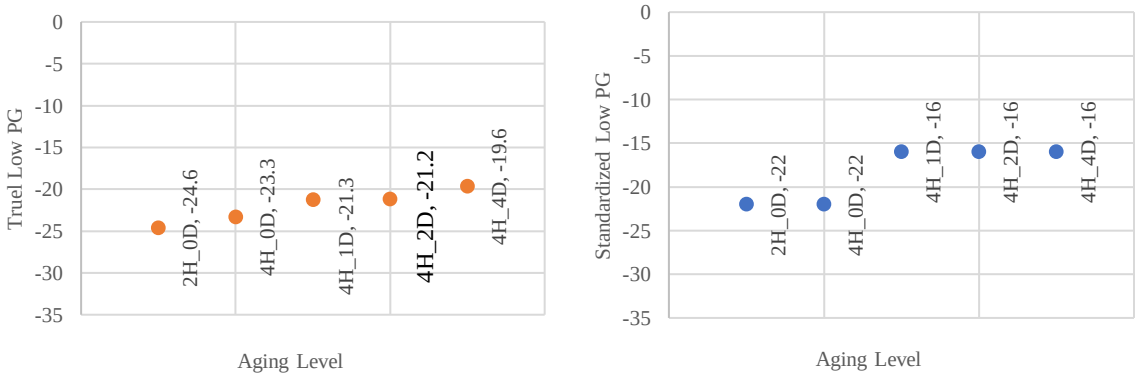

Figure 44. Recovered True low PG (left), Recovered Standardized low PG (right) - M7

Upon examining the true PG plots for both virgin and recovered binders of the M7 mixture, it's evident that the binder utilized in the M7 mixture exhibits greater resistance to aging compared to the M4 and M6 binders. This resilience is evidenced by the minimal rise in true low PG across various aging levels. Notably, the virgin Standard Low PG decreased by only one grade, transitioning from original to PAV40, providing additional evidence supporting the earlier assertion.

5.2.2.2. Fourier Transform Infrared Test (FTIR)

The FTIR test for asphalt binders involves analyzing the infrared spectrum of the binder sample. This process helps identify and characterize the chemical components present in the binder in this case Carbonyl. By detecting molecular vibrations in the infrared region, FTIR provides information about functional groups, molecular structures, and chemical compositions, aiding in the assessment of the binder's properties and potential changes due to aging or modifications. Three replicates were tested three times for each aging duration of every mixture to ensure the results precision and accuracy.

The apparatus used in this test is the following:

Fourier transform Infrared machine, oven, data collection system.

Figure 45 shows the FTIR machine used to conduct this test.

Figure 45. Fourier Transform Infrared Machine (FTIR)

5.2.2.2.1. M4 Mixture

Shown in Figures 46 and 47 as well as Table 33 are the FTIR test outcomes illustrating the results for the M4 mixture, portraying the virgin and recovered binder, respectively.

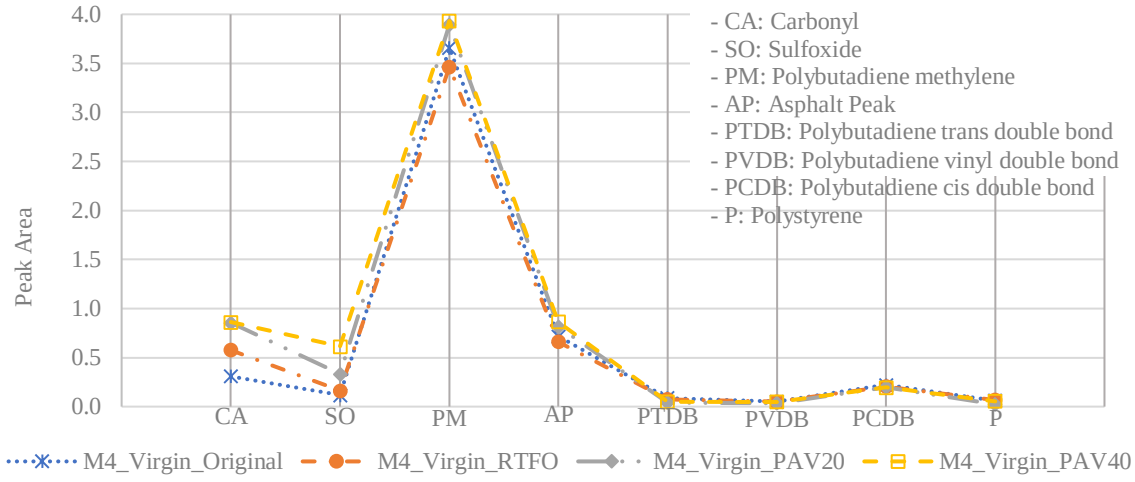

Figure 46. FTIR - M4 Virgin Binder

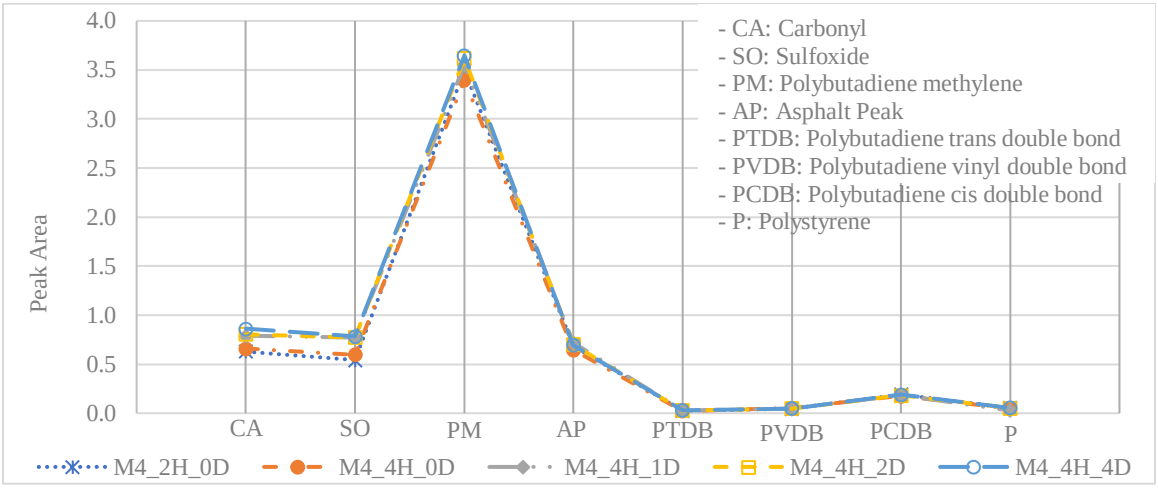

Figure 47. FTIR - M4 Recovered Binder

Table 33. M4 FTIR test results – Virgin and Recovered Binder

	Aging Level	CA	SO	PM	AP	PTDB	PVDB	PCDB	P
Recovered Binder	2H_0D	0.631	0.542	3.497	0.687	0.025	0.044	0.191	0.054
	4H_0D	0.658	0.596	3.395	0.646	0.021	0.050	0.175	0.047
	4H_1D	0.790	0.772	3.550	0.718	0.028	0.044	0.186	0.028
	4H_2D	0.805	0.773	3.618	0.702	0.027	0.048	0.182	0.052
	4H_4D	0.861	0.784	3.648	0.696	0.029	0.048	0.189	0.055
Virgin Binder	Original	0.311	0.117	3.656	0.717	0.088	0.052	0.221	0.061
	RTFO	0.577	0.162	3.465	0.661	0.076	0.052	0.204	0.066
	PAV20	0.855	0.331	3.896	0.817	0.042	0.036	0.198	0.024
	PAV40	0.861	0.612	3.933	0.863	0.049	0.050	0.197	0.056

*: H is hours of aging at compaction temperature and the D is days of aging at 95°C

The scatter plots featured in Figures 46 and 47 and the data present in table 33 display the Peak area of various binder components concerning the Virgin and Recovered M4 binder. These plots distinctly indicate that the Peak Carbonyl area remains relatively stable post 4H_1D, as the curves overlap. This observation signifies a deceleration in the growth of CA after this specific aging duration.

5.2.2.2.2. M6 Mixture

Shown in Figures 48 and 49 and table 34 are the FTIR test outcomes illustrating the results for the M6 mixture, portraying the virgin, and recovered binder from tested LMLC IDT_CT samples, respectively.

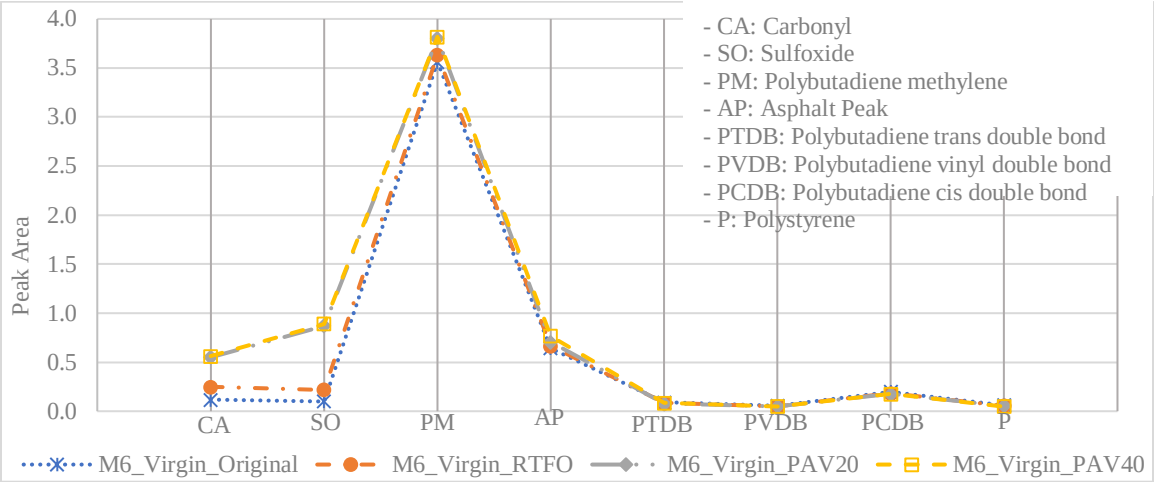

Figure 48. FTIR - M6 Virgin Binder

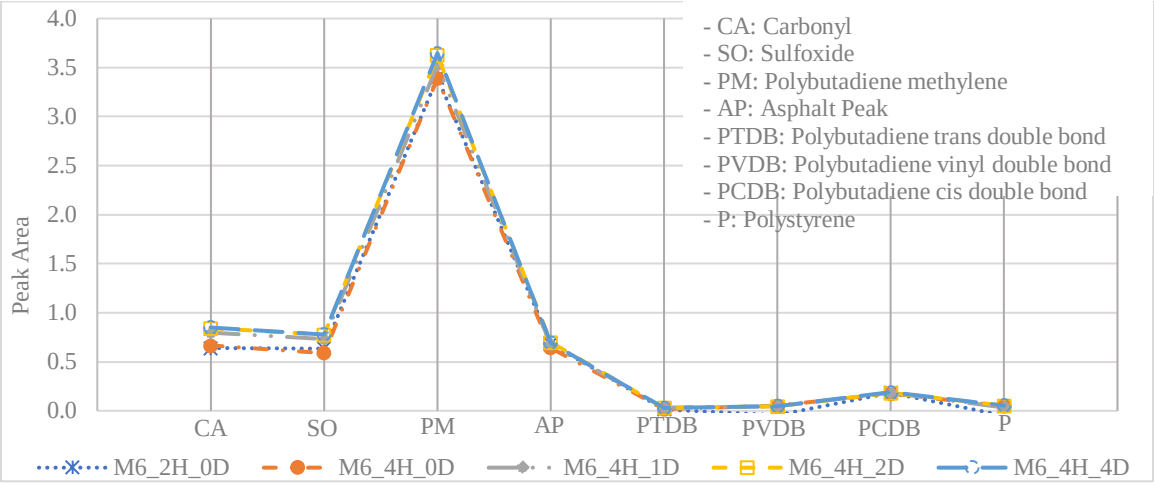

Figure 49. FTIR - M6 Recovered Binder

Table 34. M6 FTIR test results – Virgin and Recovered Binder

	Aging Level	CA	SO	PM	AP	PTDB	PVDB	PCDB	P
Recovered Binder	2H_0D	0.64	0.64	3.40	0.69	0.02	0.04	0.18	0.05
	4H_0D	0.66	0.59	3.39	0.64	0.02	0.05	0.17	0.05
	4H_1D	0.79	0.73	3.52	0.67	0.03	0.05	0.18	0.04
	4H_2D	0.84	0.77	3.62	0.70	0.03	0.05	0.18	0.05
	4H_4D	0.85	0.78	3.65	0.69	0.03	0.05	0.19	0.05
Virgin Binder	Original	0.12	0.10	3.56	0.64	0.09	0.06	0.20	0.06
	RTFO	0.25	0.22	3.63	0.67	0.08	0.05	0.18	0.06
	PAV20	0.55	0.87	3.80	0.70	0.08	0.05	0.17	0.06
	PAV40	0.56	0.89	3.82	0.76	0.08	0.05	0.18	0.05

*: H is hours of aging at compaction temperature and the D is days of aging at 95℃

As depicted in the plots, it's evident that the Peak Carbonyl area displays minimal alteration following PAV20 and 4H_1D, indicating a semblance between these aging conditions concerning CA. This observation implies a deceleration in the growth rate of CA after this specific aging duration.

5.2.2.2.3. M7 Mixture

Similarly, to the M4 and M6 mixtures, the M7 mixture was evaluated using the Fourier Transform Infrared test using both virgin and recovered binder from the tested LMLC IDT-CT samples. Shown in Figures 50 and 51 and Table 35 are the FTIR test outcomes illustrating the results for the M7 mixture.

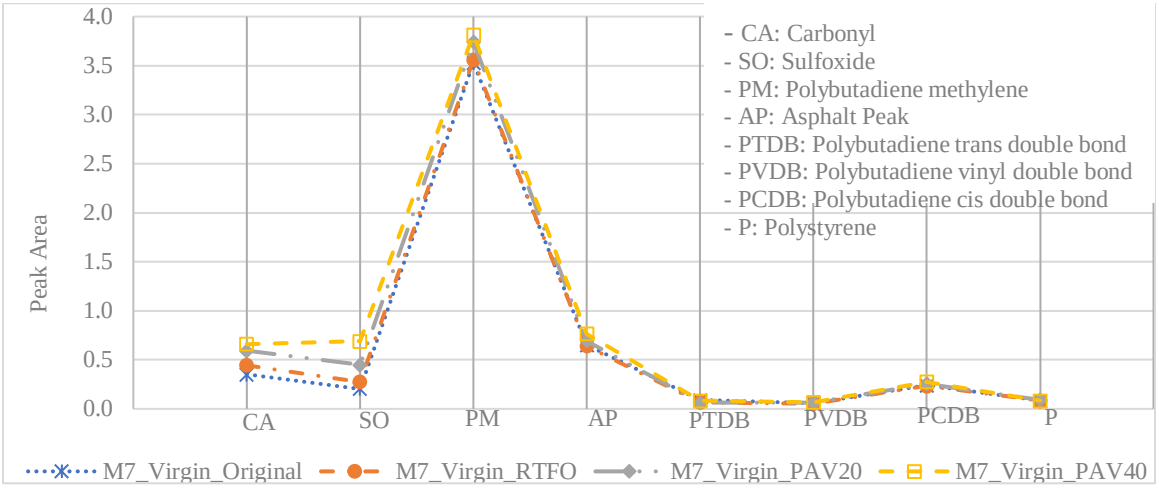

Figure 50. FTIR - M7 Virgin Binder

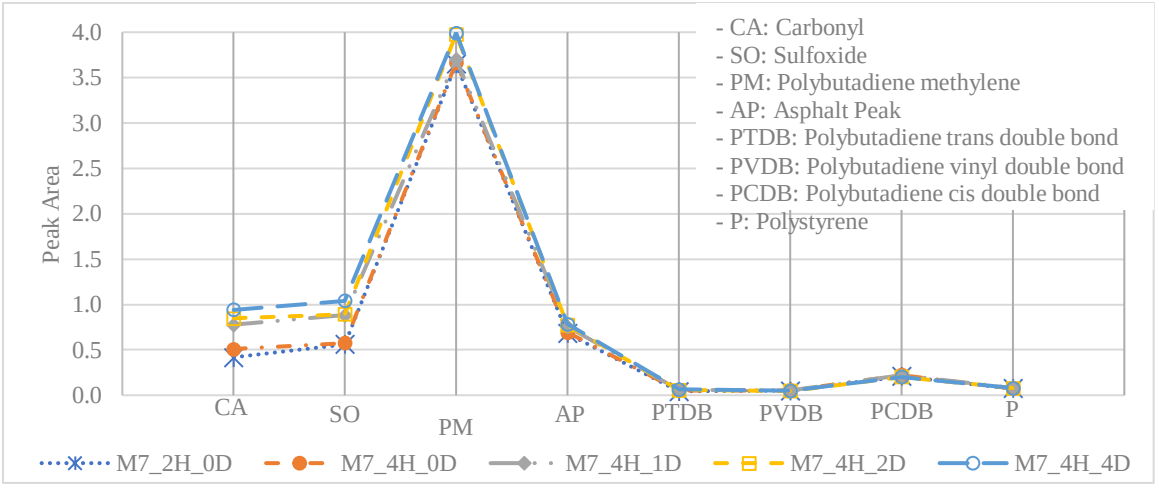

Figure 51. FTIR - M7 Recovered Binder

Table 35. M7 FTIR test results – Virgin and Recovered Binder

	Aging Level	CA	SO	PM	AP	PTDB	PVDB	PCDB	P
Recovered Binder	2H_0D	0.42	0.56	3.65	0.68	0.04	0.05	0.21	0.07
	4H_0D	0.51	0.57	3.67	0.69	0.05	0.05	0.22	0.07
	4H_1D	0.78	0.88	3.70	0.75	0.06	0.05	0.22	0.08
	4H_2D	0.85	0.89	3.98	0.77	0.06	0.05	0.20	0.08
	4H_4D	0.94	1.04	3.99	0.78	0.07	0.05	0.20	0.08
Virgin Binder	Original	0.35	0.20	3.53	0.65	0.09	0.06	0.24	0.08
	RTFO	0.44	0.27	3.56	0.64	0.07	0.05	0.23	0.08
	PAV20	0.59	0.45	3.74	0.69	0.06	0.06	0.26	0.09
	PAV40	0.66	0.69	3.82	0.76	0.08	0.07	0.28	0.08

*: H is hours of aging at compaction temperature and the D is days of aging at 95°C

As evident in the plots of Figures 50 and 51, there's a discernible stability in the Peak Carbonyl area post PAV20 and 4H_1D. Both plots exhibit a notable surge in the Carbonyl area at these specific aging levels, indicating a marked change. This observation implies a deceleration in the growth rate of CA following this aging duration.

5.2.2.3. Frequency Sweep Test (FS)

The Dynamic Shear Rheometer (DSR) machine conducts the Binder Frequency Sweep Test, which evaluates an asphalt binder's viscoelastic properties across a spectrum of frequencies and temperatures. It measures key parameters like the complex shear modulus (G*) and phase angle (δ) as they relate to varying frequencies, highlighting the binder's ability to withstand deformation at different temperatures and loading frequencies. This procedure involves exposing the binder sample to a range of oscillating frequencies while maintaining a consistent temperature, typically varying from 0.1 to 100 Hz. Through this examination, the test assesses the binder's rigidity, flexibility, and fatigue resistance across diverse conditions, providing crucial insights for pavement design and predicting

performance. Two replicates were tested per aging level for every one of the three mixtures for accuracy and precision.

The apparatus used in this test is the following:

Dynamic shear rheometer machine, rubber molds, measuring device, oven, air compressor, data collection system.

An experimental arrangement was devised for the FS test and is outlined in Table 36 for reference.

Table 36. Experimental plan for Frequency Sweep test

Range	High	Intermediate	Low
Temperatures (°C)	60, 64, 70	22, 28, 34, 40, 46	-2, 4, 10, 15
Gap (mm)	1	2	2
Measuring device	25 mm PP	8 mm PP	8 mm PP
Frequency (rad/s)	0.01-100	0.1-100	0.1-100

This examination was performed on both virgin and recovered binders. The recovered binders were extracted from tested LMLC IDT-CT samples that had a CTindex that closely aligned with the mean CT index of the respective aging level being studied. The outcome extracted from the Frequency Sweep (FS) test is the Glover-Rowe parameter, which assesses the correlation between the complex shear modulus (G*) and the phase angle (δ) of the binder across a range of frequencies. This parameter serves as an indicator of the binder's stiffness and its capability to endure deformation at varying frequencies and temperatures. High GRP values generally signify a stiffer binder, indicating reduced resilience against cracking. The test outcomes for the virgin and recovered binders for all three mixtures are presented in Figures 52 and 53, respectively. It's noteworthy that in both

charts, the onset of cracking is defined at 180 kPa, while significant cracking is identified at 600 kPa.

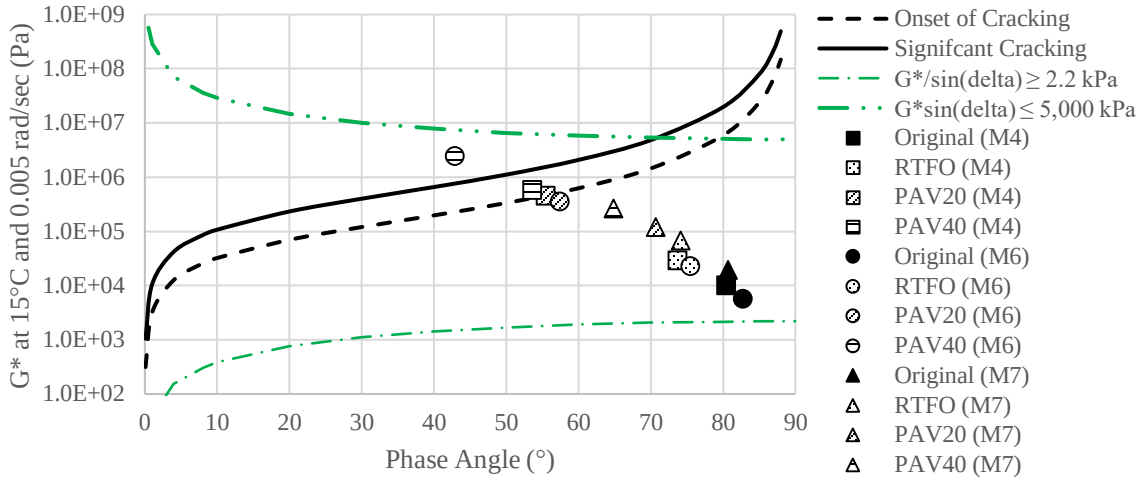

Figure 52. Black Space Diagram– Virgin Binders

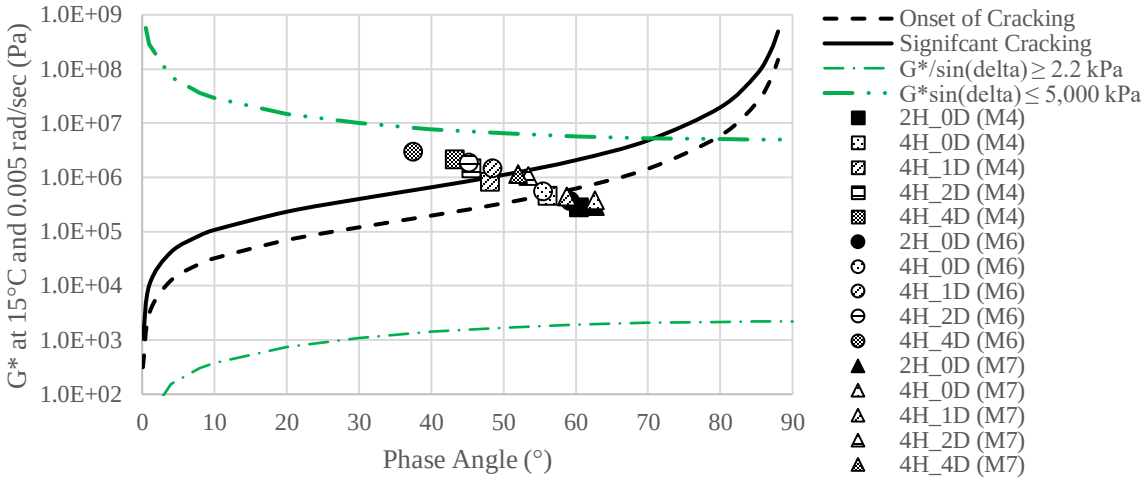

Figure 53. Black Space Diagram - Recovered Binders

Table 37 shows the complex shear modulus G* and the phase angle δ used in the calculation of the GRP.

Table 37. G* and Phase Angle - All mixtures

		M4		M6		M7	
		G (Pa)*	*Phase Angle (°)*	*G* (Pa)*	*Phase Angle (°)*	*G* (Pa)*	*Phase Angle (°)*
Recovered Binder	*2H_0D*	271,700	60.5	361,500	59.27	296,000	62.66
	4H_0D	454,400	56.17	536,000	55.56	386,000	62.68
	4H_1D	817,700	48.24	1,433,000	48.6	444,400	58.76
	4H_2D	1,446,000	45.66	1,836,000	45.32	1,058,000	53.43
	4H_4D	2,132,000	43.32	2,903,000	37.62	1,149,000	51.98
Virgin Binder	*Original*	9,864	80.54	5,680	82.86	19,850	80.73
	RTFO	28,430	73.82	22,630	75.55	68,960	74.11
	PAV20	448,400	55.56	349,900	57.46	121,300	70.68
	PAV40	568,000	53.66	2,406,000	42.95	264,700	64.87

*: H is hours of aging at compaction temperature and the D is days of aging at 95°C

Among the three virgin binders tested, the M7 variant displayed superior resistance to cracking, notably avoiding the onset of cracking envelope even after undergoing 40 hours of PAV aging. In contrast, the M6 virgin binder demonstrated the weakest performance in terms of cracking, surpassing the significant cracking envelope. Notably, all three mixtures virgin binders showcased relatively comparable aging responses at their original states and following the RTFO aging. When examining the Glover-Rowe parameter across aging durations (2H_0D, 4H_0D, 4H_1D, 4H_2D) for the recovered binders, a consistent trend emerges: the M7 recovered binder consistently displays lower GRP values than the M4 and M6 recovered binders at the same aging levels. This discrepancy indicates improved resistance to cracking for the M7 recovered binder. Additionally, all binders exhibit a notable surge in the GRP following one day of long-term aging (4H_1D). Table 38 consolidates the GRP of all the tested binders (Virgin and Recovered) for comprehensive

comparison and evaluation. For enhanced visual inspection and analysis, individual plots (Figures 54, 55, and 56) were generated for each mixture's binder for M4, M6 and M7 respectively.

Table 38. Glover-Rowe (GRP) - Virgin and Recovered Binder (All Mixtures)

Aging	Virgin Binder GRP (kPa)				Recovered Binder GRP (kPa)				
	Original	RTFO	PAV20	PAV40	2H-0D	4H_0D	4H_1D	4H_2D	4H_4D
M4	0.27	2.3	174	248	76	170	486	988	1645
M6	0.09	1.5	120	1892	109	208	835	1277	2984
M7	0.5	5.4	14	53	70	91	140	468	553

*: H is hours of aging at compaction temperature and the D is days of aging at 95°C

5.2.2.3.1. M4 Mixture

The individual mixture results are then plotted to emphasize the effect of aging on G*, δ as well as GRP. Starting with the M4 mixture shown in Figure 54 and Table 39.

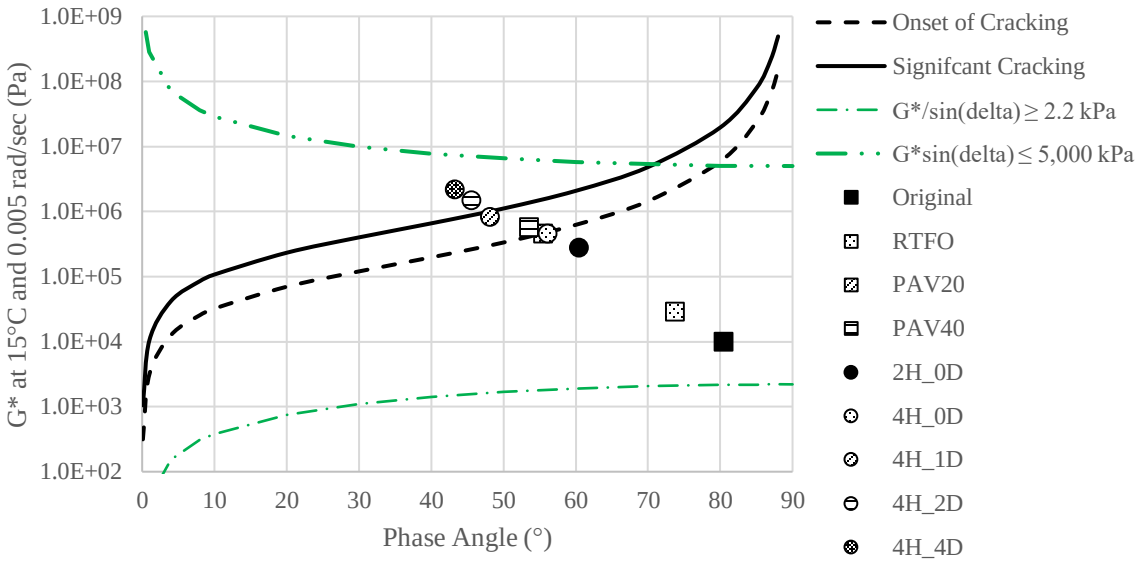

Figure 54. Black Space Diagram - M4

Table 39. G* vs Phase Angle - M4 mixture

		M4	
		G (Pa)*	*Phase Angle (°)*
Recovered Binder	*2H_0D*	271,700	60.5
	4H_0D	454,400	56.17
	4H_1D	817,700	48.24
	4H_2D	1,446,000	45.66
	4H_4D	2,132,000	43.32
Virgin Binder	*Original*	9,864	80.54
	RTFO	28,430	73.82
	PAV20	448,400	55.56
	PAV40	568,000	53.66

*: H is hours of aging at compaction temperature and the D is days of aging at 95℃

As anticipated, increased aging corresponds to higher G* values and lower δ values. Notably, the GRP value reaches the severe cracking envelope after one day of short-term aging for the recovered M4 binder. In the CT index plot shown earlier in Figure 17, an inflection point is evident after one day of long-term aging (4H_1D). Post PAV aging, the GRP value aligns with the cracking onset envelope. Comparative analysis revealed the equivalence between PAV20 of the virgin binder and 4H_1D for the recovered binder. The GRP value surpasses the significant cracking envelope after one day of Long-Term Aging (4H_1D). All the recorded data points fall within the range of $G^* \times \sin \delta < 5000$ kPa and $G/\sin \delta > 2.2$ kPa.

5.2.2.3.2. M6 Mixture

The M6 mixture black space diagram was also plotted for virgin and recovered binders and detailed in Figure 55 and Table 40.

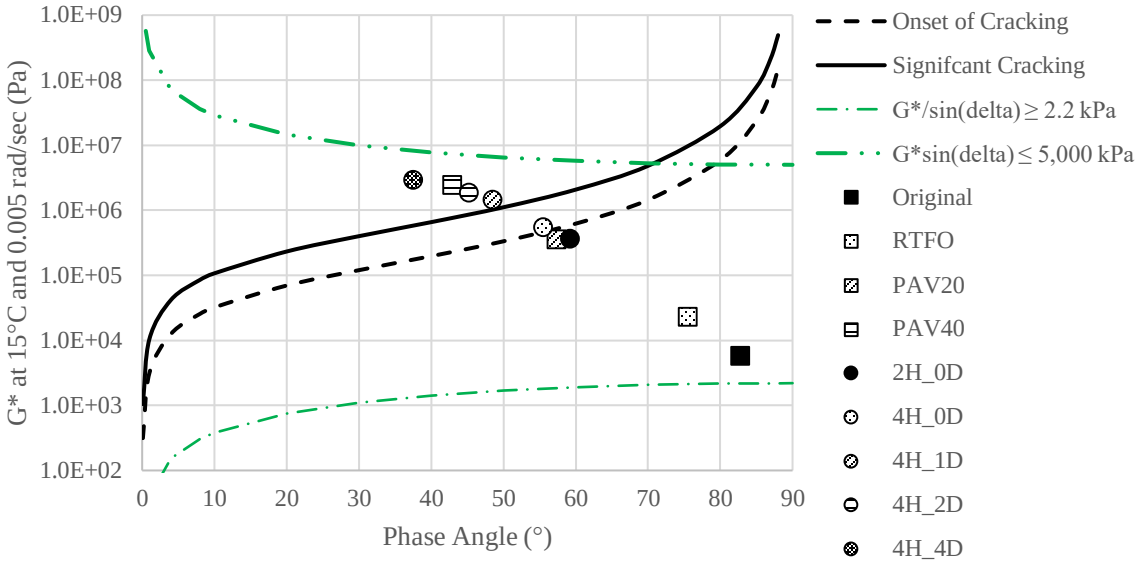

Figure 55. Black Space Diagram- M6

Based on the plot in Figure 17, the information in Figure 55 aligns with the distinct curve elbow seen in Figure 17 at the 4H_1D aging level for the recovered M6 binder. Also, for the recovered M6 binder, post PAV20 aging the GRP value aligns with the cracking onset envelope and at PAV40, the binder surpassed the significant crack envelope. The PAV20 data point of the M6 virgin binder falls between the 4H_0D and 4H_1D data points of the recovered M6 binder on the chart, highlighting the relevance of these aging levels for the M6 mixture cracking performance. The detailed G* and phase angle values are depicted in Table 40.

Table 40. G* vs Phase Angle – M6 mixture

		M6	
		G (Pa)*	*Phase Angle (°)*
Recovered Binder	*2H_0D*	361,500	59.27
	4H_0D	536,000	55.56
	4H_1D	1,433,000	48.6
	4H_2D	1,836,000	45.32
	4H_4D	2,903,000	37.62
Virgin Binder	*Original*	5,680	82.86
	RTFO	22,630	75.55
	PAV20	349,900	57.46
	PAV40	2,406,000	42.95

*: H is hours of aging at compaction temperature and the D is days of aging at 95℃

Table 40 shows that the G* value is increasing with more aging indicating a stiffer binder as well as a decreasing phase angle indicating a more brittle behavior. This is true for all aging levels for both virgin and recovered binders.

5.2.2.3.3. M7 Mixture

Similar to M4 and M6 mixtures, the M7 mixture black space diagram was also plotted to compare the different aging levels for virgin and recovered binders in terms of GRP.

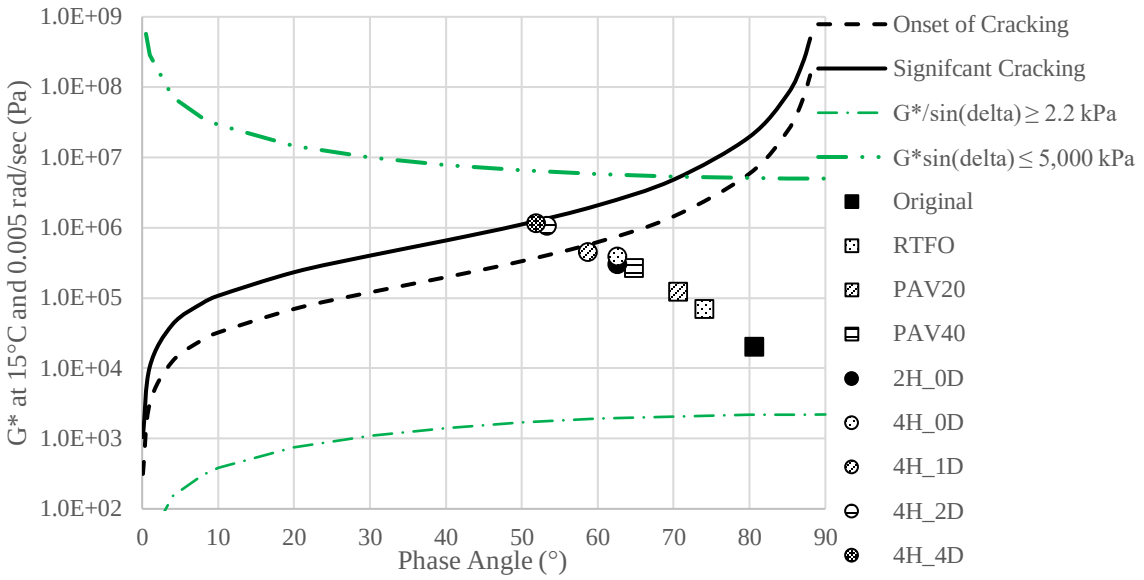

Figure 56. Black Space Diagram - M7

The detailed G* and phase angle values for the M7 mixture for virgin and recovered binders are depicted in Table 41

Table 41. G* vs Phase Angle - M7

		M7	
		G (Pa)*	*Phase Angle (°)*
Recovered Binder	*2H_0D*	296,000	62.66
	4H_0D	386,000	62.68
	4H_1D	444,400	58.76
	4H_2D	1,058,000	53.43
	4H_4D	1,149,000	51.98
Virgin Binder	*Original*	19,850	80.73
	RTFO	68,960	74.11
	PAV20	121,300	70.68
	PAV40	264,700	64.87

*: H is hours of aging at compaction temperature and the D is days of aging at 95°C

Once more, the observations for the M7 mixture are in line with those for the M4 and M6 blends, particularly regarding the GRP. This alignment is evidenced by reaching the onset of cracking curve after 4H_1D for the recovered M7 binder. The M7 mixture exhibits superior characteristics compared to the M4 and M6 mixtures as the GRP of the virgin binder never reaches the onset of the cracking curve even after PAV40. Moreover, the GRP of the recovered binder never exceeds the significant cracking curve even after 4H_4D aging. When comparing the Carbonyl against aging duration, two aging rates are observed. An initial fast aging rate and a more decelerated steady rate after 1 day of aging shown in Figure 57.

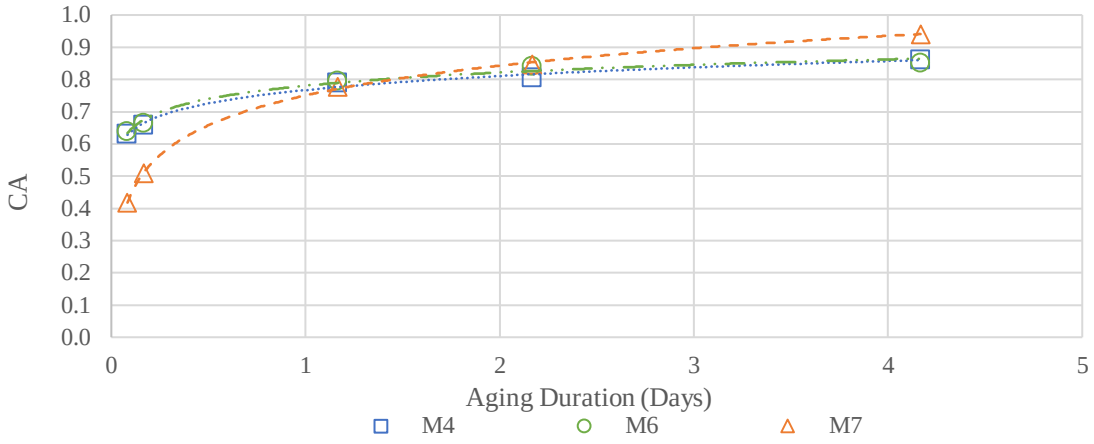

Figure 57. Carbonyl Growth vs Aging Duration

The steady state is attained after one day of aging, data points follow a logarithmic function. The aging needed to reach the steady state is compared with the plot in Figure 57 to see if the duration corresponds with the formation of the elbow shape observed in Figure 58.

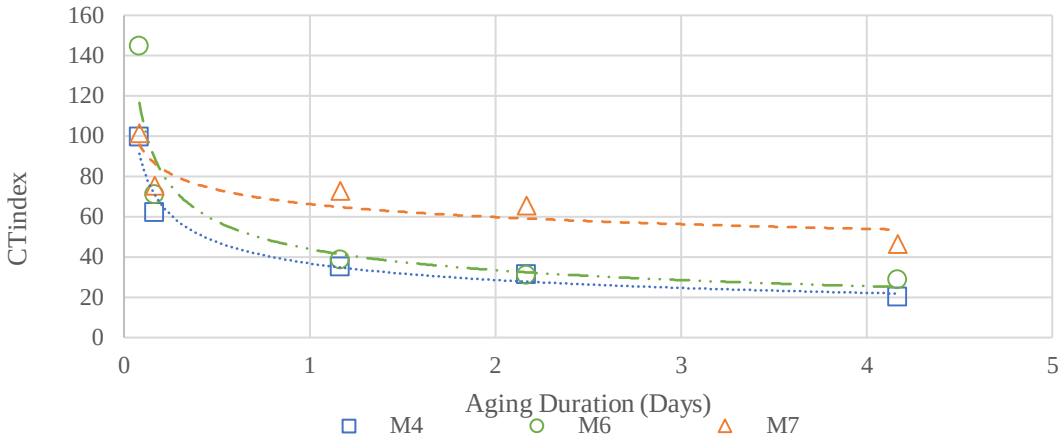

Figure 58. CTindex vs Aging Duration

The steady state starts just right after the elbow observed in Figure 58. Upon analyzing the gathered data from both mixture and binder tests, the 4H_1D aging level emerged as a crucial point for discerning performance differences among the mixtures.

5.3. Long-Term aging at Compaction Temperature:

Given the study's focus on establishing workable long-term aging protocols for better cracking resistance in Virginia, it became crucial to translate the extended aging at 95°C into a higher temperature range. This adjustment aimed to reduce the aging duration while aligning it with working hours, streamlining the implementation process for better ease and feasibility. At first, a temperature of 135°C was proposed. However, considering that the compaction temperatures for all mixtures fall within a proximity of 135°C, the decision was made to opt for compaction temperatures tailored to each mixture. This choice offers a more straightforward and seamless process for implementation, aligning specifically with the requirements of each mixture. From insights extracted from the NCHRP 9-54 study entitled: "Authentication of Loose Mixture Aging Methods for Assessing Cracking Resistance in Balanced Mix Design", a conversion chart was applied to derive preliminary long-term aging periods at the compaction temperature that suit all three mixtures M4, M6, and M7. Table 42 and Figure 59 illustrate the conversion table sourced from the NCHRP 9-54 study.

Table 42. Time equivalence conversion table for different LTA temperatures (NCHRP 9-54)

$T_{85°C, days}$	$T_{95°C, days}$	$T_{135°C, hours}$
2.4	1	1
4.6	2	2
6.8	3	4
8.9	4	6
10.8	5	8
12.7	6	11
14.5	7	15
16.2	8	19
17.9	9	23
19.6	10	27

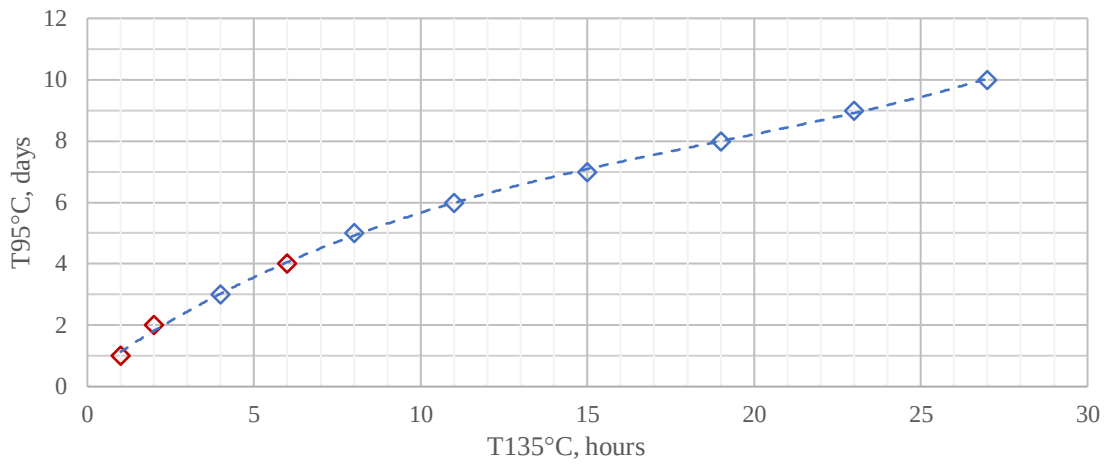

Figure 59. Time equivalence conversion curve for different LTA temperatures (NCHRP 9-54)

To establish an analogous duration at the compaction temperature to replicate the impact of 4 hours at compaction temperature and 1 day at 95°C (4H_1D), three sequential steps were necessary to consider the initial fast aging rate. Initially, the STA aging periods measured in hours at 135°C needed to be converted into days at 95°C. Subsequently, the cumulative equivalent number of days at 95°C for 4H_1D, 4H_2D, and 4H_4D was calculated. Following this, the total days at 95°C were reconverted into hours at 135°C. It's noteworthy that 135°C was assumed to be akin to the compaction temperature, approximately 149°C, for the purposes of this calculation.

Step 1: Convert STA aging periods from hours at 135°C to days at 95°C.

Step 2: Calculate cumulative days at 95°C for 4H_1D, 4H_2D, and 4H_4D.

Step 3: Reconvert total days at 95°C to hours at 135°C.

Based on the conversion outcomes, the decision was made to adopt two aging levels: the initial one involving 4 hours at compaction temperature followed by an additional 2 hours (6H_0D), and the second one consisting of 4 hours at compaction temperature followed by another 4 hours (8H_0D). The three mixtures M4, M6 and M7 were then mixed, compacted, and aged in the laboratory and after that tested for IDT-CT. Extracted binders from these tested samples were subjected to evaluations through the FTIR test and the FS test. This was done to compare the new results with the previously obtained data.

5.3.1. Mixture Testing

5.3.1.1. IDT-CT Test

Three samples were mixed, compacted, and aged to be tested. Similarly, to the first five LMLC aging levels, these samples were also conditioned at 25°C for two hours prior to testing. Table 43 compares all the aging duration's CT indices for all three LMLC mixtures.

Table 43. IDT- CT - LMLC all aging levels

M4						
Mixture ID*	**CTindex**	**l75/m75**	**Gf (Joules/m2)**	**m75 (kN/mm)**	**P100 (kN)**	**Energy to P100 (Joules/m2)**
M4[2hrs; 0d]	99.6	1.79	8361.7	2.83	13.019	3245.1
M4[4hrs; 0d]	61.9	1.21	7702.6	3.57	14.124	2962.6
M4[4hrs; 1d]	35.1	0.73	7195.6	4.62	16.404	2727.6
M4[4hrs; 2d]	31.2	0.67	6995.8	4.97	16.253	2654.2
M4[4hrs; 4d]	20.2	0.43	7009.0	6.73	18.681	2718.8
M4[6hrs; 0d]	31.4	0.63	7431.0	5.29	17.549	2922.2
M4[8hrs; 0d]	19.6	0.44	6669.0	5.89	17.505	2465.0
M6						
Mixture ID*	**CTindex**	**l75/m75**	**Gf (Joules/m2)**	**m75 (kN/mm)**	**P100 (kN)**	**Energy to P100 (Joules/m2)**
M6[2hrs; 0d]	144.5	2.07	10429.4	2.54	14.640	3279.2
M6[4hrs; 0d]	70.9	1.03	10314.8	4.25	17.552	3538.8
M6[4hrs; 1d]	38.4	0.63	9158.1	5.41	19.628	3087.1
M6[4hrs; 2d]	31.0	0.58	7969.5	5.74	21.164	2963.4
M6[4hrs; 4d]	28.6	0.50	8552.1	6.15	20.859	2840.3
M6[6hrs; 0d]	54.0	0.71	11451.7	5.48	22.057	4232.9
M6[8hrs; 0d]	44.7	0.74	9036.9	4.59	19.057	2671.2
M7						
Mixture ID*	**CTindex**	**l75/m75**	**Gf (Joules/m2)**	**m75 (kN/mm)**	**P100 (kN)**	**Energy to P100 (Joules/m2)**
M7[2hrs; 0d]	101.4	1.50	10139.1	3.11	15.820	3349.3
M7[4hrs; 0d]	75.5	1.13	10113.0	3.91	17.428	3508.6
M7[4hrs; 1d]	72.9	1.12	9769.0	3.84	16.831	3405.3
M7[4hrs; 2d]	65.4	0.99	9956.5	4.08	18.357	3545.4
M7[4hrs; 4d]	46.6	0.72	9644.1	5.11	19.611	3347.4
M7[6hrs; 0d]	78.7	1.25	9443.3	3.65	16.889	3172.7
M7[8hrs; 0d]	43.0	0.56	11449.6	6.24	23.816	3623.6

The data in Table 43 indicates a close alignment between the prediction and the actual outcomes, affirming the accuracy of the forecast. The results from the 6H_0D aging closely mirrored those of the 4H_1D, meeting the intended expectations. Furthermore, the individual mixtures CTindex versus the aging duration at 135°C was plotted in Figures 60 through 62. The data points in red are the ones belonging to 6H_0D and 8H_0D.

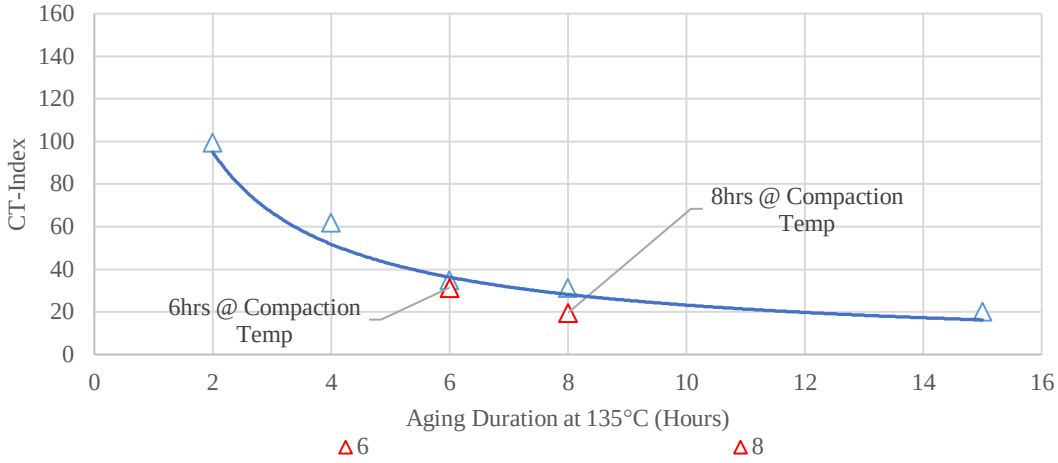

Figure 60. CT-Index M4 - LMLC all aging levels

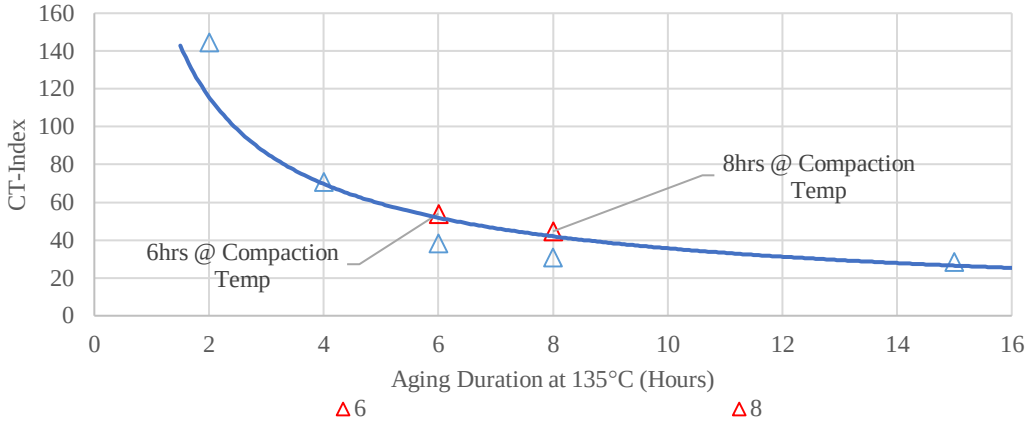

Figure 61. CT-Index M6 - LMLC all aging levels

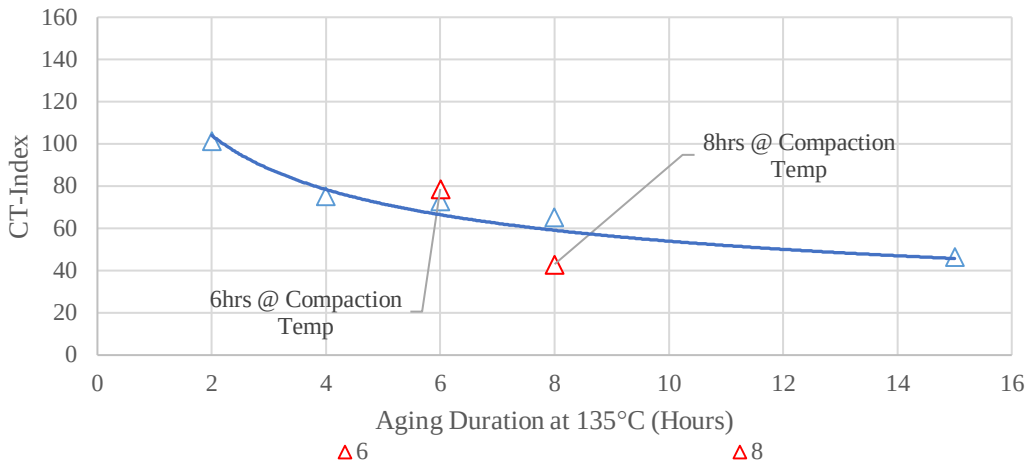

Figure 62. CT-Index M7 - LMLC all aging levels

As anticipated, the data depicted in Figures 60 to 62 corresponds closely with the projected behaviors of the mixtures.

5.3.2. Binder Testing

5.3.2.1. Fourier Transform Infrared Test (FTIR)

Two additional aging durations, namely 6H_0D and 8H_0D, were introduced for testing. The binder retrieval involved examining IDT-CT LMLC samples that closely matched the CTindex mean of the specific aging level under consideration. For each binder, three samples underwent testing, with each sample being tested three times. Figures 63 to 65 showcase the averaged FTIR test outcomes of all the LMLC recovered binders.

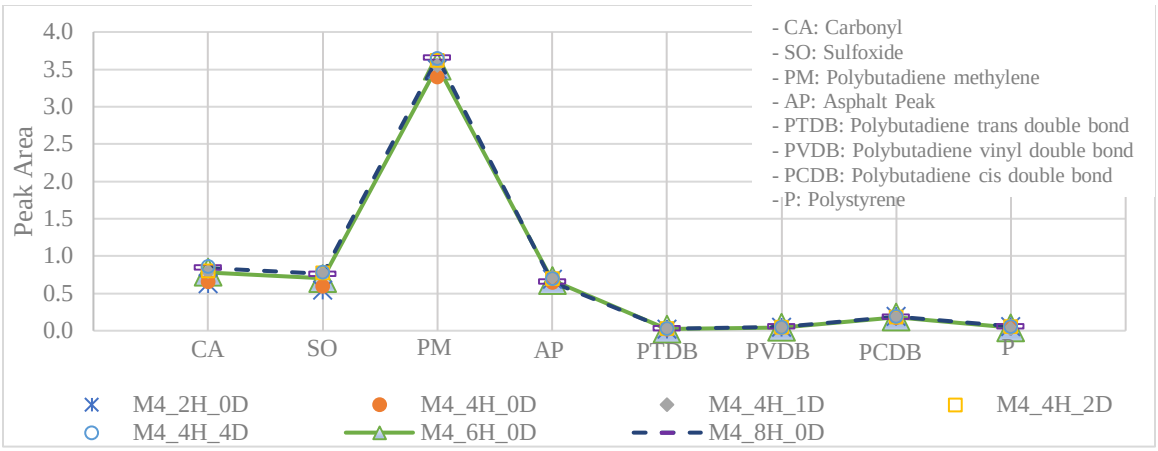

Figure 63. FTIR - M4 all aging Levels

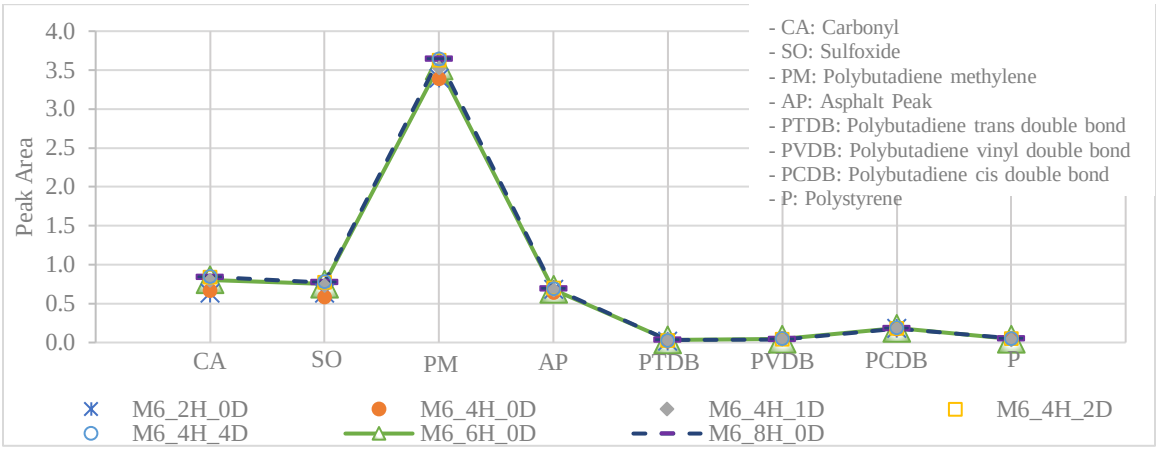

Figure 64. FTIR - M6 all aging Levels

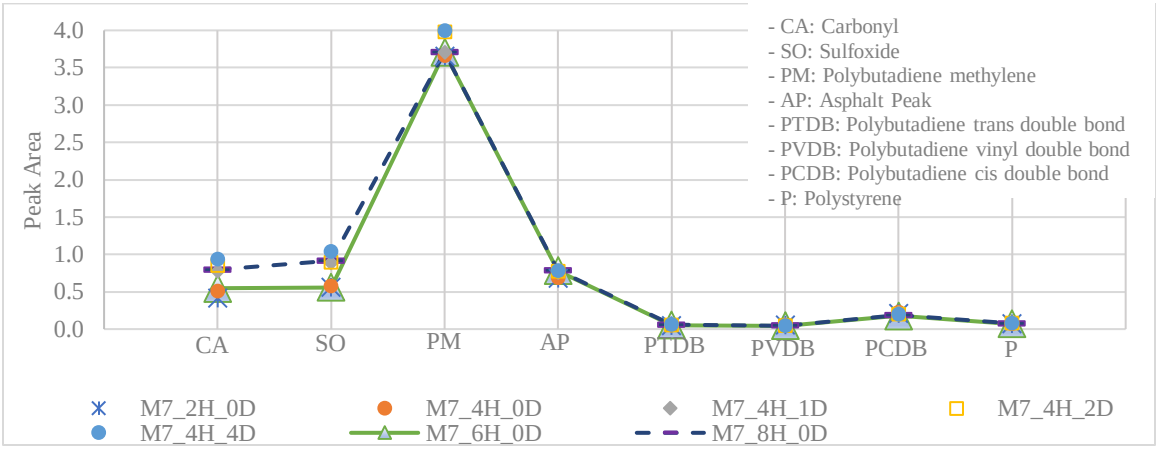

Figure 65. FTIR - M7 all aging Levels

Additionally, Table 44 depicts the different mixtures of FTIR data for the two new accelerated aging levels.

Table 44. FTIR Data Accelerated Aging levels - All mixtures

M4	6H_0D	0.78	0.70	3.54	0.68	0.02	0.05	0.18	0.04
	8H_0D	0.84	0.76	3.65	0.65	0.03	0.05	0.19	0.06
M6	6H_0D	0.80	0.75	3.55	0.68	0.03	0.05	0.18	0.04
	8H_0D	0.84	0.77	3.64	0.69	0.03	0.04	0.18	0.05
M8	6H_0D	0.55	0.56	3.70	0.78	0.05	0.04	0.18	0.07
	8H_0D	0.80	0.91	3.71	0.79	0.06	0.04	0.19	0.08

Once more, the alignment between the FTIR data at 6H_0D and 8H_0D and the predicted model reaffirms the suitability of 6H_0D in simulating the critical aging duration found earlier in the project, namely, 4H_1D. This is true for all three mixtures M4, M6 and M7 where similar results are observed.

5.3.2.2. Frequency Sweep Test (FS)

Similar to the IDT-CT and FTIR tests. Figures 66 through 68 showcase the two additional data points in red for all three mixtures M4, M6 and M7 along with all aging levels tested at an earlier stage of the study. It is worth noting that the binders used in this test were recovered from tested LMLC IDT-CT samples having the closest CTindex to the mean of the aging level in question.

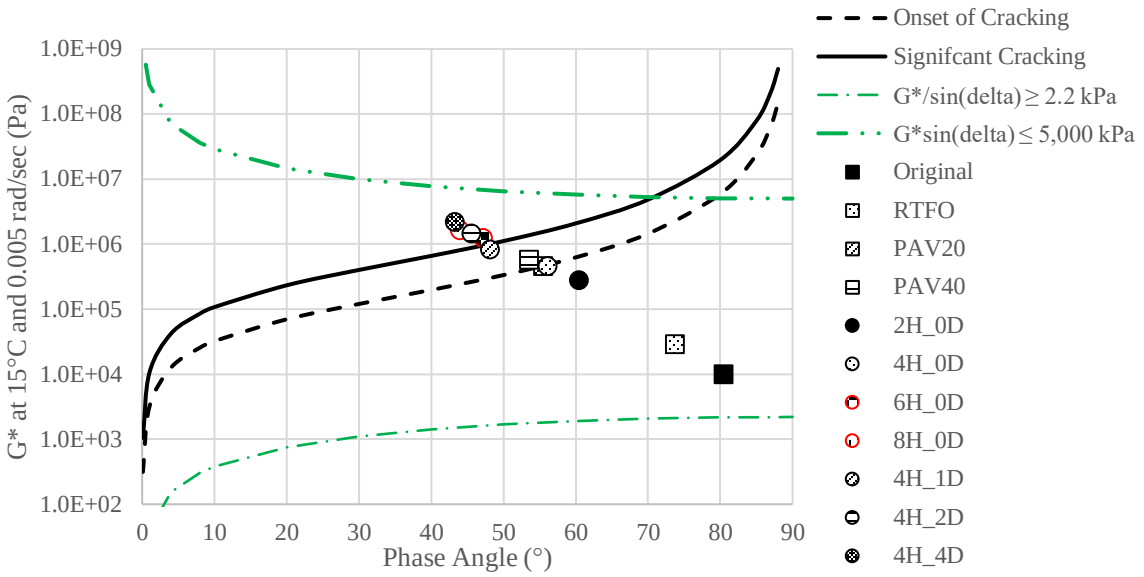

Figure 66. Black Space Diagram - M4 all aging levels

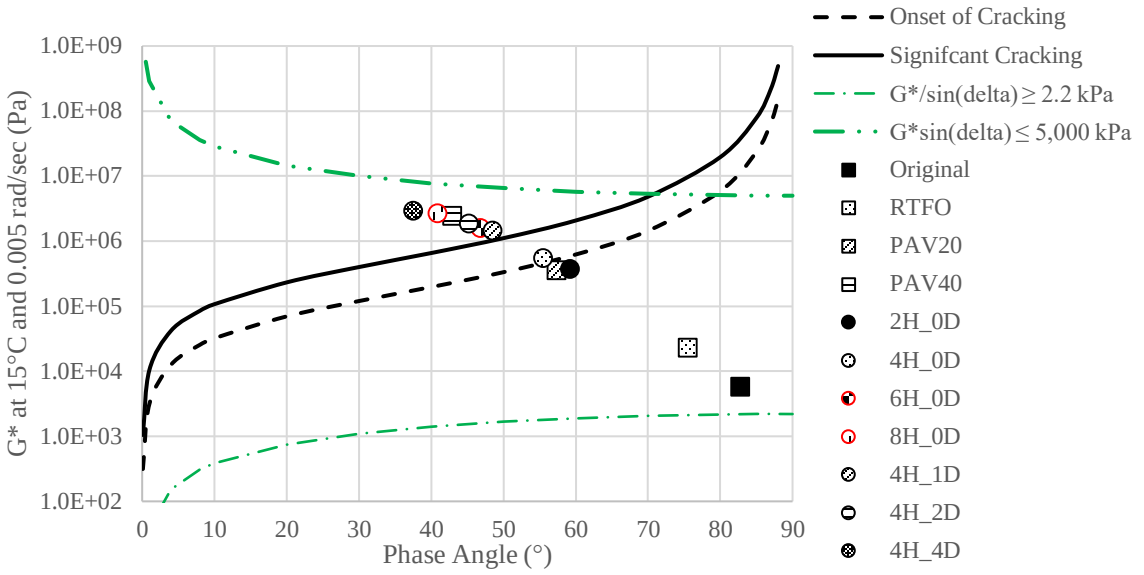

Figure 67. Black Space Diagram - M6 all aging levels

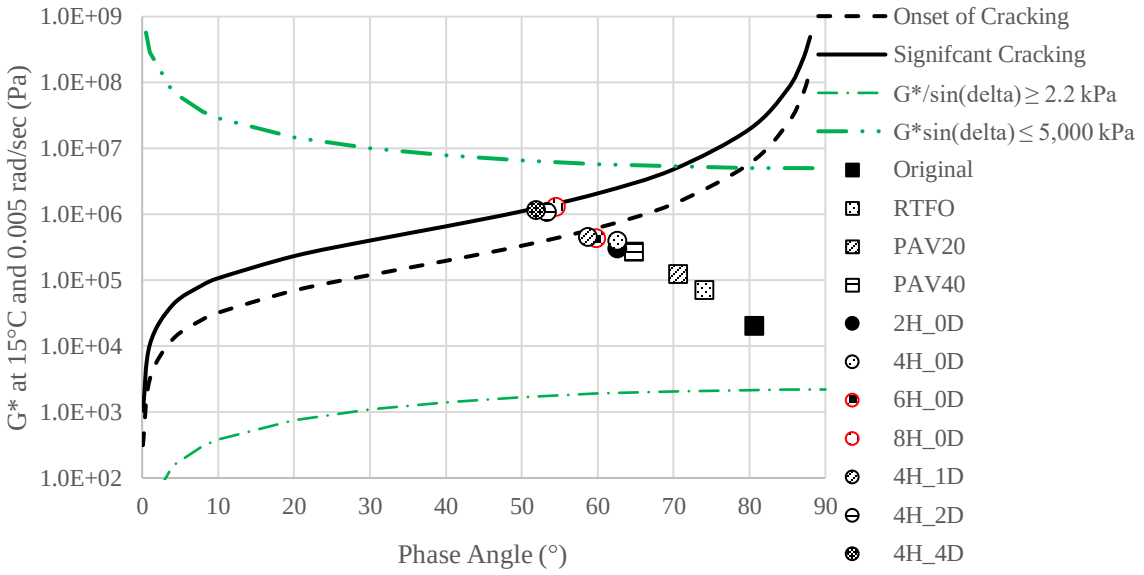

Figure 68. Black Space Diagram - M7 all aging levels

Upon reviewing the figures in the provided dataset, it's evident that the impact of the 6H_0D aging duration mirrors the effects observed at the 4H_1D level, particularly concerning the Glover Rowe parameter. Thus, it can be asserted that the 6H_0D duration effectively represents a critical aging level.

5.4. Comparison Plots

To strengthen the hypothesis suggesting that the 6H_0D aging duration mirrors the aging impact initiated by the 4H_1D level, an evaluation was conducted by plotting various parameters. These parameters encompass Glover-Rowe parameter, Carbonyl area, Carbonyl growth compared to 2h (Cag (2h)) and CTindex.

These plots are shown in Figures 69 through 72.

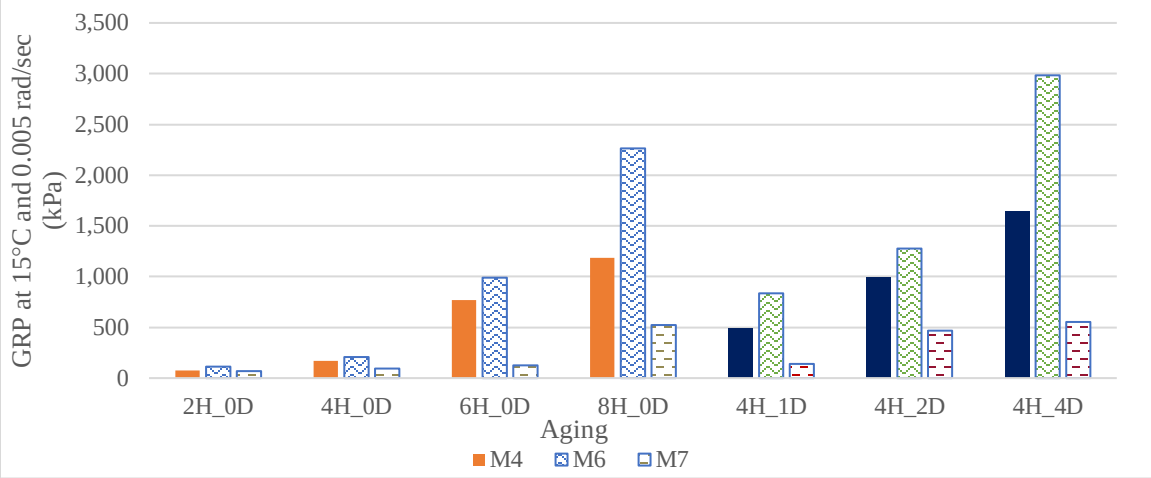

Figure 69. GRP vs Aging level – LMLC all mixtures

Displayed in the bar chart in Figure 69, the Glover-Rowe parameter for the LMLC recovered binders across all aging levels for all three mixtures. A comparison between the 6H_0D and the 4H_1D reveals a remarkable similarity and proximity in values across these two distinct aging levels for all three mixtures.

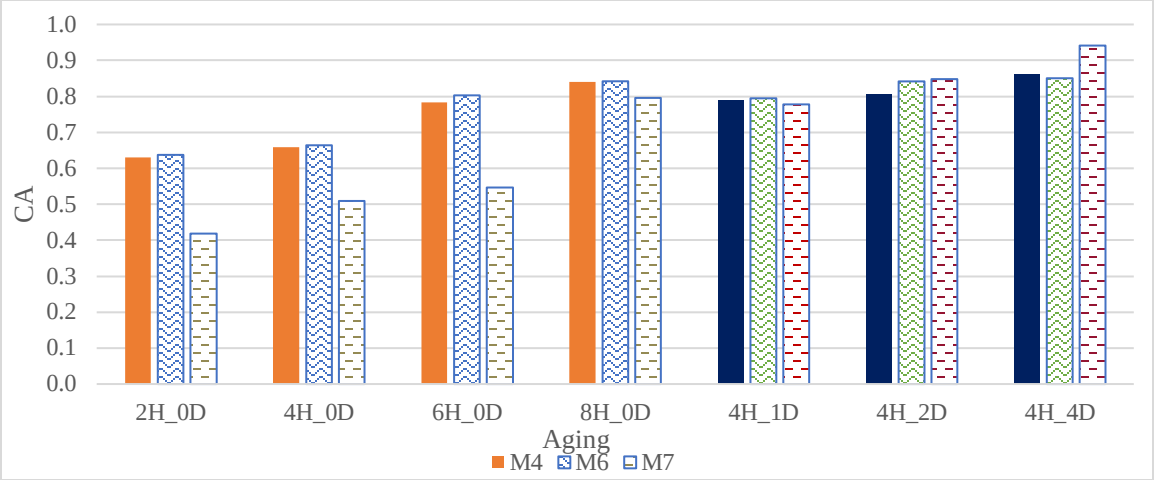

Figure 70. CA vs aging level – LMLC all mixtures

The bar chart in Figure 70 illustrates the carbonyl area of LMLC recovered binders across aging levels for all three mixtures. When comparing the 6H_0D with the 4H_1D, similarities and closeness in values are evident across these two distinct aging levels for M4 and M6 mixtures, registering values around 0.8 for CA. However, the M7 mixture showed a lower carbonyl area at 6H_0D compared to 4H_1D.

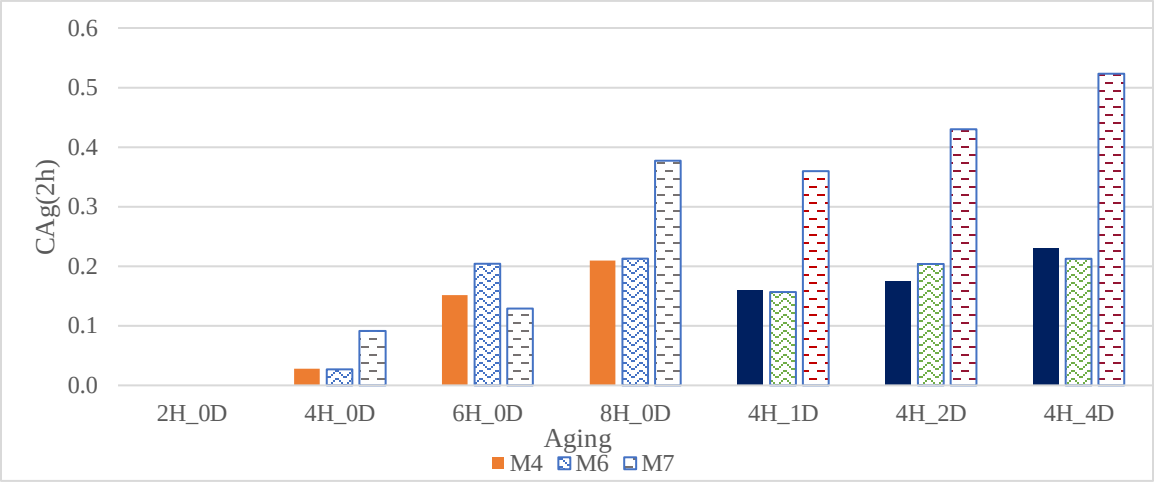

Figure 71. CAg(2h) vs Aging levels - LMLC all mixtures

Figure 71 depicts the Carbonyl growth from 2H across various aging levels for all three LMLC mixtures. Notably, the bar chart lacks data at the 2H_0D aging duration as this comparison focuses on growth from this specific aging duration, rendering a zero-growth value for all three mixtures, as it serves as the reference point. While observing 6H_0D and 4H_1D, some similarities emerge, yet these results aren't sufficient to confirm a clear correlation between the two aging durations.

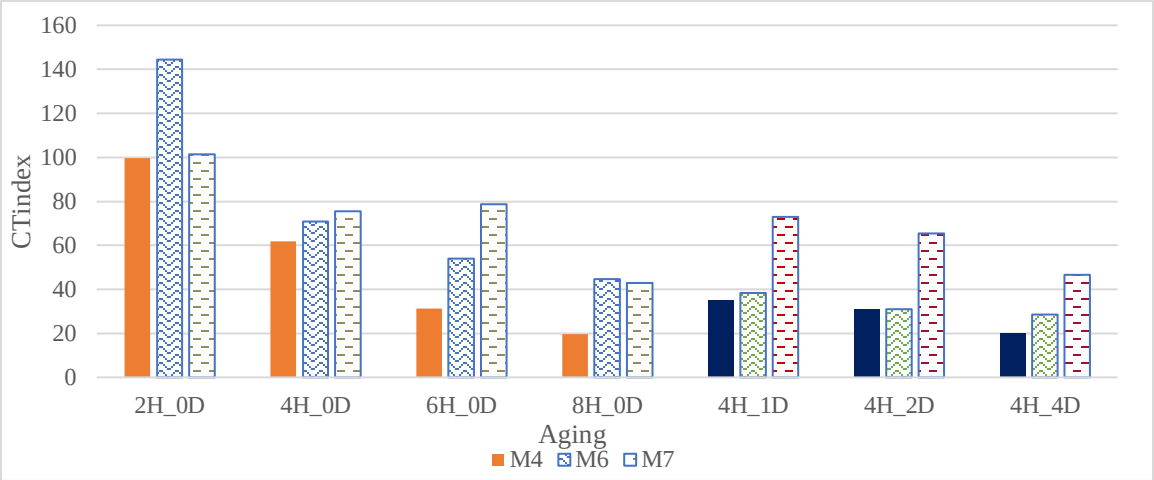

Figure 72. CTindex vs Aging levels - LMLC all mixtures

Figure 72 exhibits remarkable consistency in CTindex across the three mixtures at both 6H_0D and 4H_1D, emphasizing the significance of the 6H_0D aging level in mirroring the critical aging duration observed at 4H_1D.

5.5. Aging Criteria

The second objective of this study was to establish IDT-CT criteria for critical aging identified in the study. For that reason, a comprehensive analysis of the test data was conducted. This analysis included various test parameters gathered from both binder and mixture testing. GRP was plotted against the CTindex for all mixtures to derive cracking limits based on CTindex boundaries. Furthermore, another graph was created, plotting CTindex against aging duration to determine cracking limits based on different aging durations. Similarly, the drop in CTindex after 4 hours of aging was calculated for each aging level beyond that point and plotted against the GRP. These plots are shown in Figures 73 through 75.

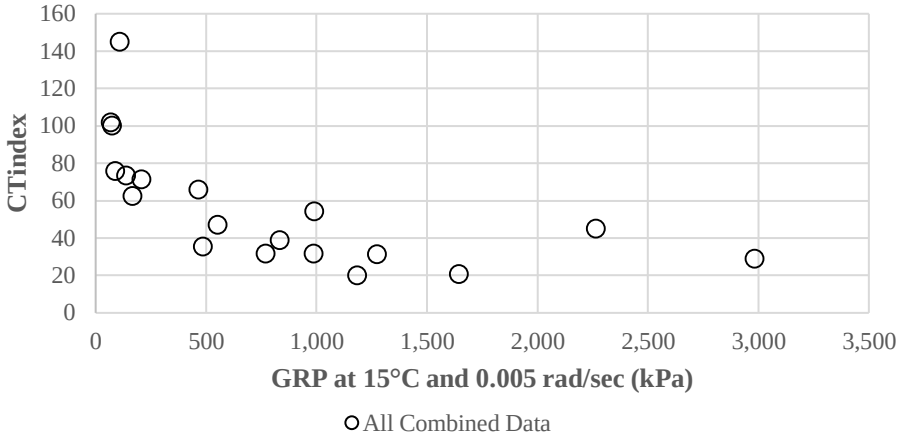

Figure 73. CTindex vs GRP - All mixtures

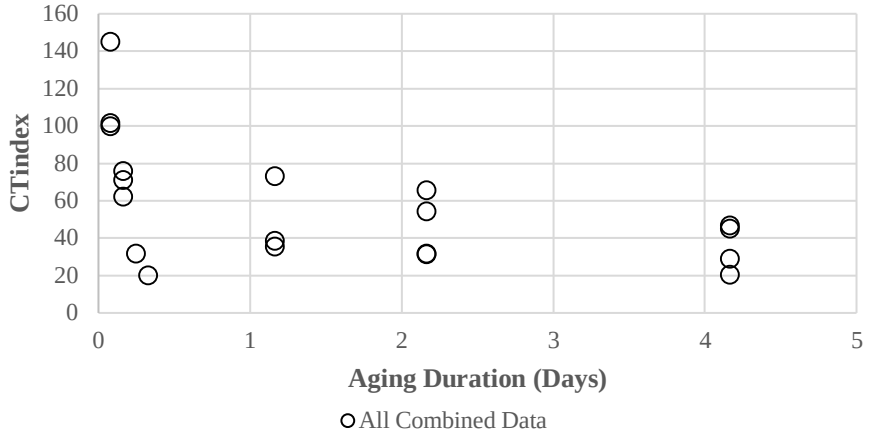

Figure 74. CTindex vs Aging Duration - All mixtures

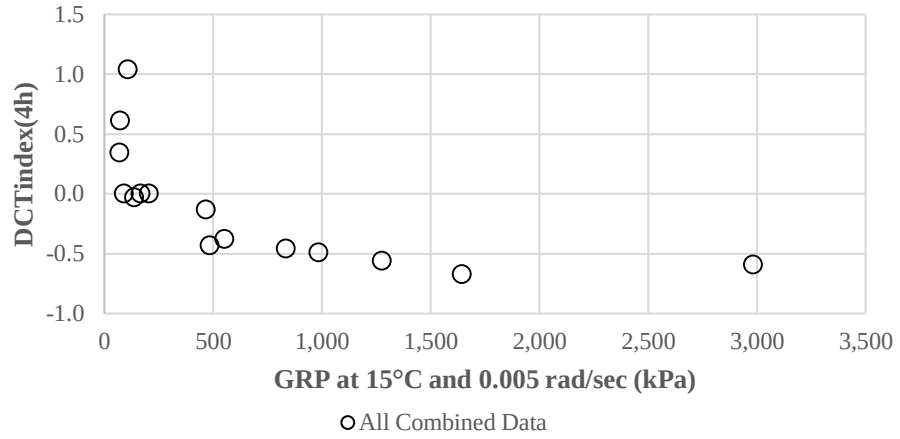

Figure 75. DCTindex (4h) vs GRP - All Mixtures

Shown in Figures 73 and 74, the resulting CTindex limits for cracking were 71.04 for onset of cracking corresponding to a GRP of 180 kPa and 42.8 for significant cracking corresponding to a GRP of 600 kPa. Furthermore, the aging durations for cracking were 0.26 days for onset of cracking corresponding to a GRP of 180 kPa and 1.41 days for significant cracking corresponding to a GRP of 600 kPa. Also, Figure 75 shows that a 10.8% drop in CTindex after 4 hours of aging signifies the onset of cracking that corresponds to a GRP of 180 kPa and a further drop reaching 29.8% signifies that the mixture has reached the significant cracking level.

Chapter 6. Summary, Conclusion and Future Steps

6.1. Summary

- This study included 11 dense-graded asphalt surface mixtures with A and D designations labeled M0 to M10, specifically selected to derive practical long-term aging protocols for cracking resistance in Virginia. The evaluation included diverse mixtures, ranging from plant mixed, laboratory compacted (PMLC) and laboratory mixed, laboratory compacted (LMLC) compositions.
- Various tests, including binder content analysis, gradation assessment, aggregate specific gravity determination, and IDT-CT evaluations, were conducted on LMLC, PMLC, and RAP samples. Specifically, the PMLC tests focused on the M6 mixture and IDT-CT analysis. Additionally, RAP testing was performed on the M4, M6, and M7 mixtures.
- LMLC testing, involving the M4, M6, and M7 mixtures, included IDT-CT assessments and further evaluations with BBR, FTIR, and FS tests on the recovered binders from the IDT-CT tested samples.
- Initial aging durations were set for LMLC, such as 2H_0D, 4H_0D, 4H_1D, 4H_2D, and 4H_4D, where "H" refers to hours of short-term aging at compaction temperature and "D" to days of long-term aging at 95°C.
- Post-evaluating of the results for mixture and binder tests across the three mixtures highlighted the critical nature of the 4H_1D aging level in predicting cracking performance.
- M7 mixture showed superior performance compared to the M4 and M6 mixtures.

- To streamline the process, accelerated aging protocols were suggested, resulting in the proposition of 6H_0D and 8H_0D aging levels based on a conversion chart from NCHRP 9-54 adjusted to fit this study's parameters.
- Further IDT-CT, FTIR, and FS tests were conducted on the three mixtures using the newly proposed aging levels to establish correlations with the 4H_1D test outcomes.
- The analysis demonstrated a notable similarity in aging effects between the 6H_0D and 4H_1D, signifying that the accelerated aging at the compaction temperature (6H_0D) mirrors the critical aging level. This equivalence indicates its capacity to effectively predict the cracking performance of the mixtures.
- CTindex limits for cracking were 71 for onset of cracking and 43 for significant cracking.
- The mixtures limit for reaching the onset of cracking is 0.26 days which represents a GRP of 180 kPa and a duration of 1.41 days for reaching the significant cracking that represents the GRP value of 600 kPa.
- The decrease in CT index (DCTindex) relative to 4hs STA at compaction temperature were 10.8% and 29.8% for the GRP onset of cracking and significant cracking limits, respectively.

6.2. Conclusion

To sum up, after careful evaluation, the 4H_1D aging period emerged as the most promising duration for assessing cracking performance, providing sufficient aging to discern between the behaviors of the mixtures. The corresponding accelerated aging period between 6H_0D and 8H_0D demonstrated a closely aligned outcome with the critical 4H_1D, signifying its potential for future implementation as an effective aging protocol. Notably, the M7 mixture consistently exhibited superior performance across multiple test results, primarily attributed to its binder characteristics and gradation.

6.3. Future Steps:

Further validations are imperative to solidify the findings outlined in this report. As an ongoing study, future endeavors will encompass comprehensive assessments of the remaining mixtures specifically, M0, M1, M2, M3, M5, M8, M9, and M10 at various aging intervals, namely 2H_0D, 4H_0D, 6H_0D, and 8H_0D, with emphasis placed once more on the critical aging level of 4H_1D. Extending the scope, intensified scrutiny will focus on the binders retrieved from tested IDT-CT samples of these eight mixtures, amplifying the credibility of the present study's conclusions. Moreover, to augment insights into performance aspects, it is pivotal to conduct two fundamental tests namely the cyclic fatigue test in accordance with AASHTO TP 107 for all mixtures. This test will offer a comprehensive view and facilitate a deeper analysis of the obtained cracking results.

References

[1] AASHTO, “Standard Practice for Laboratory Conditioning of Asphalt Mixtures” AASHTO R 30 – 22

[2] Transportation Research Board. (2022). Glossary of Transportation Terms (Report No. E-C280).

[3] *History of Asphalt Roads in The US | Dykes Paving*. (n.d.). Https://Www.dykespaving.com/.

[4] Dunlavey, B. (2015, June 22). *Asphalt Paving Throughout History*. UNIQUE Paving Materials.

[5] Diefenderfer, S. D., Nair, H., & Bowers, B. F. (2018). *Investigation of Binder Aging and Mixture Performance in Service: Reclaimed Asphalt Pavement Mixtures* (No. FHWA/VTRC 18-R26). Virginia Transportation Research Council.

[6] Saadeh, S., Hakimelahi, H., & Harvey, J. (2014, May). Correlation of semi-circular bending and beam fatigue fracture properties of asphalt concrete using non-contact camera and crosshead movement. In *T&DI Congress 2014: Planes, Trains, and Automobiles* (pp. 39-48).

[7] Diefenderfer, S. D., Boz, I., & Habbouche, J. (2021). *Balanced mix design for surface asphalt mixtures: Phase I: Initial roadmap development and specification verification* (No. FHWA/VTRC 21-R15). Virginia Transportation Research Council (VTRC).

[8] West, R., Rodezno, C., Leiva, F., and Yin, F. Development of a Framework for Balanced Mix Design. National Center for Asphalt Technology, Auburn, AL, 2018.

[9] Newcomb, D., and Zhou, F. Balanced Design of Asphalt Mixtures. MN/RC 2018-22. Minnesota Department of Transportation, St. Paul, 2018.

[10] Rodezno, C., Taylor, A., and Gu, F. Crack Resistance and Durability of RAS Asphalt Mixtures—Phase I. FHWA-OH-2018-15. National Center for Asphalt Testing, Auburn, AL, 2018.

[11] Cross, S.A., and Li, J.Q. Implement Balanced Mix Design in Oklahoma. FHWA-OK-19-01. Oklahoma State University, Stillwater, 2019.

[12] Coleri, E., Sreedhar, S., and Obaid, I.A. Development of a Balanced Mix Design Method in Oregon. FHWA-OR-RD-21-03. Oregon State University, Corvallis, 2020.

[13] Bell C. A., AbWahab Y., Cristi M. E., Sosnovske D. *Selection of Laboratory Aging Procedures for Asphalt-aggregate Mixtures*. No. SHRP-A-383. Strategic Highway Research Program, 1994.

[14] Yin, F., Martin, A. E., Arambula, E., & Newcomb, D. E. (2015). Short-term aging of asphalt mixtures. *Asphalt Paving Technology, 2016*, 2015.

[15] Islam M. R., Hossain M. I., Tarefder R. A. A Study of Asphalt Aging Using Indirect Tensile Strength Test. *Construction and Building Materials*, Vol. 95, 2015, pp. 218–223.

[16] Howard I. L., Doyle J. D. Durability Indexes via Cantabro Testing for Unaged, Laboratory-Conditioned, and One-Year Outdoor-Aged Asphalt Concrete. Presented at 94th Annual Meeting of the Transportation Research Board, Washington, D.C., 2015.

[17] Braham A. F., Buttlar W. G., Clyne T. R., Marasteanu M. O., Turos M. I. The Effect of Long-term Laboratory Aging on Asphalt Concrete Fracture Energy. *Journal of the Association of Asphalt Paving Technologists*, Vol. 78, 2009.

[18] Reinke G., Hanz A., Herlitzka D., Engber S., Ryan M. Further Investigations into the Impact of REOB & Paraffinic Oils on the Performance of Bituminous Mixtures. In Federal Highway Administration Expert Task Group Meeting, Fall River, MA, 2015, April.

[19] Elwardany, M. D., Yousefi Rad, F., Castorena, C., & Kim, Y. R. (2017). Evaluation of asphalt mixture laboratory long-term ageing methods for performance testing and prediction. *Road Materials and Pavement Design*, *18*(sup1), 28-61.

[20] Yin F., Epps Martin A., Arambula-Mercado E., Newcomb D. Characterization of Non-Uniform Field Aging in Asphalt Pavements. *Construction and Building Materials*. Vol. 153, 2017, pp. 607–615.

[21] AASHTO, “Standard Practice for Reducing Samples of Asphalt Mixtures to Testing Size” AASHTO R 47 – 19

[22] AASHTO, “Standard Method of Test for Theoretical Maximum Specific Gravity (Gmm) and Density of Asphalt Mixtures” AASHTO T 209 – 22

[23] ASTM International. ASTM D8225-19: Standard Test Method for Determination of Cracking Tolerance Index of Asphalt Mixture Using the Indirect Tensile Cracking Test at Intermediate Temperature. West Conshohocken, PA, 2019a.

[24] AASHTO, "Standard Method of Test for Quantitative Extraction of Asphalt Binder from Asphalt Mixtures" AASHTO T 164 – 22

[25] ASTM International. ASTM D5404-21: Standard Practice for Recovery of Asphalt from Solution Using the Rotary Evaporator. West Conshohocken, PA, 2021

[26] AASHTO, "Standard Method of Test for Materials Finer Than 75-μm (No. 200) Sieve in Mineral Aggregates by Washing" AASHTO T 11 – 23

[27] AASHTO, "Standard Method of Test for Specific Gravity and Absorption of Fine Aggregate" AASHTO T 84 – 22

[28] AASHTO, "Standard Method of Test for Specific Gravity and Absorption of Coarse Aggregate" AASHTO T 85 – 22

[29] AASHTO, "Standard Method of Test for Determining the Flexural Creep Stiffness of Asphalt Binder Using the Bending Beam Rheometer (BBR)" AASHTO T 313 – 22

[30] AASHTO, "Standard Practice for Accelerated Aging of Asphalt Binder Using a Pressurized Aging Vessel (PAV)" AASHTO R 28 – 22

[31] F. Yin (2022). *Validation of Loose Mix Aging Procedures for Cracking Resistance Evaluation in Balanced Mix Design* (Auburn University).

[32] AASHTO, “Standard Method of Test for Determining the Damage Characteristic Curve and Failure Criterion Using the Asphalt Mixture Performance Tester (AMPT) Cyclic Fatigue Test” AASHTO TP 107 – 18

[33] AASHTO, “Standard Method of Test for Determining the Dynamic Modulus and Flow Number for Asphalt Mixtures Using the Asphalt Mixture Performance Tester (AMPT)” AASHTO T 379 – 22